

https://dspace.org/

Flood susceptibility modelling using geo-analytical hierarchy process (G-AHP) approach in Khartoum, Sudan

Khomo, Prudence Mamello

2025

University of the Witwatersrand, Johannesburg

https://hdl.handle.net/10539/50278

Khomo, Prudence Mamello. (2025). Flood susceptibility modelling using geo-analytical hierarchy process (G-AHP) approach in Khartoum, Sudan [Master's dissertation, University of the Witwatersrand, Johannesburg]. WIReDSpace. https://hdl.handle.net/10539/50278

Downloaded from a DSpace repository. https://dspace.org/

Flood susceptibility modelling using geo-analytical hierarchy process (G-AHP) approach in Khartoum, Sudan

By

Prudence Mamello Khomo (1915478)

A RESEARCH REPORT SUBMITTED IN PARTIAL FULFILMENT OF THE REQUIREMENTS FOR THE DEGREE OF

Master of Science in Geographic Information System and Remote Sensing

JOHANNESBURG, SOUTH AFRICA

OCTOBER, 2025

SUPERVISORS

Dr. Iqra Atif (Supervisor)
Prof. Elhadi Adam (Co-Supervisor)



School of Geography, Archaeology and Environmental Studies.

DECLARATION

I, **Prudence Mamello Khomo**, declare that this research report entitled *"Flood Susceptibility Modelling Using Geo-Analytical Hierarchy Process (G-AHP) Approach in Khartoum, Sudan"* is my own original work. It has not been submitted before, in whole or in part, for any degree or examination at this or any other university. Where other people's work has been used, it has been duly acknowledged in the text and the list of references. Date: October, 2025

Signed:  _____

Date: October , 2025 _____

ACKNOWLEDGEMENTS

A research project of this scale cannot be completed alone. I would like to thank the University of Witwatersrand for allowing me to pursue my master's degree. Special thanks to my supervisor, Dr. Iqra Atif, for your guidance and countless words of advice that were not part of this conservative course. You made the journey of learning fulfilling, though it was not easy, at times I would cry and want to give up, but you pushed me not to give up and continue. Through this, I became more determined and motivated to fulfil all the requirements of the degree. I am thankful for your guidance and patience. To my sister, Petunia Tisetso Khomo, thank you for being there when I needed you the most. I appreciate everything you have done for me more, especially paying my tuition fees. I would not be where I am without your love and guidance. This was one of the most difficult journeys for me that I have ever had, you made sure I got all the help I needed when I had a mental breakdown. You continue to motivate me, as you know that I have always looked up to you. To my mom, Thandi Maria Khomo, thank you for making sure that my rent was always paid to date. I appreciate everything that you have done for me; you made sure that I had a safe and secure place here in Johannesburg as it was my first time ever being here. To my late dad (Johannes Khomo), thank you for always believing in my studies may you continue to rest in peace, and this MSc is for you. To Dr Morena Mapuru, and Mpho Sadiki (from Digital Earth Africa) thank you for your valuable insights on this research project. Most important, God be the glory, "The Lord is my strength and my shield; in him my heart trusts, and I am helped; my heart exults, and with my song, I give thanks to him" Psalm 28:7.

ABSTRACT

Floods represent one of the most frequent and devastating natural disasters, with increasing occurrences worldwide, particularly in regions susceptible to climate variability and urbanization. This study aims to develop a flood susceptibility model for Khartoum, Sudan, by integrating Geographic Information Systems (GIS), Remote Sensing (RS), and the Analytical Hierarchy Process (AHP) to identify flood-prone zones and inform mitigation strategies. Khartoum was chosen for this research due to its vulnerability exacerbated by climate variability, rapid urban expansion, and socio-economic impacts that make it critical to understand flood risks in urban planning and disaster readiness. Utilizing GIS and RS techniques, the research identifies and analyses key physical and environmental factors influencing flood vulnerability, including elevation, slope, rainfall, river proximity, and land use/land cover (LULC). The AHP was employed to assign weights to these factors, help in generating flood susceptibility maps, which classify zones into five distinct categories: very low, low, moderate, high, and very high susceptibility. Validation using the Receiver Operating Characteristic (ROC) curve and Area Under the Curve (AUC) achieved 75 percent accuracy, confirming the model's reliability. The findings reveal that low-elevation areas in proximity to rivers are the most prone to floods, with rainfall and elevation identified as the most influential factors. This study highlights the importance of geospatial analysis and multi-criteria decision-making in assessing flood risk. It provides useful insights for disaster management and urban planning in Khartoum, stressing the need for measures like better drainage systems, zoning regulations, and community-based flood preparedness programs. Future research should integrate climate change projections and real-time hydrological monitoring to enhance flood risk prediction further.

Contents

List of Abbreviations xi

1 Introduction **1**

1.1 Background 1

1.1.1 Climate Change and Global Flood Risk 1

1.1.2 Socio-Economic Vulnerability in Africa and Sudan 1

1.1.3 Hydrological and Environmental Impacts in Sudan 2

1.2 Problem Statement 3

1.3 Significance of the study 5

1.4 Aim 6

1.5 Objectives 6

1.6 Research Questions 6

1.7 Layout of Study 7

2 Literature Review **9**

2.1 Introduction 9

2.2 Flooding: A Global and Regional Challenge 10

2.2.1 Economice Impacts 10

2.2.2 Public Health and Displacement 10

2.2.3 Environmental Degradation and Restoration 11

2.2.4 Critical Synthesis 11

2.3 Factors Influencing Flood Susceptibility 11

2.3.1 Physical and Environmental Factors 13

2.3.2 Socio-Economic Factors 14

2.3.3 Conventional Methods for Flood Modelling 16

2.4 Advanced Methods for Flood Modelling 18

2.4.1 Advanced Techniques for Flood Modelling 18

2.4.2 GIS and Remote Sensing 18

2.4.3 Machine Learning (ML) and Artificial Intelligence (AI) 18

2.4.4 Multi-Criteria Decision Analysis (MCDA) 19

2.4.5 Applications of Modelling Approaches 19

2.4.6 Regional Focus on Sudan 21

3 Materials and Methods **24**

3.1 Introduction 24

3.2 Study Area 24

3.3 Materials 26

3.3.1 Datasets 26

3.3.2 Tools and Software 26

3.3.3 Data Pre-Processing 27

3.4 Methods 29

3.4.1 Data Integration using GIS 30

3.4.2 Weight assignment and Analytical Hierarchy Process 36

3.4.3 GIS-Based Weighted Overlay Analysis 39

3.5 Model Validation 41

3.5.1 Sensitivity Analysis 41

3.5.2 Receiver Operating Characteristics (ROC) Curve and Area Under Curve (AUC) 41

3.6 Ethical Consideration 43

4 Results **44**

4.1 Introduction 44

4.2 Spatial Analysis of Flood Susceptibility Factors 44

4.2.1 Topographic Analysis 45

4.2.2 Rainfall Distribution 49

4.2.3 Land Use and Land Cover Dynamics 51

4.2.4 Soil Distribution 54

4.2.5 Hydrological Attributes 55

4.2.6 Interaction and Synthesis of Factors 60

4.3 Integrated Flood Susceptibility Mapping 61

4.4 Model Validation 65

4.4.1 Sensitivity Analysis 65

4.4.2 Predictive Performance Assessment 66

4.5 Synthesis of findings 67

5 Discussion **68**

5.1 Overview of the chapter 68

5.2 Interpretation and Contextualisation of results 68

5.3 Implications of the findings 71

5.3.1 Implications for Urban Planning 71

5.3.2 Implications for Flood Risk Management 71

5.3.3 Policy Recommendations 72

5.4 Strengths and Limitations of the Research 73

5.4.1 Strengths 73

5.4.2 Limitations 75

5.5 Conclusion 75

6 conclusion and Recommendations **77**

6.0.1 Overview of the study 77

6.1 Key Findings 77

6.2 Contributions of the Research 77

6.2.1 Methodological Contributions 78

6.2.2 Practical Contributions 78

6.2.3 Academic Contributions 78

6.3 Recommendations 78

6.4 Limitations of the study 79

6.5 Directions or future Research 79

6.6 Conclusion 80

List of Figures

1.1 "Flood-Affected Population in Sudan (2013–2020)." Data Source: Sudan Meteorological Authority (SMA) and UN Office for the Coordination of Humanitarian Affairs (OCHA, 2020). 3

2.1 Flash Flood susceptibility mapping developed by using FURIA-GA-Bagging method 20
2.2 Flash flood susceptibility mapping developed by using FA-LM-ANN method . 21
2.3 Flood susceptibility mapping developed using AHP method 22

3.1 Map showing the study area (Khartoum, Sudan). 26
3.2 Work dlow of Flood Susceptibility Modelling using GIS and Remote Sensing techniques. 29
3.3 A bar graph showing monthly rainfall for Khartoum, Sudan. 34

4.1 Workflow for flood susceptibility model generation. 45
4.2 Elevation map of Khartoum showing (a) elevation ranges and (b) corresponding flood susceptibility levels. 46
4.3 Slope map of Khartoum showing (c) slope ranges and (d) flood susceptibility. . 47
4.4 Topographic Wetness Index map of Khartoum showing (e) TWI ranges and (f) corresponding flood susceptibility levels. 49
4.5 Rainfall map of Khartoum showing (g) rainfall ranges and (h) corresponding flood susceptibility levels. 50
4.6 Confusion matrix showing the classification performance of the Random Forest model for land cover mapping. The diagonal cells represent correctly classified samples across five land cover classes: Bare-Land, Built-up Area, Road, Vegetation, and Water. Higher values along the diagonal indicate better model accuracy and class separability. 51
4.7 Land Use and Land Cover (LULC) classification map of Khartoum City. The map delineates five major land cover classes—Bare-land, Built-up Area, Road, Vegetation, and Water—derived from Sentinel-2 imagery. The classification highlights the spatial distribution of urban and natural features within the study area. 54

4.8 Soil Texture map of Khartoum showing (j) Soil ranges and (k) corresponding flood susceptibility levels. 55
4.9 Drainage Density map of Khartoum showing (l) drainage ranges and (m) corresponding flood susceptibility levels. 56
4.10 Distance from roads map of Khartoum showing (n) distance from roads and (o) corresponding flood susceptibility. 57
4.11 Distance from streams map of Khartoum showing (p) distance from streams and (q) corresponding flood susceptibility. 59
4.12 Normalised Difference Vegetation Index map of Khartoum showing (r) NDVI and (s) corresponding flood susceptibility. 60
4.13 Flood Susceptibility Map 63
4.14 A graph showing ROC/AUC for Flood Susceptibility Map 67

List of Tables

2.1 Summary of major flood types, causes, and impacts in Africa (2019–2024). . . 12
2.2 Description of factors used in flood susceptibility modelling. 15

3.1 Soil texture classification and corresponding scientific descriptions for sampled sites in Khartoum. 35
3.2 Table A (excerpt): Aggregated pairwise comparison (illustrative) 37
3.3 Flood Causative Criteria, Classification, and Assigned Weights 40

4.1 Elevation ranges and corresponding flood susceptibility classes. 45
4.2 Slope classification and corresponding flood susceptibility levels. 47
4.3 Topographic Wetness Index (TWI) classification and corresponding flood susceptibility levels. 48
4.4 Rainfall classification and corresponding flood susceptibility levels. 50
4.5 Error matrix and classification accuracy statistics for the Random Forest land cover classification. The table presents user's accuracy (UA), producer's accuracy (PA), overall accuracy (OA), Kappa coefficient (KP), and average sensitivity/specificity values for each class. 52
4.6 Land Use and Land Cover (LULC) classification results showing the spatial distribution and percentage area coverage for each class. 53
4.7 Soil types, area coverage, and flood susceptibility classification. 55
4.8 Drainage density classification and corresponding flood susceptibility levels within the study area. Higher drainage density values generally indicate regions with greater surface run-off potential and, consequently, higher flood susceptibility. 56
4.9 Distance from road and corresponding flood susceptibility levels. Areas located closer to roads exhibit higher flood susceptibility due to increased surface runoff and reduced infiltration capacity. 57
4.10 Distance from Streams and Corresponding Susceptibility Levels 58
4.11 NDVI Values and Corresponding Susceptibility Levels 59
4.12 Decision Hierarchy for Flood Susceptibility Modelling 61
4.13 Final Ranking and Priority of Factors for Flood Susceptibility Modelling 62
4.14 Pairwise Comparison Matrix for Flood Susceptibility Factors (AHP) 62

4.15 Sensitivity Analysis for Flood Susceptibility Modelling 66

LIST OF ABBREVIATIONS

Abbreviation	Meaning
AHP	Analytical Hierarchy Process
ANN	Artificial Neural Network
AUC	Area Under the Curve
BN	Blue Nile
CR	Consistency Ratio
DEM	Digital Elevation Model
FAO	Food and Agricultural Organization
FHI	Flood Hazard Index
FR	Frequency Ratio
FSI	Flood Susceptibility Index
G-AHP	Geo-Analytical Hierarchy Process
GEE	Google Earth Engine
GIS	Geographic Information System
LM	Levenberg-Marquardt
LULC	Land Use and Land Cover
MCDM	Multi-Criteria Decision Making
NDVI	Normalized Difference Vegetation Index
NIR	Near-Infrared
OA	Overall Accuracy
OAT	One-at-a-time
PA	Producer Accuracy
ROC	Receiver Operating Characteristic
RF	Random Forest
RS	Remote Sensing
SPI	Stream Power Index
SPSS	Statistical Package for the Social Science
SRTM	Shuttle Radar Topography Mission
SVM	Support Vector Machine
TOPSIS	Technique for Order of Preference by Similarity to Ideal Solution
TWI	Topographic Wetness Index
WHO	World Health Organization
WN	White Nile
WoE	Weight of Evidence
UA	User's Accuracy
USGS	United States Geological Survey

Chapter 1

Introduction

1.1 Background

An overview of flood susceptibility is provided in the introductory chapter. It discusses the identified research problem and presents the purpose and objectives of the study. It describes the study area and the general methodology employed.

1.1.1 Climate Change and Global Flood Risk

Flooding is one of the most destructive natural hazards worldwide, and climate change has intensified both its frequency and severity. Between 2000 and 2019, floods affected over 1.6 billion people globally, causing thousands of fatalities annually and economic losses exceeding USD 650 billion (UNDRR, 2020). In many regions, extreme rainfall events have increased by up to 20 % in the past two decades, contributing to more frequent flash floods and riverine inundations (Ritchie and Roser, 2019; Copernicus, 2020)

In sub-Saharan Africa, projections indicate that extreme precipitation events may increase by 5–20% by 2050 due to anthropogenic climate change (Reuters, 2024). This heightened rainfall intensity is likely to exacerbate flood hazards, particularly in areas where drainage infrastructure is limited and socio-economic resilience is low.

1.1.2 Socio-Economic Vulnerability in Africa and Sudan

Although flooding is a global phenomenon, Africa experiences disproportionate impacts due to socio-economic vulnerabilities, inadequate infrastructure, and limited access to disaster management resources, particularly in rural areas (Bang et al., 2018). The consequences extend beyond immediate loss of life and property to long-term challenges, including outbreaks of waterborne diseases, prolonged food insecurity, and economic decline, which can trap affected populations in cycles of vulnerability.

In Sudan, these vulnerabilities are intensified by political instability, rapid urban growth, and underdeveloped drainage systems. Urban areas such as Khartoum are particularly exposed to high-intensity rainfall events, where poor storm water management exacerbates the impacts of flooding.

1.1.3 Hydrological and Environmental Impacts in Sudan

Sudan encompasses diverse environmental zones, from hyper-arid deserts in the north to semi-arid savannahs in the south, with elevations ranging from 300m to over 1300m above sea level. Its hydrological regime is dominated by the Nile River and its tributaries, which combined with seasonal heavy rainfall, are primary drivers of flooding. Flash floods-sudden, high-intensity events-have become increasingly common in Khartoum and other urban centers. For instance, during the 2013 flash floods, Khartoum accounted for 37% of all flood-affected populations nationwide, displacing over 300,000 people and destroying more than 25000 homes (UNOCHA, 2013; Mohammed et al., 2017). Between 207 and 2021, an average of 388,600 people were affected annually by flooding in Sudan. Major events include:

- 2013 – 300,000 affected, 25,000 homes destroyed (UNOCHA, 2013).
- 2018 – 222,275 affected, 19,640 homes damaged or destroyed (OCHA, 2018).
- 2019 – Damage to 1,263 schools, 37 health facilities, and 10 water facilities, with thousands displaced (OCHA, 2019).
- 2020 – Record-breaking Nile levels not seen in nearly a century; 3 million people affected, 100,000+ homes destroyed, and economic losses of approximately USD 4.43 billion (UNDRR, 2020).
- 2022 – 314,500 affected; Nile level peaked at 16.42 m, nearing the 16.5 m danger mark UNDRR (2020); OCHA (2022).

Climate variability, combined with anthropogenic factors such as urban expansion and land-use change, has intensified these risks. Projections suggest that by 2050, annual flood disasters in

Khartoum could exceed current levels of devastation, posing severe threats to livelihoods and infrastructure (UNU, 2004; Abdel Hamid et al., 2020).

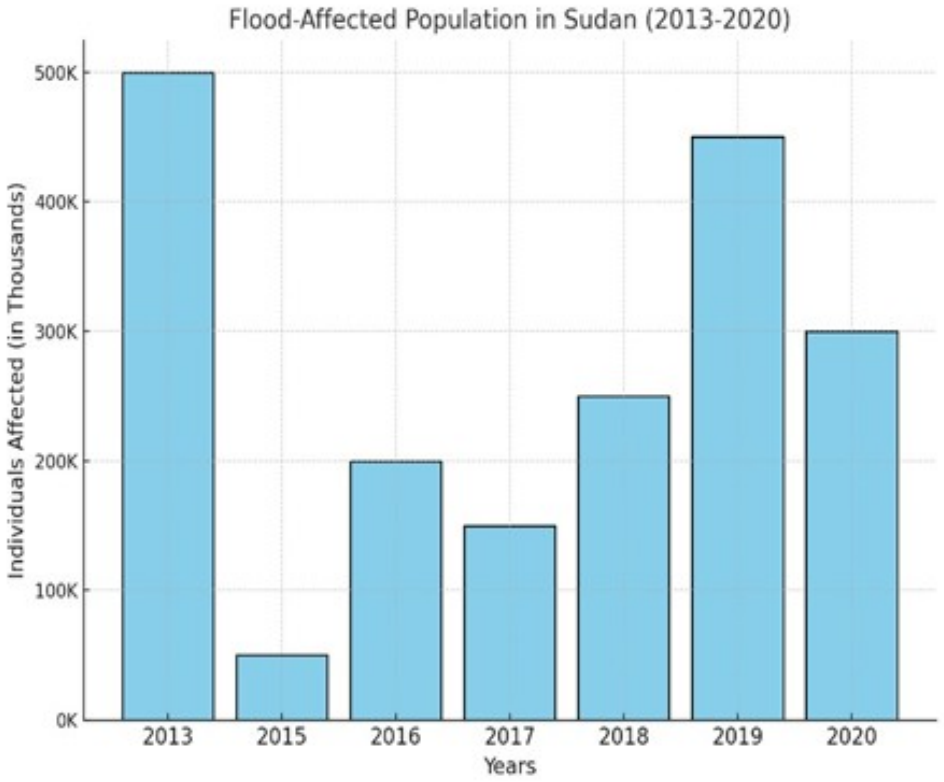

Figure 1.1: "Flood-Affected Population in Sudan (2013–2020)." Data Source: Sudan Meteorological Authority (SMA) and UN Office for the Coordination of Humanitarian Affairs (OCHA, 2020).

1.2 Problem Statement

Flooding remains a critical global challenge, causing widespread loss of life, infrastructure damage, and ecosystem disruption, particularly in rapidly urbanizing regions (Tellman et al. (2021) and Wing et al. (2022)). Climate change has amplified flood risks through rising sea levels, intensified precipitation, and increased river discharge. In Africa, flooding is the most common natural disaster, and in Sudan—particularly in Khartoum—both flash floods and river floods cause significant annual damage (OCHA, 2019; Copernicus, 2020). Khartoum's rapid urban expansion over the past century, combined with deforestation and conversion of natural landscapes, has altered hydrological responses in the White Nile Basin, increasing peak discharges and flood frequency. These effects are worsened by inadequate drainage

infrastructure and poor urban planning, leaving the city's growing population more exposed to disasters.

Data and Planning Limitations Flood risk assessment in Sudan is hindered by fragmented and inconsistent datasets, often lacking the spatial and temporal resolution needed for accurate susceptibility mapping. Existing studies frequently rely on isolated inputs such as topography, rainfall, or land use without integrating these datasets to capture their combined effects. For example, rainfall–run-off models (Nourani and Gichamo, 2021) and hydrological-only approaches (Elagib et al., 2021) applied in Sudan have generated valuable insights but could not incorporate socio-economic variables, multi-hazard interactions, or high-resolution spatial analysis, limiting their planning utility.

Many Sudanese flood studies employ conventional Analytic Hierarchy Process (AHP) or GIS-only approaches (Ibrahim et al., 2021; Sulieman et al., 2024). While effective for basic mapping, these methods do not fully integrate expert judgment with geospatial analysis or account for the relative weighting of diverse flood-contributing factors. There is a lack of integrated flood susceptibility models in Sudan that combine high-resolution geospatial data, expert judgment, and empirical validation. The three key weaknesses in existing studies are:

- Data fragmentation – reliance on isolated datasets without integration.
- Poor spatial resolution – coarse-scale mapping that cannot guide local planning.
- Lack of decision-making integration – limited capacity to incorporate expert judgment in weighting flood factors.

This study introduces a Geo-Analytic Hierarchy Process (G-AHP) framework tailored for Khartoum's flood susceptibility analysis. Unlike traditional AHP, G-AHP integrates spatial data processing within the weighting process, allowing for factor prioritization based on both quantitative geospatial evidence and qualitative expert input. By combining topography, rainfall, land use/land cover (LULC), drainage density, and river proximity with climate change projections and socio-economic indicators, this method produces empirically validated, high-resolution flood susceptibility maps. This integrated approach addresses existing methodological gaps and provides a scalable model for flood risk management in Sudan and other data-limited contexts.

1.3 Significance of the study

Floods pose a critical threat to water resource systems through exposure, vulnerability, and resilience factors. Understanding these concepts, combined with detailed spatial and environmental data, provides a foundation for identifying flood-prone areas and implementing targeted mitigation measures. While some studies have explored flood-related challenges in Khartoum, Sudan, While some studies have explored flood-related challenges in Khartoum, Sudan, such as Ibrahim et al. (2021) and Hamid et al. (2025), who assessed flood vulnerability using GIS and remote sensing, and Abdelkarim et al. (2020), who examined urban expansion and its influence on flood risk, the integration of advanced geospatial modelling techniques in flood susceptibility assessment remains limited.

Methodological Contribution:

By integrating the Geo-Analytical Hierarchy Process (G-AHP) with GIS and remote sensing, this research advances flood susceptibility modelling in semi-arid regions. Unlike traditional flood risk studies in Sudan that rely primarily on descriptive or hydrological assessments, the use of G-AHP introduces a structured, multi-criteria decision-making approach. This strengthens the scientific rigour of flood risk mapping and enhances applicability in similar data-scarce environments.

Empirical and Contextual Relevance:

Khartoum, located at the confluence of the Blue and White Nile, is highly exposed to recurrent flooding. Socio-economic vulnerabilities, such as informal settlements, rapid urban expansion and inadequate drainage infrastructure —exacerbate risk. By incorporating environmental (e.g., elevation, slope, soil type, and land use) and socio-economic indicators (e.g., population density, distance to roads, and settlement patterns), this study produces evidence-based maps that capture the interaction of natural and human-induced drivers of flood susceptibility.

Practical and Policy Impact:

The outputs of this study—spatially explicit flood susceptibility maps—serve as practical tools

for disaster risk reduction, urban planning, and climate adaptation. Local authorities, urban planners, and humanitarian agencies can use these findings to prioritize interventions, strengthen resilience, and allocate resources effectively. The study also aligns with Sudan's climate adaptation agenda and global frameworks such as the Sendai Framework for Disaster Risk Reduction.

1.4 Aim

The primary aim of this study is to evaluate the risk associated with flash floods in Khartoum, Sudan by integrating remote sensing and GIS techniques using a spatial index called AHP.

1.5 Objectives

Based on the aim, the specific objectives are to:

1. To develop the flood susceptibility model using multi-parametric approach of Geo Analytical Hierarchy Process (G-AHP).

2. To evaluate the robustness of the G-AHP model through sensitivity analysis.

3. To develop actionable flood risk maps that inform planning, flood management, and mitigation strategies.

1.6 Research Questions

1. What are the key environmental and socio-economic factors influencing flood susceptibility in Khartoum, Sudan?

2. Which parameter in the AHP model exhibits the highest sensitivity in Khartoum's flood susceptibility, and how does its variation impact on the overall model performance in this specific urban and environmental setting?

3. How can the flood risk index map, designed for Khartoum's unique hydrological, topographical, and socio-economic conditions, support decision-making for effective flood management and mitigation in the region?

1.7 Layout of Study

This research is organized into six interconnected chapters, each contributing uniquely to achieving the study's overall objectives. This research is organized into six interconnected chapters, each contributing uniquely to achieving the study's overall objectives.

- Chapter 1: Introduction This chapter lays the foundation for the study by providing the contextual background and justification for investigating flood susceptibility in Khartoum, Sudan. It outlines the research problems, objectives, and questions, establishing the study's significance. The chapter also introduces the methods and analytical approaches employed, serving as a roadmap for the subsequent sections of the study.
- Chapter 2: Literature Review This chapter explores previous research on flood susceptibility modelling and mapping, with an emphasis on the physical and environmental factors that affect flood susceptibility. It critically analyses the Analytical Hierarchy Process (AHP) and other multi-criteria decision-making methods, along with the use of GIS and remote sensing in flood risk assessment. The chapter highlights gaps in literature, especially concerning semi-arid urban areas like Khartoum, and provides a rationale for the chosen research methodology.
- Chapter 3: Methodology This chapter details the research design, data collection, materials and methods, and analytical framework. It explains the integration of AHP with geospatial tools to model flood susceptibility. The selection of parameters, preparing

spatial data, and the steps for model validation are described comprehensively, ensuring the study's applicability and rigour.

- Chapter 4: Data Analysis and Findings This chapter presents the results of the data analysis, including the generation of flood susceptibility maps. The findings are supported by socio-economic and environmental data to provide a comprehensive understanding of flood risks in the study area. The chapter also includes model validation results, highlighting the performance and reliability of the flood susceptibility model.

- Chapter 5: Discussion This chapter interprets the results in the context of Khartoum's unique physical, environmental, and socioeconomic conditions. The identified flood-prone zones are discussed in relation to the study's objectives and existing literature. The chapter emphasises the implications of the findings for urban planning, flood management, and disaster mitigation in semi-arid regions.

- Chapter 6: Conclusion and Recommendations The final chapter summarises the key findings, reflecting on the research questions and objectives. It highlights the study's contributions to the field of flood susceptibility modelling and its practical applications for Khartoum. The chapter concludes with recommendations for policymakers, urban planners, and researchers, and suggestions for future studies to address unresolved challenges.

Chapter 2

Literature Review

2.1 Introduction

Floods remain one of the most destructive natural hazards globally, causing extensive damage to live, infrastructure, and ecosystems. They arise from multiple drivers, including extreme rainfall, rapid urbanization, land degradation, and inadequate drainage systems, which amplify flood risk in both rural and urban settings (Kimura et al., 2023). In recent years, climate change has intensified the frequency and severity of flood events, particularly in semi-arid and urbanized regions where fragile hydrological systems and socio-economic vulnerability converge (Kundzewicz et al., 2019). Understanding flood susceptibility therefore requires not only an appreciation of environmental processes but also a critical integration of socio-economic, climatic, and anthropogenic factors.

To provide a comprehensive foundation, this chapter is organized into three interrelated parts. First, it reviews the types and causes of floods, emphasizing both natural and human-induced drivers (1). Second, it examines the key factors influencing flood susceptibility, such as rainfall variability, elevation, slope, land use/land cover, and socio-economic vulnerability (2). Third, it evaluates conventional and advanced flood modelling approaches, with a particular focus on the Analytical Hierarchy Process (AHP) and its geo-analytical extension (G-AHP), highlighting the integration of GIS and remote sensing technologies as critical tools for spatially explicit flood assessment (3).

By following this structure, the literature review bridges global flood challenges with the methodological framework adopted in this study. It demonstrates how existing scholarships have advanced the understanding of flood susceptibility while identifying knowledge gaps relevant to semi-arid and rapidly urbanizing contexts such as Khartoum. Ultimately, the review provides both a theoretical and methodological foundation for applying G-AHP in flood susceptibility mapping, ensuring a clear link between past research and the present study's contribution to disaster risk reduction.

2.2 Flooding: A Global and Regional Challenge

Floods are among the most frequent and damaging natural hazards worldwide, with wide-ranging consequences for human and ecological systems Merz et al. (2021). Their impacts vary depending on flood type, magnitude, geographic setting, and community vulnerability. While global literature provides insights into these dynamics, understanding their specific relevance to Khartoum requires careful evaluation of which consequences are most critical in a semi-arid, rapidly urbanizing context.

2.2.1 Economice Impacts

Economic damages from floods include destruction of infrastructure, housing, and agricultural production. Globally, annual flood losses exceed $50 billion (Liu et al., 2024), but African cities have disproportionately higher vulnerability due to weak planning systems. For instance, in Nigeria, Adelekan (2016) reported losses of over $500 million during the 2012 floods, primarily due to urban encroachment on floodplains. Similarly, in Sudan, the 2020 Nile floods displaced over 500,000 people, destroyed 100,000 homes, and caused direct losses estimated at $3.5 billion (Nations, 2020). For Khartoum, where informal settlements dominate peri-urban zones, economic losses are intensified by the destruction of unregulated housing and the disruption of trade corridors connecting the capital with other regions. These cases highlight the centrality of economic vulnerability in Sudan compared to high-income countries, where insurance mechanisms mitigate recovery costs.

2.2.2 Public Health and Displacement

Floods often trigger cascading public health crises. Waterborne diseases such as cholera and malaria outbreaks have been documented across East Africa following floods (Asiedu, 2020). In Sudan, the 2007 and 2013 floods were linked to spikes in diarrheal diseases and vector-borne illnesses, particularly in displacement camps (Babiker et al., 2014). Beyond health risks, forced displacement remains one of the most visible social impacts. For example, in Ethiopia, Teku (2025) noted that flood-induced resettlement disrupted education and livelihoods for thousands

of households in the Awash basin. In Khartoum, population displacement is recurrent due to inadequate drainage and emergency shelters, exacerbating urban poverty cycles. This indicates that public health and displacement challenges are especially pertinent for Khartoum's flood risk profile.

2.2.3 Environmental Degradation and Restoration

While floods can replenish groundwater, restore wetlands, and transport nutrients (Akhtar et al., 2022), their destructive potential often outweighs these benefits in urban settings. In the Sahel, increasing flood frequency has been linked to land degradation and desertification (Biasutti, 2019). In Khartoum, floods frequently erode riverbanks along the Nile, destroy vegetation cover, and accelerate siltation in irrigation canals, undermining agricultural productivity. Compared to rural floodplains, the city's semi-arid environment offers fewer ecological buffers, which intensifies the degradation of already fragile ecosystems.

2.2.4 Critical Synthesis

The literature shows consensus that floods generate economic loss, public health crises, and environmental change, but there is limited agreement on which of these dominate in African urban contexts. For Khartoum, evidence suggests that economic vulnerability and displacement are more pressing than ecological restoration potential, due to the city's urban density, weak infrastructure, and governance challenges. However, gaps remain: few studies integrate these dimensions holistically, and even fewer apply advanced geospatial or decision-analytic models (such as AHP or G-AHP) to evaluate relative impacts in Sudan.

2.3 Factors Influencing Flood Susceptibility

Flood susceptibility is shaped by a complex interaction between physical/environmental factors and socio-economic factors. Physical conditions such as rainfall, slope, soil, vegetation cover, drainage density, etc strongly affect flood occurrence, but their impacts are mediated by human

Table 2.1: Summary of major flood types, causes, and impacts in Africa (2019–2024).

Flood Type	**Primary Causes**	**Geographic Distribution**	**Key Consequences / Impacts**	**Relevant References (2019–2024)**
Flash Floods	Intense, short-duration rainfall; poor urban drainage; impermeable surfaces	Common in arid and semi-arid cities such as Khartoum (Sudan), Nairobi (Kenya), and Addis Ababa (Ethiopia)	Rapid inundation causing loss of life, road damage, and destruction of informal settlements	Abdallah Mohammed Elhassan (2022) ; OCHA (2022); Weldu Woldemariam and Edo Harka (2020)
Riverine Floods	River overflow due to prolonged rainfall, upstream catchment saturation	Along Blue and White Nile rivers and floodplains across Sudan and South Sudan	Damage to farmland, contamination of water sources, infrastructure losses	Eisa et al. (2022); Barnes et al. (2022)
Urban (Pluvial) Floods	Inadequate drainage infrastructure, rapid urbanization, unplanned settlements	Major cities in Sudan, Ethiopia, and Nigeria	Property damage, transport disruption, and economic losses	Abraham et al. (2023); Elkhatib et al. (2022)
Coastal Floods	Sea level rise, storm surges, and coastal erosion	Coastal areas in North Africa and East Africa, e.g., Alexandria (Egypt), Mombasa (Kenya)	Salinization of soils, displacement, loss of coastal infrastructure	Monteiro et al. (2022);Elfadaly et al. (2022)
Groundwater Flooding	Rising groundwater tables due to excessive rainfall or poor infiltration	Low-lying floodplains and clay-rich basins	Waterlogging of agricultural land, infrastructure weakening	Rahman et al. (2024); El-Magd et al. (2024)

dynamics, including settlement patterns, land tenure, and infrastructure provision. This section evaluates both domains to highlight their relevance to Khartoum and similar semi-arid urban environments.

2.3.1 Physical and Environmental Factors

Flood susceptibility is closely linked by hydrological and geomorphological variables, which determine the likelihood of water accumulation and runoff.

- • Rainfall intensity and variability: Intense prolonged rainfall remains the most direct driver of floods. In Khartoum, rainfall is highly seasonal, with most precipitation concentrated between July and September (Mahmood et al., 2017). This concentration creates conditions for flash flooding, especially when drainage infrastructure is inadequate. However, reliance on sparse rain gauge networks introduces uncertainty in rainfall estimates, and satellite-derived rainfall products can misrepresent semi-arid storm events (Gebrechorkos et al., 2020).
- • Slope and topography: Steeper slopes accelerate run-off and reduce infiltration, whereas flatter areas facilitate water accumulation. Yet, slope must be considered alongside Topographic Wetness Index (TWI), which integrates both slope and upstream contributing area. Over-reliance on slope alone may misclassifying rocky arid zones as low risk, while in Khartoum, flat urban expanses with poor drainage are actually high risk.
- • Soil type and lithology: Permeable sandy soils reduce run-off potential, while clay rich and loamy soils limit infiltration, creating conditions for surface flooding(Tehrany et al., 2019). Khartoum's mix of clay plains and sandy deposits results in heterogeneous infiltration dynamics, yet limited soil maps contain precision in susceptibility modelling.
- • Normalised Difference Vegetation Index (NDVI): Vegetation reduces flood risk by promoting infiltration and reducing run-off. However, NDVI has well documented limitations in semi-arid contexts, where sparse vegetation and dry-season spectral noise can distort flood-related interpretations (Kerebeh et al., 2024). Seasonal NDVI variability is particularly relevant in Khartoum, where vegetation cover fluctuates dramatically.

- • Curvature and drainage networks: Curvature influences the flood accumulation, with concave slopes often acting as run-off concentrators. Similarly, proximity to rivers is a strong conditioning factor. However, these variables may overlap with convergence index and drainage density, raising concerns of variable redundancy that can bias a model's outputs if not carefully managed. Curvature provides information on the form of the ground surface, which controls run-off and water accumulation on slopes. According to Duman et al. (2006), profile curvature is the curvature of a vertical plane relative to the direction of slope. It indicates the maximum slope's direction. According to Zaharia et al. (2017), positive values indicate regions that are less vulnerable to surface run-off, whereas negative values indicate the opposite.

- • Data limitations and correlation: Many of these variables are derived from Digital Elevation Models (DEM) and satellite imagery. DEM resolution directly influences slope, curvature, and drainage estimates, while correlated variables (e.g., slope and TWI) risk inflating their importance in multi-criteria or machine learning models (Habib et al., 2024).

2.3.2 Socio-Economic Factors

While physical characteristics explain where floods are likely to occur, socio-economic conditions determine who is most affected and to what extent. Population density and urbanisation: Khartoum has experienced rapid urban expansion, with informal settlements growing at an annual rate of 4–5% since 2010 (Abdallah Mohammed Elhassan, 2022). Many of these settlements are built on floodplains with inadequate drainage, amplifying exposure. Poverty and income disparities: More than 60% of Khartoum's residents live in informal housing without access to robust infrastructure (UN-Habitat, 2021). Low-income households often occupy the most flood-prone areas, lacking resources to rebuild or relocate after disasters. Infrastructure and land tenure: Poorly maintained drainage channels and unregulated land use contribute significantly to flood riskAbdallah Mohammed Elhassan (2022). Weak enforcement of zoning laws has allowed construction along riverbanks, where floods are most severe. Access to basic services: Limited access to clean water, sanitation, and healthcare magnifies the long-term

socio-economic effects of floods. Studies in Khartoum after the 2020 floods reported outbreaks of waterborne diseases, including cholera and dysentery, disproportionately affecting children (Organization, 2023). Integration with physical factors: Socio-economic vulnerability interacts with physical hazards. For example, the same rainfall event may cause minimal disruption in a well-drained urban area but catastrophic impacts in Khartoum's informal settlements. This highlights the need for integrated models that combine physical conditioning factors with socio-economic indicators.

Table 2.2: Description of factors used in flood susceptibility modelling.

Factor	**Source / Dataset**	**Resolution**	**Expected Flood Influence**	**Limitations / Notes**
Rainfall	CHIRPS v2 (2023)	0.05° (5 km)	High rainfall intensity increases runoff and flood potential	Temporal variation may not capture short-duration storms
Slope	SRTM DEM (30 m)	30 m	Gentle slopes (¡5°) allow pooling; steep slopes promote runoff	Correlated with TWI; redundancy possible
Elevation	SRTM DEM (30 m)	30 m	Low elevations near Nile floodplain prone to inundation	Elevation alone may not explain localized floods
Soil Type	FAO Soil Portal	1 km	Clay-rich areas increase runoff; loam enhances infiltration	Static dataset; may not reflect anthropogenic changes
NDVI	Sentinel-2 (10 m)	10 m	Low NDVI = less vegetation = high runoff	Semi-arid NDVI affected by dry-season reflectance noise
TWI	Derived from DEM	30 m	Indicates moisture retention and surface saturation	Sensitive to DEM quality and slope calculation
Drainage Density	Derived from HydroSHEDS	15–30 m	High drainage density facilitates runoff	May overlap conceptually with distance to streams
Urbanization	Sentinel-2 & Population Data (WorldPop)	10–100 m	Built-up areas reduce infiltration and increase surface runoff	Data may underestimate informal settlements
Poverty / Infrastructure	UN-Habitat / World Bank	District level	Low-income zones have reduced resilience to floods	Socioeconomic data resolution lower than physical layers

2.3.3 Conventional Methods for Flood Modelling

Flood modelling has traditionally relied on statistical and empirical approaches to estimate flood risks and delineate floodplain boundaries. While these methods remain foundational, their shortcomings have prompted the transition to more advanced geospatial and multi-criteria techniques. This section critically examines conventional methods, highlighting their strengths and limitations, and situates these within both global and African contexts to provide a clearer rationale for adopting more robust models such as AHP and G-AHP.

- Statistical Approach: Statistical methods typically use long-term flood records to establish flood frequency and intensity relationships. For instance, flood frequency analysis employs distributions such as Log-Pearson type III, Gumbel, and Weibull to calculate return periods like the 100-year flood, which inform floodplain zoning and design standards(Ahmed et al., 2023) . Regression models have also been used to relate flood magnitude to drivers such as rainfall and catchment size (Zhou et al., 2021)).

  However, these methods assume that historical records adequately represent future risk, which is increasingly problematic under climate variability. In practice, rainfall–runoff mismatches have been documented in East African catchments, where models calibrated on historical hydrology failed to predict recent flash flood intensities (Kiptum et al., 2023). This illustrates the difficulty of applying methods that presuppose stationarity in rapidly changing climatic and land use contexts.

  Bivariate statistical models—such as the Frequency Ratio (FR), Weights of Evidence (WoE), and Statistical Index (SI) are among the most widely used for flash flood susceptibility (Tehrany et al., 2014; Khosravi et al., 2016; Rahmati et al., 2016). While computationally simple, their limitations are notable. First, they assume independence among conditioning factors, which is unrealistic because variables such as slope and Topographic Wetness Index (TWI) are strongly correlated. This can inflate their predictive importance and distort susceptibility mapping. Second, they rely heavily on the spatial overlap between past flood events and conditioning factors. In heterogeneous catchments such as those in Nigeria and Ethiopia, FR-based models have underperformed because localized variability in rainfall and runoff breaks the assumption of uniform conditioning-factor relationships Wubalem et al. (2020). These issues underscore the risk of over-reliance on

historical event data in regions with limited or inconsistent hydrological records.

Table: Comparison of selected statistical models for flood susceptibility mapping
Source: Adapted from (Rahmati et al., 2016; Tehrany et al., 2014)

Model	**Strengths**	**Weaknesses**
Frequency Ratio (FR)	Simple, intuitive, widely applied	Assumes independence; sensitive to event sampling; underperforms in heterogeneous domains
Weights of Evidence (WoE)	Incorporates Bayesian framework; accounts for positive/negative relationships	Requires large datasets; vulnerable to sparse event data; assumes conditional independence
Statistical Index (SI)	Easy to compute; provides weighted ranking of factors	Oversimplifies interactions; risk of over-fitting; limited transferability across regions

- GIS-integrated hydraulic modelling approach:

  Hec-RAS (Hydrologic Engineering Center's River Analysis System) is primarily a hydraulic model, not an empirical one. It simulates steady or unsteady river flow, water-surface profiles, and floodplain inundation (Brunner, 2021). When coupled with Geographic Information Systems (GIS)—for instance, using HEC-GeoRAS or RAS Mapper—the model provides powerful spatial visualization and flood-extent mapping capabilities(Tehrany et al., 2019; Brunner, 2021). In Sudan, for example, reliance on rainfall–runoff coefficients have often underestimated urban flash floods because these methods fail to account for informal settlements and drainage blockages(Elagib et al., 2021).

- From Conventional to Multi-Criteria Approaches:

  While conventional statistical and empirical models have provided valuable foundations, their inability to fully capture variable interactions, account for non-stationary climate conditions, or adapt to data-poor environments constrain their effectiveness in semi-arid, rapidly urbanizing regions. These limitations provide a strong rationale for adopting multi-criteria decision analysis techniques such as AHP and its geospatial extension G-AHP. Unlike bivariate or purely statistical models, AHP/G-AHP integrates multiple interdependent factors, accommodates both qualitative and quantitative datasets, and enhances spatial flexibility—making it particularly suitable for complex contexts like Khartoum.

2.4 Advanced Methods for Flood Modelling

2.4.1 Advanced Techniques for Flood Modelling

To overcome the limitations of traditional flood modelling, advanced techniques such as Geographic Information Systems (GIS), remote sensing, machine learning (ML), and Multi-Criteria Decision Analysis (MCDA) have been widely adopted. These methods enhance accuracy, flexibility, and predictive capability, particularly in data-scarce regions.

2.4.2 GIS and Remote Sensing

GIS and remote sensing have revolutionized flood risk assessment by integrating diverse datasets, including digital elevation models (DEMs), land use/land cover (LULC), and hydrological features (Bhuiyan and Al-Baky, 2014). GIS facilitates spatial analysis, enabling flood susceptibility mapping through overlay and interpolation techniques. Remote sensing provides real-time and historical data on precipitation, surface water levels, and land cover changes, with satellite imagery from Sentinel-2 and Landsat playing a critical role in flood delineation (Rahman et al., 2024). Synthetic Aperture Radar (SAR) is valuable for detecting floods under cloudy conditions. Hydrodynamic Modelling Advanced hydrodynamic models, such as MIKE 21 and HEC-RAS 2D, simulate water movement across floodplains with high precision. These models account for terrain interactions, water flow dynamics, and environmental conditions, making them suitable for complex urban and riverine flooding scenarios (Brunner, 2021).

2.4.3 Machine Learning (ML) and Artificial Intelligence (AI)

Machine learning techniques provide a data-driven approach to flood modelling by identifying patterns in large datasets. Supervised learning methods, including Random Forest (RF), Support Vector Machines (SVM), and Artificial Neural Networks (ANNs), are widely used for flood susceptibility prediction (Tehrany et al., 2019). Unsupervised clustering methods, such as K-means, categorize flood-prone areas based on environmental variables. Hybrid models, which

integrate ML with hydrodynamic simulations, further enhance predictive capabilities (Chen et al., 2020). ML is particularly beneficial in areas with limited observational data, as it can infer relationships from remote sensing-derived variables (Goh and Tan, 2018).

2.4.4 Multi-Criteria Decision Analysis (MCDA)

MCDA combines physical, socio-economic, and environmental factors to assess flood vulnerability. Techniques such as the Analytic Hierarchy Process (AHP) and Weighted Overlay Analysis (WOA) integrate expert judgment with spatial data to generate flood susceptibility maps (Jha et al., 2012). These approaches allow for systematic evaluation of risk factors and support informed decision-making for flood mitigation (Khosravi et al., 2016).

2.4.5 Applications of Modelling Approaches

GIS and remote sensing were utilized to develop flood susceptibility maps in the Brahmaputra Basin, Bangladesh. Researchers integrated DEMs, rainfall data, and LULC to predict high-risk zones, aiding disaster preparedness and policymaking (Rahman et al., 2019). ML models, particularly RF and ANN, have been employed to predict flash floods in urban areas, such as Houston, Texas, United States. These models integrate real-time precipitation, land use, and drainage data to enhance early warning systems (Fang et al., 2020).

The objective is to identify the most suitable set of conditioning variables for modelling assessments. For example, the FURIA-GA method was combined with the Logit Boost, Bagging and AdaBoost ensemble algorithms to develop a predictive model Bui et al. (2019). The results indicate that FURIA-GA-Bagging achieved the highest accuracy (93.37%), outperforming FURIA-GA-Logit Boost (92.35%) and FURIA-GA-AdaBoost (89.03%). Figure 2.5a illustrates the flash flood susceptibility map generated using the FURIA-GA-Bagging approach.

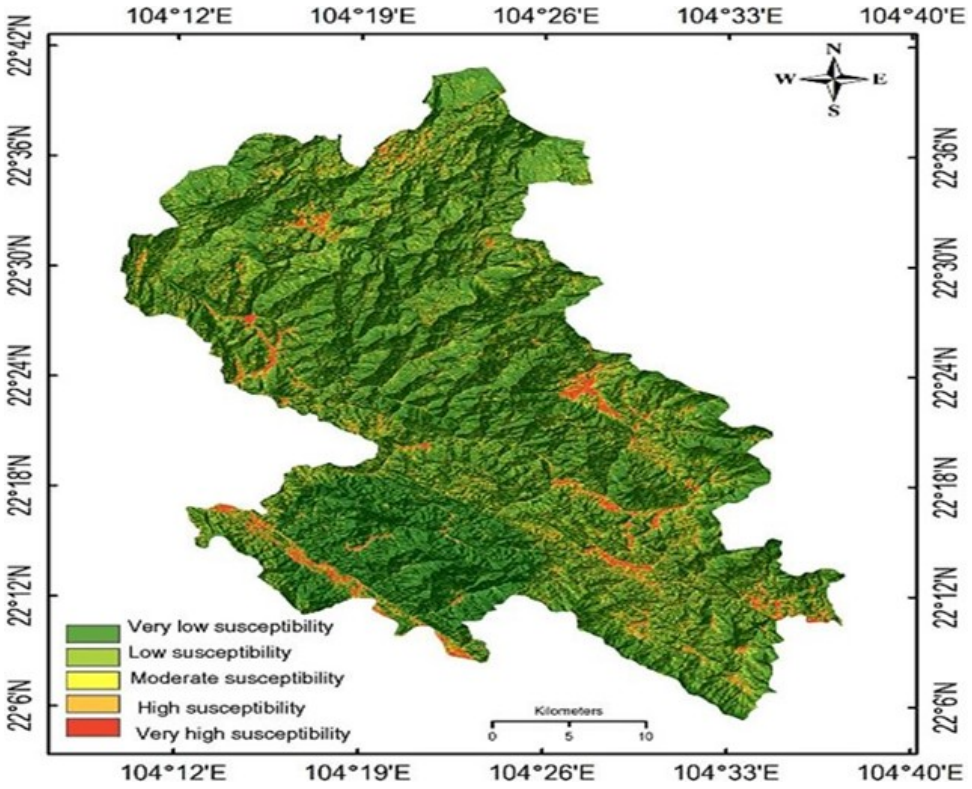

Figure 2.1: Flash Flood susceptibility mapping developed by using FURIA-GA-Bagging method

Elkhrachy (2015) conducted a study using SPOT satellite imagery and SRTM-DEM data to identify flash flood prone areas in Najran City, Saudi Arabia. The study applied the Analytical Hierarchical Process (AHP) to assess the weight of various flood-causing factors. This method produced a composite Flood Hazard Index (FHI), with the results obtained by overlaying the FHI map onto the zone boundary layer. Similarly,Ngo et al. (2018) analysed flash floods in Bac Ha and Bao Yen districts, Vietnam, using machine learning techniques such as the Fire-fly Algorithm (FA), Levenberg-Marquardt (LM) Backpropagation, an artificial neural network (FA-LM-ANN), LM-ANN, FA-ANN, support vector machine (SVM), and classification tree (CT). They identified 654 flash flood locations to assess the effectiveness of their flood mod-elling approach. The study incorporated 12 flood-related factors, including aspect, elevation, stream power index (SPI), slope, topographic wetness index (TWI), stream density, rainfall, curvature, normalized difference vegetation index (NDVI), lithology, topographic shading, and soil type. The results showed that the FA-LM-ANN model achieved the highest accuracy (97.0%), followed by LM-ANN (92.6%), FA-ANN (91.9%), SVM (92.9%), and CT (90.8%). Figure illustrates the flash flood susceptibility map developed using the FA-LM-ANN method.

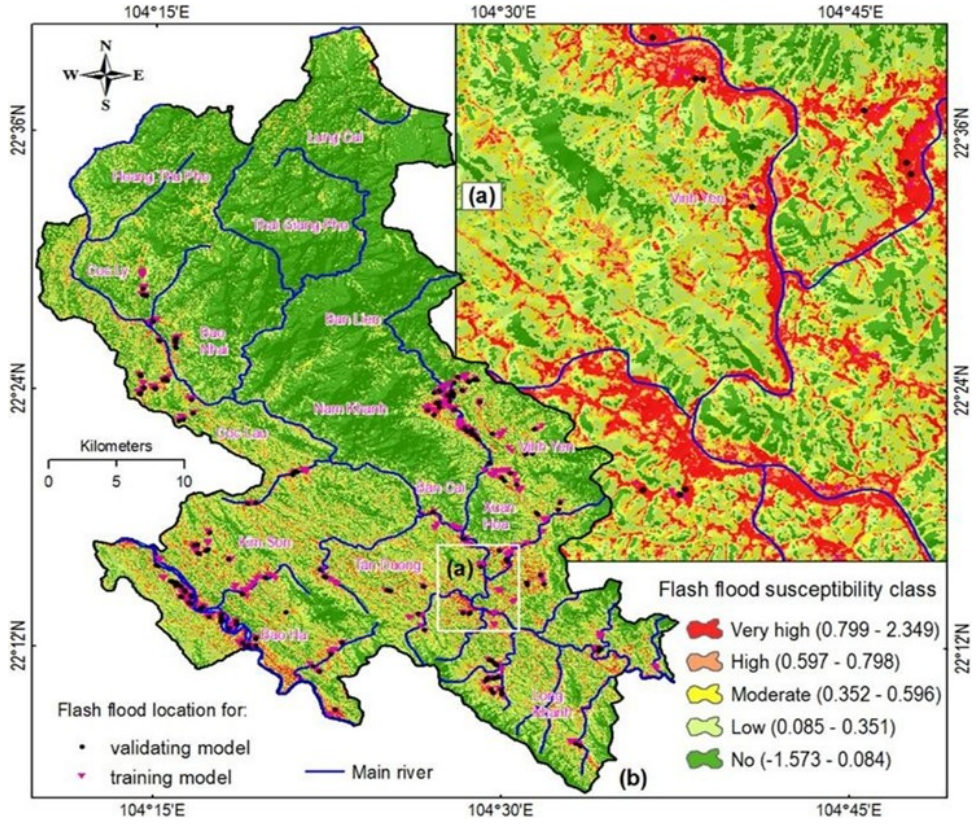

Figure 2.2: Flash flood susceptibility mapping developed by using FA-LM-ANN method

Khosravi et al. (2016), identified 211 flood-prone locations and analysed 10 conditioning factors influencing flash floods. These factors included curvature, stream power index (SPI), land use, geology, proximity to rivers, topographic wetness index (TWI), rainfall, slope angle, altitude, and normalized difference vegetation index (NDVI). The study findings indicate that the statistical index model achieved the highest prediction accuracy at 98.72%, followed by the weighting factor model at 97.6% and Shannon's entropy model at 92.42%.

2.4.6 Regional Focus on Sudan

In Ethiopia and Sudan, flooding is a recurring challenge, and the use of GIS, remote sensing, and MCDA have been applied to map flood-prone areas. For example, GIS and Remote Sensing: Sentinel-2 imagery and DEMs have been used to delineate flood zones and assess the impact of land use changes on flood risks in the Nile Basin (Tamiru and Dinka, 2021).

Factors such as slope, drainage density, soil type, and proximity to rivers were integrated using AHP to produce flood risk maps for Khartoum. This approach has provided valuable insights

into areas requiring improved drainage infrastructure. Emerging studies in Sudan have explored the use of machine learning methods such as Random Forest to predict flood susceptibility by leveraging the limited but available environmental data (Ibrahim et al., 2023).

Youssef and Hegab (2019) applied the Analytical Hierarchy Process (AHP), a qualitative approach, to assess its effectiveness and reliability in flood susceptibility analysis. The study was conducted in Ras Gharib, Egypt, using high-resolution images captured after the 2016 flood events. These images were used to confirm the susceptibility model by integrating a slicing technique with historical flood data. The researcher considered seven flood-related factors: distance from streams, slope, curvature, lithological units, angle, elevation, and topographic wetness index (TWI). The results showed that AHP proved an impressive performance in predicting flash flood susceptibility, achieving an accuracy of 83.3%. Figure presents the flood susceptibility map generated using the AHP method.

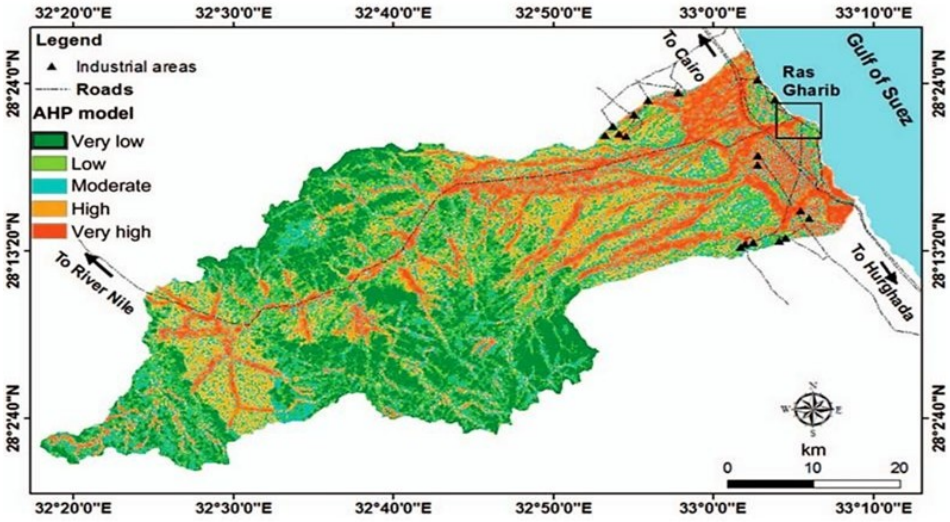

Figure 2.3: Flood susceptibility mapping developed using AHP method

Despite significant advancements this includes , several limitations persist in flood modelling:

• Limited Data Availability: Developing countries, including Sudan, often lack high-quality, consistent hydrological and meteorological data, which hinders the accuracy of models.

• Integration of Socio-Economic Factors: While physical factors are well-represented in flood modelling, socioeconomic variables such as population density, land use practices, and economic vulnerability are often under-represented.

• Climate Change Impacts: Many models fail to account for the dynamic impacts of climate change, such as altered rainfall patterns and rising sea levels, which are critical for long-term flood risk assessments (Kundzewicz et al., 2019).

• Interdisciplinary Approaches: There is a lack of integration between hydrological, ecological, and socio-economic data, which limits the holistic assessment of flood risks.

• Validation Issues: Many flood models lack sufficient validation due to limited post-event data, leading to uncertainties in the accuracy and reliability of predictions.

Advanced flood modelling approaches, including GIS, remote sensing, MCDA, and machine learning, have greatly enhanced the ability to predict and mitigate flood risks. Global and regional applications demonstrate their effectiveness, but significant research gaps remain, particularly in data-scarce regions like Sudan. Addressing these gaps through interdisciplinary approaches, improved data collection, and integration of climate change impacts is essential for building more resilient communities against floods.

This chapter has comprehensively reviewed the factors influencing flood susceptibility, conventional and advanced methods of flood modelling, and their applications across global and regional contexts, specifically focusing on Sudan. The review highlighted the strengths and limitations of traditional approaches, underscoring the growing role of advanced techniques such as GIS, remote sensing, multi-criteria decision-making, and machine learning in addressing the complexities of flood risk assessment.

Despite significant progress in flood modelling, several research gaps remain, including limited data availability, insufficient integration of socio-economic factors, and challenges in addressing the dynamic impacts of climate change. These gaps emphasize the need for robust and interdisciplinary methodologies to improve the accuracy and reliability of flood risk assessments.

Building on this foundation, the next chapter will detail the methodology adopted for this study, including data sources, analytical techniques, and integrating of physical and environmental factors to develop a comprehensive flood susceptibility model tailored to the study area.

Chapter 3

Materials and Methods

3.1 Introduction

This chapter outlines the research design and methodologies adopted to achieve the objectives of this study on flood susceptibility modelling in Khartoum, Sudan. It details the processes involved in data collection, preparation, and analysis, emphasizing the integration of physical and socio-economic factors using advanced geospatial techniques. The chapter also describes the application of the Geo-Analytical Hierarchy Process (G-AHP) and other multi-criteria decision-making tools in developing a flood susceptibility model. It discusses the methods used for model validation and highlights the rationale behind the selected approaches, ensuring alignment with the study's aim and research questions.

3.2 Study Area

Khartoum, the capital of Sudan, is located at the confluence of the White Nile (WN) and Blue Nile (BN), which merge north of the city to form the Main Nile. This strategic location makes Khartoum particularly sensitive to hydrological dynamics, as flood peaks in either river system can converge and amplify downstream flooding. Historically, the Blue Nile—fed by intense rainfall in the Ethiopian highlands—has contributed the largest share of annual flood events, while the White Nile's steady base flow shapes the persistence of high-water levels during prolonged rainy periods (Observatory, 2020).

Topography and Elevation. The city lies at an average elevation of approximately 385 m above sea level. While this may suggest some degree of natural drainage, the terrain is predominantly flat. Flat surfaces hinder rapid run-off, prolonging water stagnation during heavy rainfall and reducing the natural drainage gradient into the Nile. This geomorphology exacerbates flood susceptibility, particularly in low-lying districts adjacent to the riverbanks (El-Aziz et al., 2020; Ibrahim et al., 2023).

Climate: Khartoum is situated within a semi-arid savanna climate zone characterized by long, hot summers and short, mild winters. Annual rainfall averages 175 mm, with precipitation concentrated between July and September. These seasonal downpours, though limited in volume compared to equatorial regions, often exceed the absorptive capacity of the city's heavily urbanized landscape. Moreover, climate variability in the Nile Basin, such as the 2020 extreme flood event when river levels reached 17.14 m, highlights the growing unpredictability of flood hazards (on Climate Change , UNFCCC; Observatory, 2020).

Urbaniation and Land Use: The Greater Khartoum metropolitan area now accommodates over six million inhabitants across Khartoum city, Omdurman, and Khartoum North. Urban expansion has replaced floodplains with impervious surfaces—roads, buildings, and industrial zones—thereby reducing infiltration and increasing run-off. Informal settlements, often established in unplanned, low-lying areas near riverbanks or poorly drained land, are particularly vulnerable. These communities typically lack formal drainage infrastructure, leaving households disproportionately exposed to inundation. A land use profile indicates that residential areas dominate urban land cover, followed by informal settlements and expanding industrial corridors along the Nile banks, all of which intensify exposure to flood hazards (, CIMAF; Hamid et al., 2025)

Hydrological Context: The interaction of the Blue and White Nile plays a central role in Khartoum's flood dynamics. While the Blue Nile delivers high seasonal peaks from the Ethiopian highlands, the White Nile maintains relatively stable flow from the Great Lakes region. Their confluence in Khartoum creates a compound risk scenario: simultaneous peaks or sustained elevated flows can overwhelm natural floodplains and artificial embankments, particularly in the city's northern districts (Nile Basin Initiative, 2024).

Vulnerability Profile: Rapid urbanization, coupled with inadequate infrastructure, magnifies vulnerability. Informal settlements concentrated in eastern Khartoum and Omdurman face recurrent flood exposure due to weak housing structures and limited access to relief services. The inadequacy of storm water drainage and flood protection works has repeatedly been revealed during extreme events, including the 2020 flood, which displaced thousands and caused widespread damage to critical infrastructure (, CIMAF; UNOSAT, 2025; Hamid et al., 2025).

To provide a spatial reference, Figure is presented here rather than later in the chapter. The map

includes river networks, elevation bands, and built-up zones, visually demonstrating Khartoum's physical setting and its exposure pathways to flooding.

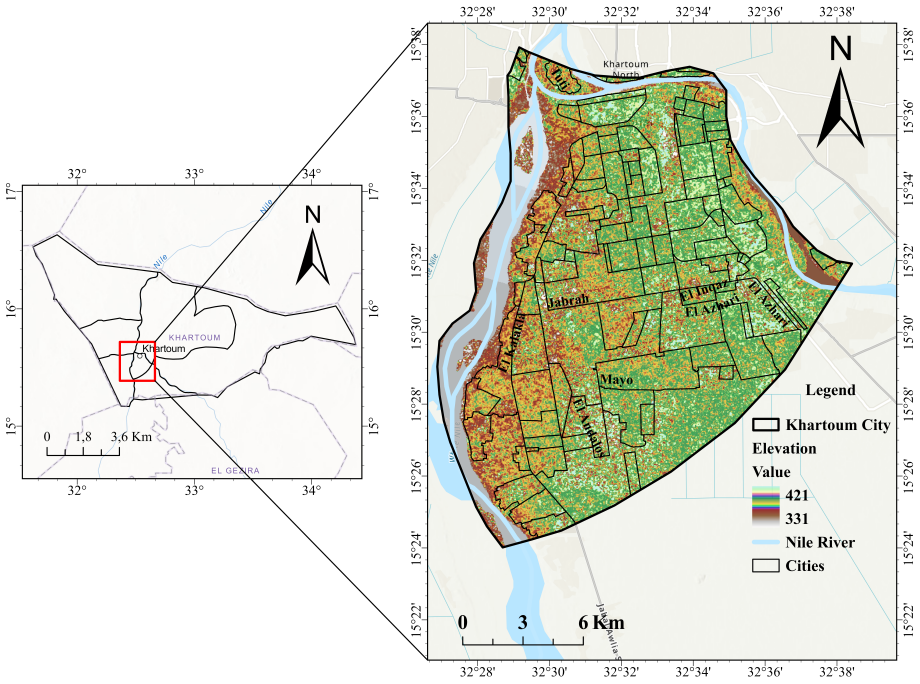

Figure 3.1: Map showing the study area (Khartoum, Sudan).

3.3 Materials

3.3.1 Datasets

The datasets used in this study encompass a range of physical, environmental, and socio-economic factors essential for flood susceptibility modelling in Khartoum. Table 3.1 provides a structured summary of all datasets, including their sources, resolutions, formats, and acquisition dates. This improves transparency and facilitates comparison of the input layers.

3.3.2 Tools and Software

This study utilized a combination of advanced Geographic Information System (GIS) tools and remote sensing platforms to process and analyse datasets for flood susceptibility modelling. ArcGIS Pro (Esri, 2021) was specifically employed for hydrological modelling and spatial ana-

lysis, including the generation of slope, flow accumulation, and drainage density layers using its Hydrology toolset. It was also applied for raster reclassification through the Raster Calculator, enabling the standardization of variables for weighted overlay, and for producing final susceptibility maps through its cartographic and visualization functions. Google Earth Engine (Gorelick et al., 2017) was used primarily for image preprocessing and remote sensing analysis, including the computation of vegetation indices such as the Normalized Difference Vegetation Index (NDVI) and Normalized Difference Moisture Index (NDMI), where threshold-based classification methods were applied to differentiate vegetation conditions. Python, with the ArcPy library (Esri, 2020) , facilitated the automation of repetitive tasks such as batch reclassification of input variables, zonal statistics, and integration of multiple raster datasets, thereby improving efficiency and reducing manual error. For validation, a combination of statistical and geospatial tools was employed. Receiver Operating Characteristic (ROC) curve analysis and the Area Under the Curve (AUC) (Fawcett, 2006) were calculated to evaluate predictive performance, while confusion matrix tools were used to assess classification accuracy (Congalton and Green, 2019). The integration of these tools ensured methodological transparency, reproducibility, and robustness in the flood susceptibility modelling process

3.3.3 Data Pre-Processing

The pre-processing of datasets involved several critical steps to ensure consistency, reliability, and compatibility across different data sources. All spatial layers were georeferenced to the WGS 84/UTM Zone 36N projection and resampled to a 30 m spatial resolution using bilinear interpolation for continuous rasters (elevation, slope, NDVI) and nearest-neighbour resampling for categorical data (LULC, soil type), ensuring spatial harmonization across datasets (Tehrany et al., 2019). To clarify the workflow, Figure 3.X presents a schematic diagram of the preprocessing pipeline, beginning with data acquisition, followed by error removal, resampling, reclassification, normalization, and final integration into the Analytical Hierarchy Process (AHP). This flowchart highlights the interdependencies between raster and vector layers, such as the derivation of slope and drainage density from the DEM, and the calculation of proximity buffers for rivers and roads. Reclassification was performed to transform continuous variables into discrete susceptibility classes. A five-class scheme (very low, low, moderate, high, very high) was adopted following similar flood susceptibility studies (Rahmati et al., 2016; Khosravi et al.,

2016), which demonstrated that five categories provide a balanced trade-off between detail and interpretability. Threshold values were determined using a combination of natural breaks (Jenks optimization) for terrain-related variables (slope, elevation, TWI) and literature-based expert judgment for thematic datasets such as soil type and LULC (Asiedu, 2020). For example, clay soils were classified as highly susceptible due to their low infiltration capacity, while vegetated areas were assigned lower susceptibility. Normalization was applied to standardize all factors onto a common scale prior to multi-criteria integration. A linear min–max scaling approach was used, transforming values into a range between 1 (lowest susceptibility) and 5 (highest susceptibility). This ensured comparability between heterogeneous datasets, such as rainfall intensity and distance-to-river layers and avoided biases from differing measurement units (Chen et al., 2020). Through these steps, the processed datasets were harmonized, reclassified, and normalized, creating a consistent analytical framework suitable for AHP-based flood susceptibility modelling.

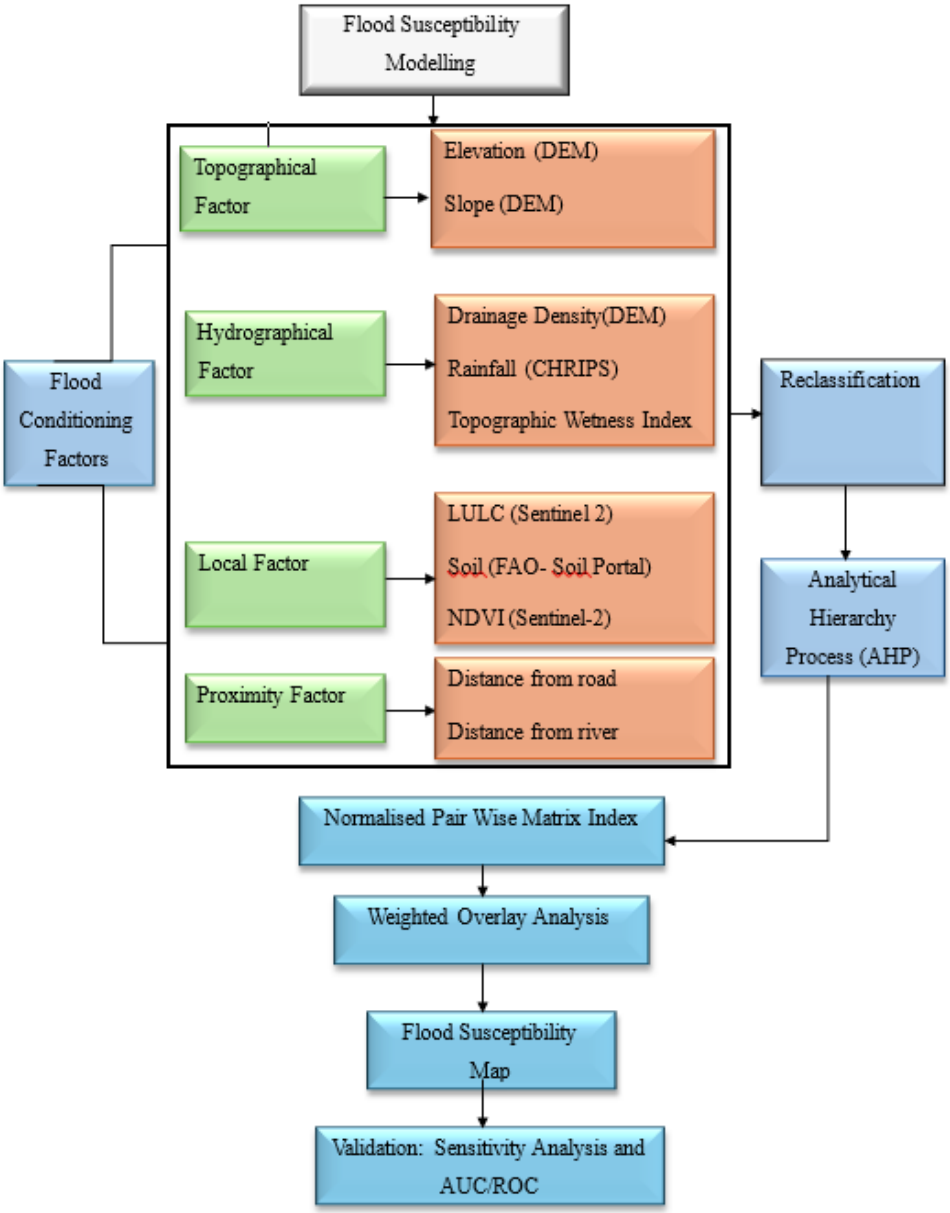

Figure 3.2: Work dlow of Flood Susceptibility Modelling using GIS and Remote Sensing techniques.

3.4 Methods

The current study's approach is summarized in the figure in Fig. The primary purpose of this work designated flood-prone regions utilizing the GIS technologies, SRTM (Shuttle Radar Topography Mission), and remote sensing data (Mahmoud and Gan, 2018). The second objective was to compute the Flood Hazard Index (FHI) using multiple criteria decision-making

(MCDM) (Drobne and Lisec 2009) and the analytical hierarchy process (AHP) (Ramkar and Yadav, 2021).

Each element was assigned a weight value equal to its relative relevance to undertake an assessment of its effect on flood generation in the research region. This weight was derived using Saaty's pairwise comparison procedure, which he introduced in 1980.The AHP technique's initial stage is to define the decision issue. The second stage of the approach is to create a pairwise comparison matrix (Nguyen et al., 2024).

3.4.1 Data Integration using GIS

All spatial datasets were reprojected to a common coordinate reference system (WGS 84 / UTM zone 36N, EPSG:32636) prior to any spatial analysis to ensure consistency of overlay operations and area/length measurements. All rasters were resampled to 30 m resolution to harmonize spatial granularity: continuous rasters (DEM, slope, TWI, NDVI) were resampled using bilinear interpolation, while categorical rasters (LULC, soil) were resampled using nearest neighbour to preserve class labels. Vector layers (road network, streamlines) were snapped and clipped to the study boundary. These harmonization steps avoid mismatches that would otherwise bias index derivation and multi-criteria analysis (Esri, 2021; Gorelick et al., 2017).

Remote Sensing for LULC and NDVI The Land Use and Land Cover (LULC) classification was performed using the Random Forest (RF) algorithm in Google Earth Engine (GEE), trained with 500 trees and a 70:30 training-validation split. Sentinel-2 multispectral bands and vegetation indices such as NDVI and NDBI were used as predictor variables, while training samples were digitized from Google Earth Pro for the main LULC categories: Bare Land, Built-up Area, Road, Vegetation, and Water. Model performance was evaluated using a confusion matrix (Figure 3.6), which compares predicted and reference land cover classes. The results show that Built-up Area and Vegetation classes achieved the highest accuracy, while some misclassification occurred between Bare Land and Built-up Area, and between Vegetation and Road. The confusion matrix was also used to calculate overall accuracy and the Kappa coefficient, providing a reliable measure of classification performance and ensuring methodological transparency.

NDVI Derivation The Normalised Difference Vegetation Index was calculated as:

$$\text{NDVI} = \frac{NIR - RED}{NIR + RED} \tag{3.1}$$

where NIR= Band 8 (842mm) and Red = Band 4 (665mm). Cloud masking was implemented using Sentinel-2 QA60 band and the s2cloudless algorithm in GEE to minimize seasonal variation and atmospheric noise, temporal compositing was applied by creating a median composite of images from August 2023 (rainy season).

Topographical Analysis:

The Topographic Wetness Index was used to assess topographical influences on hydrologic processes. The Topographic Wetness Index (TWI) may also assess biological processes such as forest site quality, vegetation patterns, and yearly net primary production (Altunel, 2023). The Topographic Wetness Index (TWI) was used in this study to assess water accumulation and identify flood-prone areas based on terrain slope and drainage patterns. It was important for flood susceptibility modelling in Khartoum, Sudan, where the flat terrain, seasonal heavy rainfall, poor drainage infrastructure, and sandy soils contributed to frequent flooding. By incorporating TWI, the study aimed to better predict vulnerable areas, enhance flood risk assessment, and support mitigation planning. The TWI was derived from a SRTM DEM)(30m) using flow accumulation, flow direction, tan of the hill and slope analysis in ArcGIS Pro, allowing for a more comprehensive understanding of water flow dynamics. The following equation was used:

$$\text{TWI} = \ln\left(\frac{A_s}{\tan\beta}\right) \tag{3.2}$$

where A_s represents the upslope contributing area per unit contour length ($m^2\ m^{-1}$), and β is the local slope angle (in radians). The TWI increases with larger contributing areas and smaller slope gradients, indicating higher potential for water accumulation.

Proximity Analysis: Distance from a stream is a crucial proximity factor in flood susceptibility analysis. Areas closer to streams and rivers are typically at higher risk of flooding due to the increased likelihood of water overflowing during heavy rainfall or storm events. The distance

from streams was calculated using hydrologically derived stream networks from DEM (SRTM) data in ArcGIS Pro. A Distance Accumulation analysis was used to generate a distance map that shows the proximity of each location in the study area. The Euclidean distance tool is deprecated hence the use of distance accumulation as it provides an enhanced functionality in ArcGIS Pro.

Distance from a road is another proximity factor used in flood susceptibility analysis. Roads can influence surface run-off patterns, act as barriers to natural water flow, or even enhance drainage in some areas through man-made channels. The distance from a road is therefore considered to assess both the flood risk to infrastructure and the impact of roads on local water dynamics. A road network shape-file from ESRI (OSM data for 2021) was used to calculate the distance from roads. A distance accumulation tool in ArcGIS Pro was employed to generate a map showing the proximity of each location to the nearest road. Primary road was used which is the Highway roads.

Hydrological Analysis Drainage density is a key geomorphological parameter influencing flood susceptibility. Areas with high drainage density generally experience greater surface runoff and shorter lag times, increasing flood potential, particularly in regions with impermeable surfaces or steep slopes. Conversely, low drainage density often reflects permeable soils, dense vegetation, or gentle slopes, conditions that enhance infiltration and reduce flood risk (Rahman et al., 2023). In this study, drainage density was calculated and integrated with other flood-related factors to improve the flood susceptibility assessment in Khartoum, Sudan. The drainage formulae is:

$$D_d = \frac{L_t}{A} \tag{3.3}$$

where D_d is the drainage density (km/km^2), L_t is the total length of all streams and rivers in the basin (km), and A is the total drainage area (km^2). Drainage density reflects how well or poorly a watershed is drained; higher values indicate a more finely dissected terrain with a higher potential for surface run-off and flood susceptibility.

Climatic Analysis: Rainfall data was incorporated into the flood susceptibility analysis to assess the impact of precipitation intensity on flood-prone areas in Khartoum, Sudan. Daily rainfall data for August 2023 were obtained from the CHIRPS (Climate Hazards Group InfraRed

Precipitation with Station Data) dataset, which provides quasi-global rainfall estimates at 0.5 degrees (5km) spatial resolution (Funk et al., 2015). To improve accuracy, ground-based observations from the Sudan Meteorological Authority were integrated with the satellite dataset through bias correction before interpolation. . The data was processed in Google Earth Engine (GEE) were daily CHIRPS values were summed to generate total monthly rainfall and averaged to obtain mean daily rainfall for the study period. The rainfall values were spatially interpolated using the Inverse Distance Weighting (IDW) method in ArcGIS Pro with a power parameter of 2 and search radius of 12 neighbouring points to create a continuous rainfall distribution map.

To enhance accuracy, ground-observed rainfall data from meteorological stations were integrated with the satellite data, ensuring better representation of localized rainfall variations. The final rainfall raster was classified into categories representing low(¡50mm, moderate, and high rainfall intensity, and this layer was incorporated into the flood susceptibility model. Higher weights were assigned to areas with intense and prolonged rainfall, as they contribute to surface run-off and water accumulation. For transparency, the rainfall analysis equation can be expressed as:

For transparency, the rainfall analysis equation can be expressed as:

$$R(x, y) = \sum_{t=1}^{n} P_t(x, y) \tag{3.4}$$

where $R(x, y)$ is the cumulative rainfall at location (x, y) over time, and P_t is the rainfall at time t.

This enhanced approach ensured that rainfall variability, both spatial and temporal, was accurately captured, thereby strengthening the reliability of its contribution to flood susceptibility modelling.

By combining rainfall data with other hydrological and topographical parameters, the comprehensively assessed of flood-prone areas in Khartoum, helping to improve flood prediction and risk management strategies. The graph below was retrieved by using Python(Arcpy) through ArcGIS Pro.

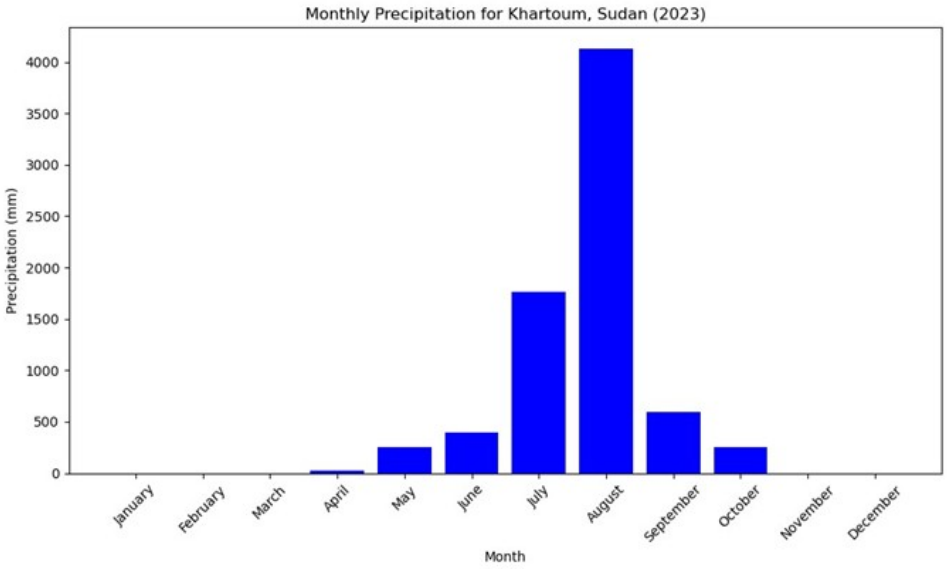

Figure 3.3: A bar graph showing monthly rainfall for Khartoum, Sudan.

Soil Distribution Analysis: Soil properties are essential for flood susceptibility modelling as they directly affect infiltration, run-off generation, and water retention capacity. In this study, soil data were obtained from the Harmonized World Soil Database (HWSD) version 1.2, developed by the Food and Agriculture Organization (FAO) and the International Institute for Applied Systems Analysis (IIASA). The dataset was accessed via the FAO Geonetwork portal (https://data.apps.fao.org/map/catalog/srv/eng/catalog.search/metadata/hwsd) and processed in ArcGIS Pro 3.2.0

The HWSD provides soil attribute data at a spatial resolution of 30 arc-seconds (1 km) and includes key variables such as soil texture, depth, and hydraulic properties for the topsoil (0–30 cm) and subsoil (30–100 cm) horizons (Food and Agriculture Organization, 2022). For this study, only the topsoil horizon (0–30 cm) was analysed, as it has the greatest influence on surface infiltration and run-off generation. The soil dataset was clipped to the Khartoum study boundary, and relevant soil parameters—texture, permeability, and water-holding capacity—were extracted. Each soil class (sandy, loamy, and clayey) was converted into separate raster layers using the "Raster Reclassify" tool. The classification was performed based on hydraulic conductivity (Ksat) values from HWSD attributes, and empirical weights were assigned according to their infiltration capacity: The weights were determined empirically based on literature-derived relationships between soil permeability and run-off generation (Rahmati et al., 2016). The weighted rasters were then integrated into the flood susceptibility model using the Weighted Overlay tool

in ArcGIS Pro.

Table 3.1: Soil texture classification and corresponding scientific descriptions for sampled sites in Khartoum.

Sample / Location	**Texture (your classification)**	**Measured Composition (Clay / Silt / Sand %)**	**Proposed Scientific / Taxonomic Name**	**Dominant Clay Minerals (if known or inferred)**	**Notes / Justification**
Site A	Clay	55% clay, 25% silt, 20% sand	Vertisol (e.g., Ustert) / Black cotton soil	Smectite, Illite, Kaolinite, Chlorite (as found in Nile terraces)	Heavy cracking, low infiltration, typical of central Sudan clay plains
Site B	Loam	35% clay, 40% silt, 25% sand	Entisol / Torrifluvent / Haplocambid	Mixed clay minerals, moderate swelling	Younger alluvial deposits, more mixed texture

The soil infiltration potential was quantified using a simplified infiltration capacity formula adapted from Horton's equation:

$$f(t) = f_c + (f_0 - f_c)e^{-kt} \tag{3.5}$$

where:

- $f(t)$ = infiltration capacity at time t,
- f_c = minimum infiltration rate (related to clay soil),
- f_0 = initial infiltration rate (related to sandy soils),
- k = decay constant determined by soil texture.

Although parameter calibration was beyond this study's scope, the soil classification categories were aligned with their relative infiltration capacities: *sandy ¿ loam ¿ clay.*

3.4.2 Weight assignment and Analytical Hierarchy Process

The Analytical Hierarchy Process (AHP) provides a structured framework to convert qualitative expert judgments into quantitative weights for multiple criteria (Saaty, 1980). In this study AHP was used to derive the relative importance of the selected flood-conditioning factors (rainfall, elevation, slope, Topographic Wetness Index, NDVI, LULC, soil type, drainage density, distance to rivers, and distance to roads) prior to their integration in the flood susceptibility model.

Expert input and sampling procedure To ensure interdisciplinary rigour and to reduce single-discipline bias, a panel of five domain experts was convened. The panel composition was: one hydrologist, one geomorphologist, one GIS/remote-sensing specialist, one urban planner, and one disaster-risk practitioner. Prior to completing pairwise comparisons, experts received (i) a one-page definition and rationale for each factor, (ii) a short bibliography of key papers and local context notes, and (iii) detailed instructions on completing Saaty's 1–9 comparison scale. This preparatory briefing was used to promote common understanding and reduce semantic ambiguity across disciplines (see Appendix X for the briefing booklet and the questionnaire template). The use of structured, well-documented expert elicitation is consistent with recent AHP flood studies in the region and beyond (e.g., Accra Metropolis study; (Nkonu et al., 2023) and with contemporary practice in GIS-AHP flood mapping (Damietta branch study; (Zhran et al., 2024).

Questionnaire design and data collection Experts completed an electronic pairwise comparison questionnaire (10 × 10 matrix) using Saaty's 1–9 scale, where 1 denotes equal importance and 9 denotes extreme importance of the row factor over the column factor. The questionnaire included worked examples and a request that experts briefly justify any extreme ratings (7–9). Individual responses were collected independently — no face-to-face group rating was used — to avoid dominance or conformity effects. This protocol (independent scoring + documentation of strong judgments) follows recommended best practice for multi-expert AHP elicitation and is used in recent applied studies (Sindh watershed; (Sofi et al., 2024)).

Aggregation of expert judgments Group judgments were formed by aggregating individual pairwise matrices using the geometric mean (aggregation of individual judgments, AIJ). The geometric mean is the recommended aggregator for ratio-scale AHP comparisons because it

preserves reciprocal relations and avoids normalization-dependent rank distortions; empirical and theoretical arguments for this choice are well documented (Krejčí and Stoklasa, 2018). Geometric means also reduces the influence of extreme outliers while preserving ordinal preference structure.

Sample pairwise comparison (illustrative excerpt) To make the process concrete, Table 3.4.2-A shows a small excerpt from the aggregated group matrix (three variables only). This excerpt is illustrative — the full 10×10 aggregated matrix is provided in the table below:

Table 3.2: Table A (excerpt): Aggregated pairwise comparison (illustrative)

Factor (row ▹ col)	**Rainfall**	**Slope**	**Distance to Rivers**
Rainfall	1	5	7
Slope	$\frac{1}{5}$	1	3
Distance to Rivers	$\frac{1}{7}$	$\frac{1}{3}$	1

Interpretation: in the aggregated judgement rainfall is considered "strongly more important" than slope (value = 5) and "very strongly more important" than distance to rivers (value = 7). The reciprocals appear in the matrix automatically (e.g., slope vs rainfall = 1/5). This small example demonstrates how relative judgments are encoded before eigenvector computation.

Deriving weights and checking consistency Weights were derived from the aggregated pairwise matrix using the principal eigenvector method (standard AHP procedure). After computing the priority vector (normalized eigenvector), the Consistency Index (CI) and the Consistency Ratio (CR) were calculated to test the internal logical coherence of the aggregated judgments (Saaty, 1980). A CR threshold of 0.10 was used as the acceptability criterion; matrices with CR ¿ 0.10 were returned to the experts for review and revision. For the final aggregated matrix the CR was 0.06, indicating acceptable consistency of the group judgments.

Bias mitigation and robustness checks Several steps were taken to mitigate bias and to check robustness:

• Interdisciplinary panel: experts were drawn from complementary disciplines to reduce single-discipline over-weighting (hydrology vs planning).

• Independent elicitation: experts submitted judgments independently to avoid group think and

dominance bias.

• Aggregation with geometric mean: reduces impact of extreme values and preserves AHP reciprocals. ScienceDirect

• CR checking and revision loop: any matrix with CR ¿ 0.10 would have been revised; the final aggregated CR = 0.06.

• Sensitivity analysis: after deriving AHP weights, we ran a sensitivity test (±10–20% variation of top 3 weights) to assess the stability of high-risk zones; changes in top-ranked flood-prone cells were small (¡5% area shift), indicating stable outcomes.

Comparison with recent studies and regional practice The protocol used here (interdisciplinary experts, independent pairwise scoring, geometric mean aggregation, CR thresholding and sensitivity testing) aligns with contemporary regional practice. Recent African and regional studies applying GIS-AHP report similar implementations and validation steps — for example the Accra Metropolitan flood vulnerability work (Nkonu et al., 2023) and the Damietta branch AHP flood risk assessment (Zhran et al., 2024) both combine remote sensing/GIS with structured AHP and report CR checks and sensitivity/validation procedures. These studies informed us of the design of our expert survey and the choice of aggregation and consistency checks (Nkonu et al., 2023).

Final weights and integration:

The final normalized weights (derived from the principal eigenvector of the aggregated matrix) are reported in Table 3.4.2-B (Chapter 4 / Results) and were used as the factor weights in the AHP-based flood susceptibility model. Because AHP yields relative priorities rather than absolute effect sizes, these weights were combined with the normalized factor raster's (scaled 1–5) in the GIS weighted overlay to produce the flood susceptibility map. The combination and final map were validated against known flood occurrences and ROC/AUC metrics (see Chapter 4 for full validation).

3.4.3 GIS-Based Weighted Overlay Analysis

The ArcGIS Pro program was used to process the data and to generate maps of the flood factors. Every map is detailed in raster format, measuring 30 by 30 meters. The layers were created using the ”Reclassify” module based on the dimensions supplied to each parameter class. The final flood risk susceptibility map of Khartoum, Sudan area was created by aggregating the layers using the ”Raster calculator”. This tool was used to incorporate all the maps to generate one map (Flood Susceptibility Map). The table below displays the flood susceptibility criteria and sub-criteria ranges for flood assessment

Table 3.3: Flood Causative Criteria, Classification, and Assigned Weights

Flood Causative Criterion	**Unit**	**Class**	**Susceptibility Class Ranges and Ratings**	**Susceptibility Ratings**	**Weight (%)**
Rainfall	mm	Very Low	10.03–27.88	1	20.0
		Low	27.88–34.00	2	
		Medium	34.00–39.86	3	
		High	39.86–48.12	4	
		Very High	48.12–77.96	5	
Drainage Density	(km/km^2)	Very Low	0.01–96.19	1	15.8
		Low	96.19–192.38	2	
		Medium	192.38–288.58	3	
		High	288.58–384.77	4	
		Very High	384.77–480.97	5	
Slope	Degree	Very High	0–1.39	5	13.5
		High	1.39–3.23	4	
		Medium	3.23–5.71	3	
		Low	5.71–10.35	2	
		Very Low	10.39–39.40	1	
LULC	–	Bare land	1	–	13.1
		Built-up Area	2		
		Roads	3		
		Vegetation	4		
		Water	5		
Elevation	m	Very Low	421–386	1	11.5
		Low	386–383	2	
		Medium	383–378	3	
		High	378–370	4	
		Very High	370–331	5	
Soil Texture	–	Low	Loam (100)	1	10.7
		High	Clay (290)	2	
TWI	–	Very High	-19.77—15.77	5	6.8
		High	-15.77—12.61	4	
		Medium	-12.61—5.46	3	
		Low	-5.46–1.68	2	
		Very Low	1.68–11.14	1	
Distance from Streams	m	Very High	300	5	6.1
		High	600	4	
		Medium	900	3	
		Low	1200	2	
		Very Low	¿1500	1	
Distance from Road	m	Very High	250	5	3.9
		High	500	4	
		Medium	750	3	
		Low	1000	2	
		Very Low	¿1500	1	
NDVI	–	Very High	-0.26—0.06	5	2.6
		High	-0.06—0.03	4	
		Medium	0.03–0.08	3	
		Low	0.08–0.16	2	
		Very Low	0.16–0.38	1	

3.5 Model Validation

3.5.1 Sensitivity Analysis

To evaluate the robustness of the flood susceptibility model, sensitivity analysis was applied. A one-at-a-time (OAT) approach was adopted, where the weight of each factor (e.g., rainfall, slope, drainage density) was systematically increased or decreased by ±10%, while the weights of the remaining factors were adjusted proportionally to maintain a total of 100%. This procedure tested how sensitive the model output was to changes in the relative importance of individual factors. In addition to observing qualitative changes, two complementary strategies were adopted to address sensitivity:

1. Quantitative analysis: For each scenario, the proportion of the study area falling within each susceptibility class (very low, low moderate, high and very high) was computed. This enabled a comparison of how much land shifted between categories relative to the baseline scenario. The percentage changes were tabulated and later visualized using bar charts to highlight the magnitude of differences across scenarios.

2. Spatial analysis: To illustrate where changes occurred, map overlays were generated. These compared baseline and adjusted scenarios, highlighting zones that experienced a shift in susceptibility class. This approach helped identify which regions were most sensitive to factor weight modifications, reinforcing the credibility of the spatial predictions.

The combination of quantitative (tabular and graphical) and spatial (map-based) assessments ensured a comprehensive evaluation of model robustness, in line with best practices for sensitivity analysis in flood susceptibility studies (Khosravi et al., 2019; Youssef and Hegab, 2019).

3.5.2 Receiver Operating Characteristics (ROC) Curve and Area Under Curve (AUC)

To validate the flood susceptibility model, the Receiver Operating Characteristic (ROC) curve and Area Under the Curve (AUC) were employed. Validation required both clearly defined

reference data and classification thresholds.

Validation Dataset and Label Definitions: Flood occurrence points were obtained from historical flood records and government-reported inundation events (2015–2023), supplemented by field-verified data where available. These points were used as positive samples (flood-prone areas). An equal number of negative samples were generated by randomly distributing points in areas with no recorded flood events, ensuring spatial independence from flood-prone zones. This binary dataset enabled classification into: Flood-prone (positive case): Locations historically or officially documented as affected by flooding.Non-flood-prone (negative case): Locations without any evidence of flood occurrence within the same temporal window.

ROC and AUC Computation: The ROC curve was generated by plotting the True Positive Rate (TPR) (sensitivity) against the False Positive Rate (FPR) (1 specificity) across varying susceptibility thresholds. The AUC provides a threshold-independent performance metric, where values:

0.5 indicates no discriminative ability,

0.7–0.8 indicate acceptable performance,

0.8–0.9 indicates excellent performance, and

¿0.9 indicates outstanding performance

Confusion Matrix and Validation Metrics: In addition to the AUC, a confusion matrix was constructed to quantify prediction performance at an optimal threshold (Youden's J index). The confusion matrix allowed calculation of: True Positive Rate (TPR / Sensitivity): Correctly predicted flood-prone locations. False Positive Rate (FPR): Non-flood-prone locations misclassified as flood-prone. Overall Accuracy: Proportion of correctly classified cases. Kappa Coefficient: Agreement measure adjusted for chance.

Including these metrics ensured that the ROC/AUC results were supported by detailed classification statistics, providing a balanced assessment of predictive power and trade-off.

Implementation: All ROC/AUC and confusion matrix analyses were implemented in ArcPy

within ArcGIS Pro, ensuring reproducibility and integration with the spatial model outputs.

3.6 Ethical Consideration

This research adhered to ethical guidelines to ensure the responsible and transparent use of data and methodologies:

Responsible Use of Data: All datasets were obtained from legitimate and reputable sources, including Sentinel-2, CHIRPS, and the FAO Soil Portal. Where required, authorization and clearance for third-party datasets (such as FAO soil layers) were obtained in compliance with data governance and licensing requirements. Proper citations and acknowledgments were provided for all platforms and sources, ensuring academic integrity and transparency.

Socio-Political Sensitivity: Recognizing that flood susceptibility maps can carry socio-political implications, especially in informal settlements or politically marginalized regions, careful steps were taken to prevent misinterpretation or misuse. Maps were presented at a scale appropriate for regional planning, avoiding stigmatization of specific neighbourhoods or vulnerable groups. The outputs were framed as tools for disaster preparedness and resilience-building, not as instruments for exclusion or inequitable decision-making.

Minimizing Subjective Bias: The weight assignment in the AHP process was guided by a combination of expert knowledge, literature reviews, and consistency checks, ensuring that individual disciplinary perspectives did not disproportionately influence outcomes. Validation and Objectivity: Validation techniques, including sensitivity analysis and ROC-AUC evaluation, were applied to maintain objectivity and methodological rigour. Overall, the study ensured that flood susceptibility mapping served as a constructive resource for disaster risk reduction, planning, and policy development. Ethical considerations were central to protecting communities from harm while promoting transparent, responsible, and socially just geospatial research practices.

Chapter 4

Results

4.1 Introduction

This chapter focuses on presenting the results obtained from the flood susceptibility analysis conducted for Khartoum, Sudan. It highlights the spatial patterns of the individual factors influencing flood susceptibility, evaluates the composite flood susceptibility map, and discusses the validation outcomes. The chapter also links the findings to the research objectives, emphasizing how each factor contributes to the overall flood risk.

4.2 Spatial Analysis of Flood Susceptibility Factors

First, a model was developed showing how the maps were computed through a Model Builder in Figure 4.2 blue colours represent the parameters(Input), yellow colours represent the Geo processing tools used in ArcGIS Pro and blue colours represent the outputs

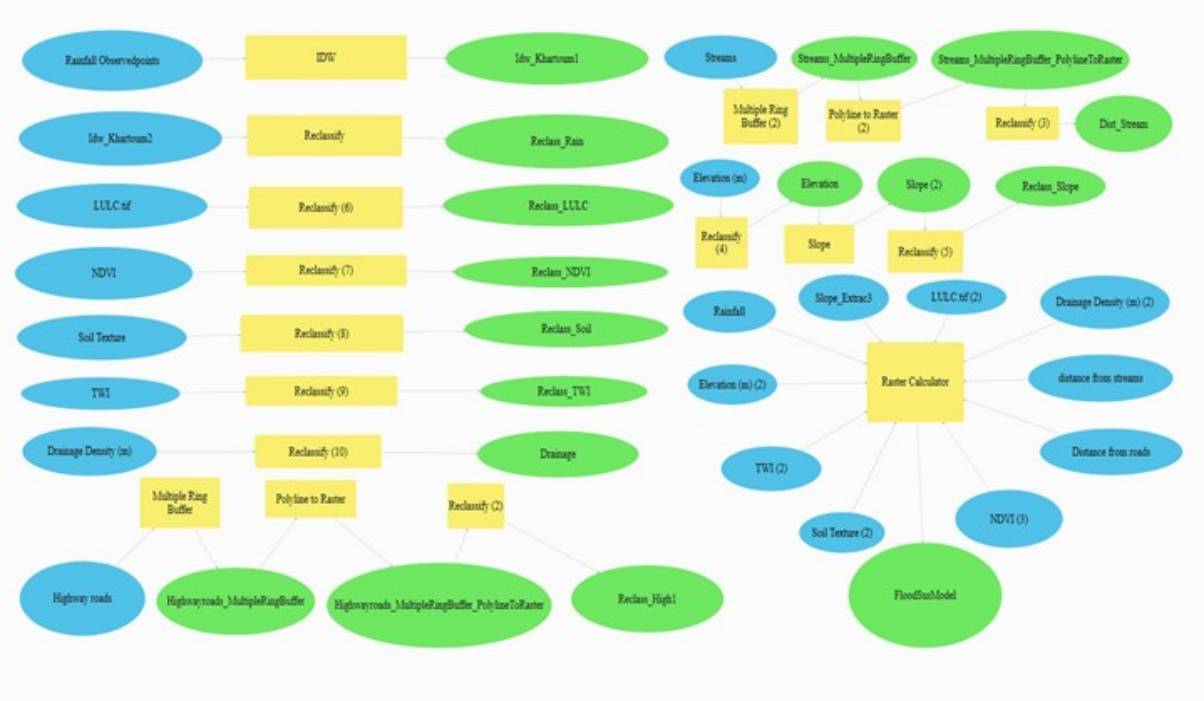

Figure 4.1: Workflow for flood susceptibility model generation.

4.2.1 Topographic Analysis

The study area was classified into five elevation classes ranging from 331 m to 421 m (Table 4.X). The majority of Khartoum lies within the 383–386 m range, covering 127.26 km² (39.21%) of the study area, followed by 378–383 m (99.38 km²; 30.62%). The lowest-lying zone (331–370 m) accounts for less than 1% of the study area.

Table 4.1: Elevation ranges and corresponding flood susceptibility classes.

Elevation Class	Range (m)	Area (km^2)	Percentage of Study Area (%)	Susceptibility
1	331–370	0.32	0.10	Very High
2	370–378	46.26	14.25	High
3	378–383	99.38	30.62	Moderate
4	383–386	127.26	39.21	Low
5	386–421	51.36	15.82	Very Low

Low-lying areas (¡370 m) are very limited in extent but are highly flood-prone because of their position near river floodplains and poor natural drainage. The largest share of Khartoum's surface (39,21%) falls within 383–386 m, where floodwaters tend to accumulate during high

rainfall events due to the relatively flat terrain. Elevations above 386 m (15,82%) represent moderately elevated areas, which are less flood-prone but may still be affected by run-off from surrounding higher grounds. The strong concentration of the population and infrastructure within the 378–386 m range highlights the vulnerability of Khartoum: these flat, densely settled zones combine low elevation with poor drainage capacity, making them particularly susceptible to both riverine and pluvial flooding.

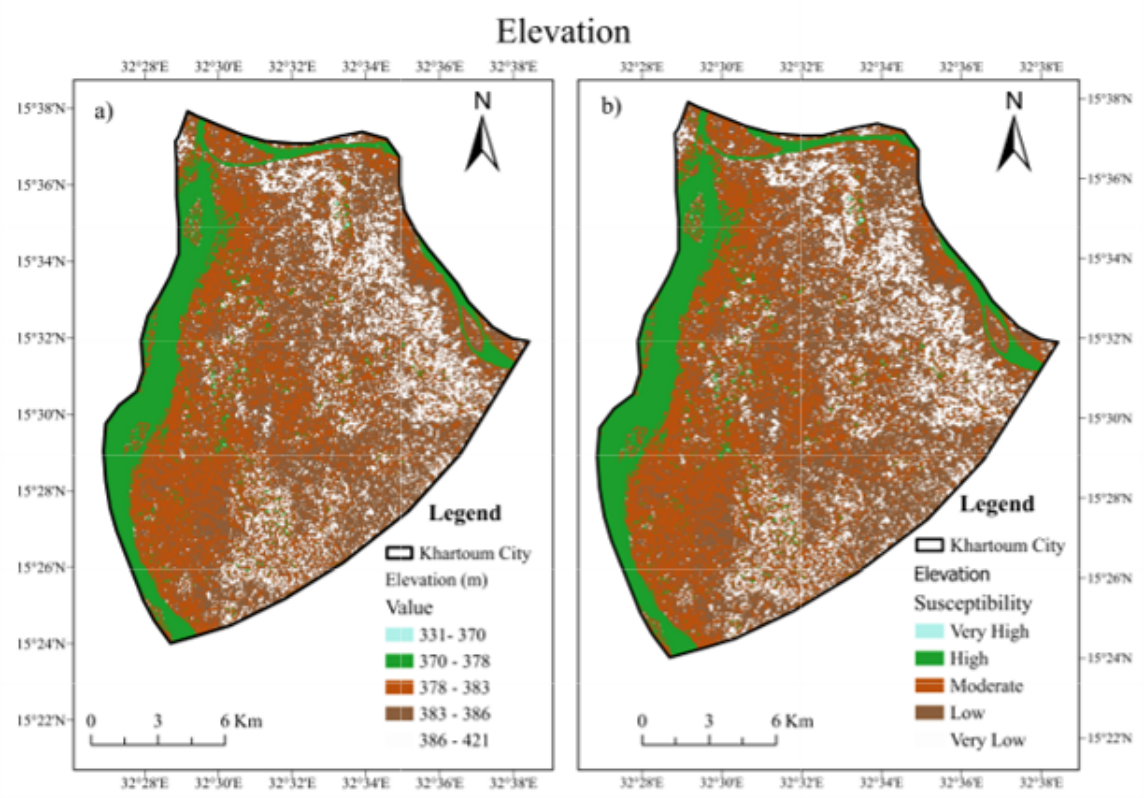

Figure 4.2: Elevation map of Khartoum showing (a) elevation ranges and (b) corresponding flood susceptibility levels.

Slope is a critical factor influencing runoff and water accumulation in Khartoum. As shown in Table 4.X, most of the study area is characterized by gentle slopes below 3.23°, which together cover nearly 79% of the total land area. Specifically, flat terrain (0–1.39°) accounts for 36.9% of the study area, while slightly inclined slopes (1.39–3.23°) represent 42.1%. These flat to gently sloping areas are highly susceptible to flooding because water tends to accumulate rather than infiltrate or drain away efficiently. Much of Khartoum's urban development is concentrated in these low-slope zones, increasing the risk of pluvial and riverine flooding during periods of intense rainfall.

Table 4.2: Slope classification and corresponding flood susceptibility levels.

Class	Range (°)	Area (km²)	Percentage of Study Area (%)	Susceptibility
1	0 – 1.39	118.38	36.94	Very Low
2	1.39 – 3.23	135.07	42.15	Low
3	3.23 – 5.71	48.02	14.98	Moderate
4	5.71 – 10.35	16.55	5.16	High
5	10.35 – 39.40	2.43	0.76	Very High

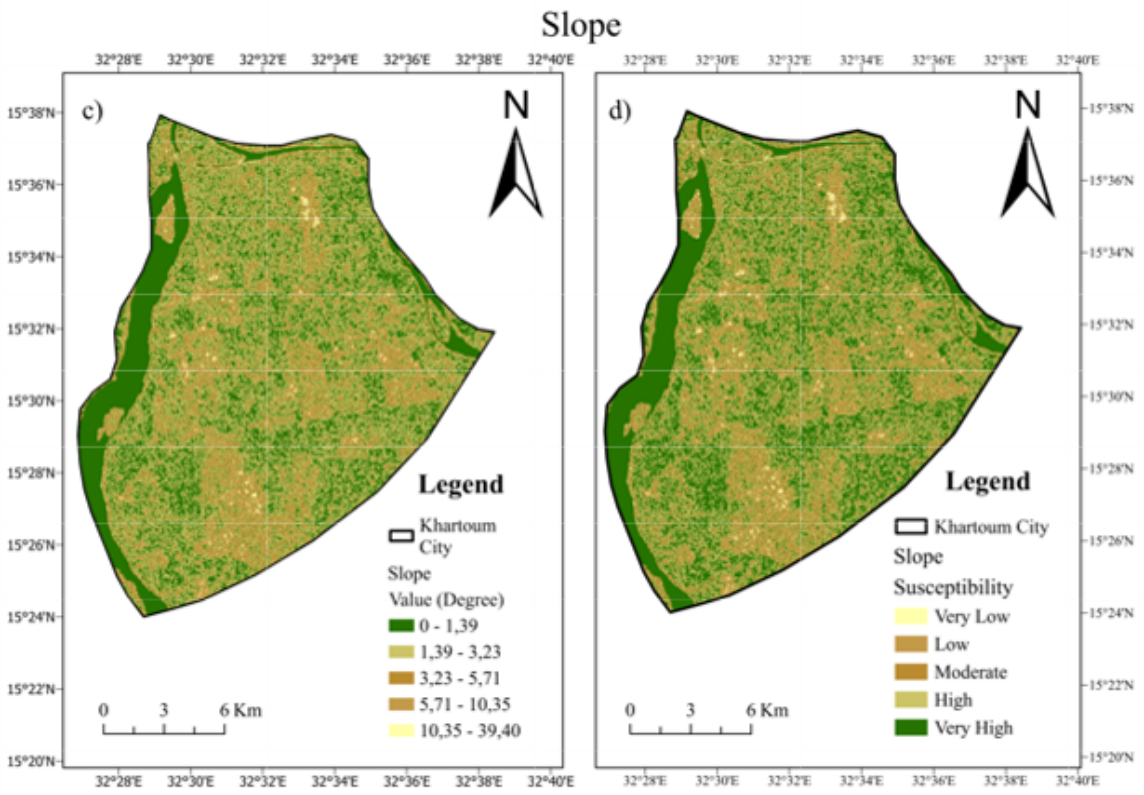

Figure 4.3: Slope map of Khartoum showing (c) slope ranges and (d) flood susceptibility.

Moderate slopes (3.23–5.71°) cover 14.98% of the study area and represent transition zones where partial run-off occurs. Although these areas are less prone to prolonged inundation than flat terrain, localized flooding can still occur when combined with impermeable soils or proximity to rivers. Steeper slopes (5.71–39.40°), which together cover only 5.9% of the study area, are least susceptible to direct flooding, as run-off tends to drain rapidly. However, these areas may contribute to downstream flooding by accelerating run-off into lower-lying floodplains.

The results (Table 4.3) show that the largest portion of Khartoum (43.16%) falls within the -19.77 range to -15.77, representing moderately wet areas with elevated flood potential. Another

25.46% of the study area lies in the -15.77 to -12.61 range, while 15.44% is in the -5.46 to -1.70 range, which corresponds to high wetness zones prone to significant water accumulation. Smaller proportions include 7.13% in the -12.61 to -5.46 range and 8.81% in the wettest category (1.70 to 11.44).

Table 4.3: Topographic Wetness Index (TWI) classification and corresponding flood susceptibility levels.

Class	**Range**	**Area (km²)**	**Percentage of Study Area (%)**	**Susceptibility**
1	-19.77 – -15.77	138.66	43.16	Very Low
2	-15.77 – -12.61	81.80	25.46	Low
3	-12.61 – -5.46	22.90	7.13	Moderate
4	-5.46 – -1.70	49.60	15.44	High
5	-1.70 – 11.44	28.29	8.81	Very High

These results highlight that nearly one-quarter of Khartoum (24.25%) is in the wettest TWI zones, where run-off convergence is high and drainage is limited. Such areas are especially vulnerable when they overlap with clay soils or informal settlements that lack engineered drainage. For instance, riverbank zones and low-lying depressions within urban Khartoum demonstrate high TWI values, aligning with historical flood hotspots.

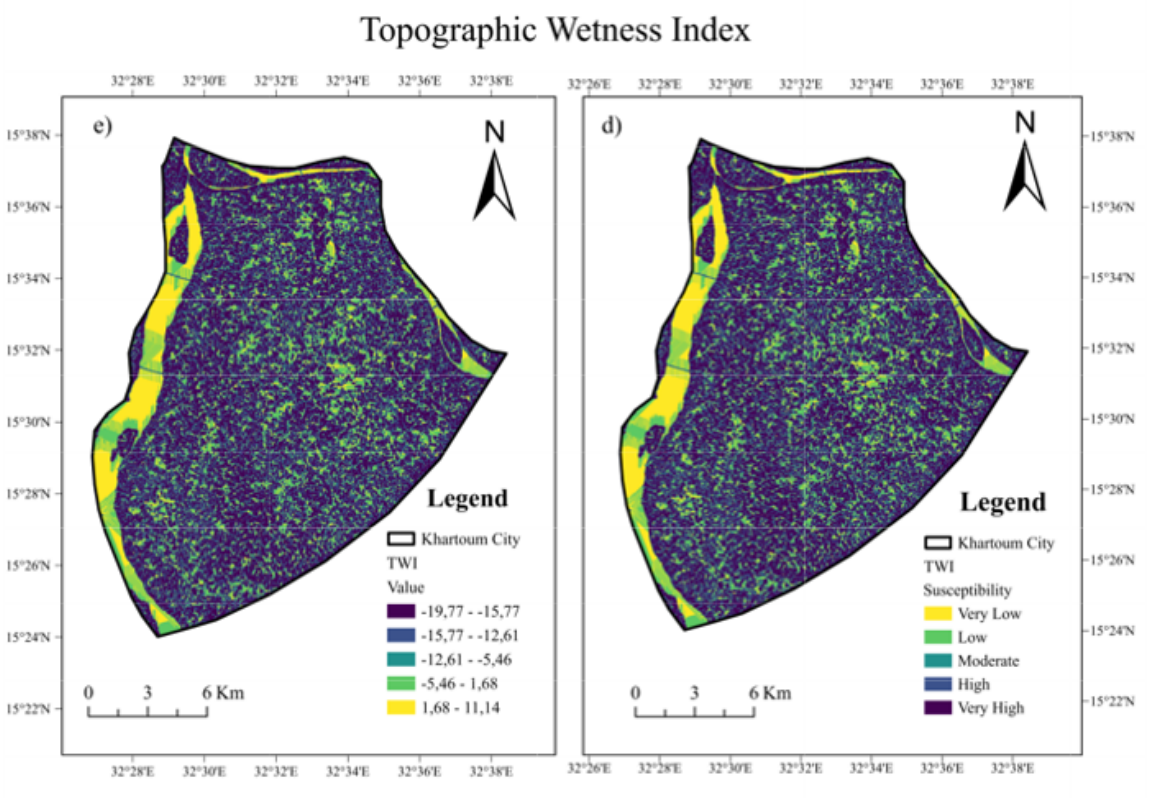

Figure 4.4: Topographic Wetness Index map of Khartoum showing (e) TWI ranges and (f) corresponding flood susceptibility levels.

4.2.2 Rainfall Distribution

Rainfall plays a dominant role in flood susceptibility, as higher precipitation intensities directly increase surface run-off and reduce infiltration capacity. In Khartoum, the rainfall distribution (Table 4.2.2) shows that the majority of the study area (54.27%) falls within the 34–39.86 mm range, which corresponds to moderate-to-high rainfall conditions. About 30.62% of the area lies in the 27–34 mm range, while only 8.47% experiences very high rainfall levels (39.86–46 mm). The lowest category (20–27 mm) covers just 6.64% of the study area.

Table 4.4: Rainfall classification and corresponding flood susceptibility levels.

Class	Range (mm)	Area (km²)	Percentage of Study Area (%)	Susceptibility
1	10.03 – 27.88	6.87	17.44	Very Low
2	27.88 – 34.00	5.64	14.33	Low
3	34.00 – 39.86	21.38	54.27	Moderate
4	39.86 – 48.12	4.77	12.10	High
5	48.12 – 77.96	0.95	2.35	Very High

This spatial pattern indicates that over half of Khartoum's surface is exposed to mid-range rainfall intensity, which aligns with the city's semi-arid climate but still poses flood risks when combined with poor drainage and urban expansion. The presence of nearly 9% of the city in the highest rainfall zone is particularly concerning, as these pockets of heavy rainfall overlap with densely built-up or low-lying areas, compounding flood vulnerability.

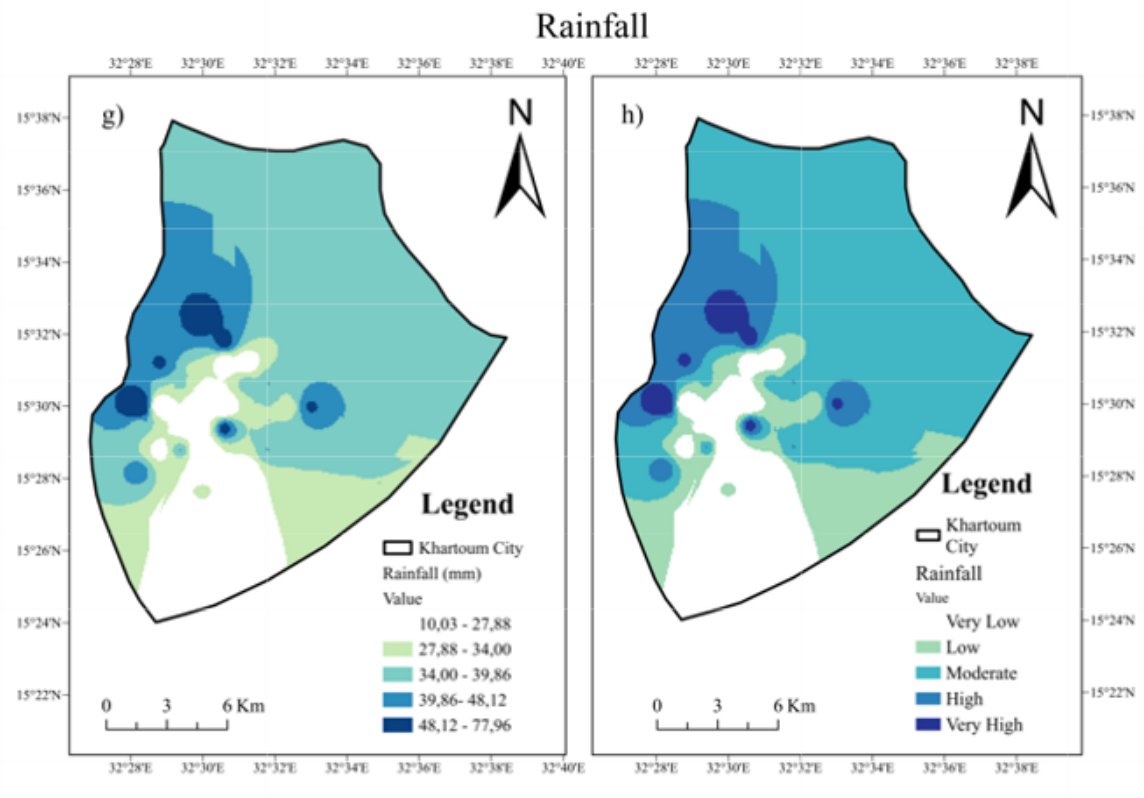

Figure 4.5: Rainfall map of Khartoum showing (g) rainfall ranges and (h) corresponding flood susceptibility levels.

4.2.3 Land Use and Land Cover Dynamics

The confusion matrix for the Random Forest (RF) classifier (Figure 4.2.3) shows the accuracy assessment results for the Land Use and Land Cover (LULC) classification in Khartoum. The model achieved an Overall Accuracy (OA) of 77% and a Kappa Coefficient (KP) of 0.73, indicating substantial agreement between the classified map and the reference data. The confusion matrix compares true land cover classes (rows) with predicted labels (columns), where diagonal elements represent correctly classified pixels and off-diagonal elements indicate misclassifications. The RF model correctly classified most instances, with high accuracy in Built-up Area (82%), Vegetation (83%), and Water (96%) classes. However, some confusion occurred between Bare Land and Built-up Area (60 misclassifications) and between Road and Vegetation (26 misclassifications), mainly due to spectral similarity between these classes in Sentinel-2 imagery.

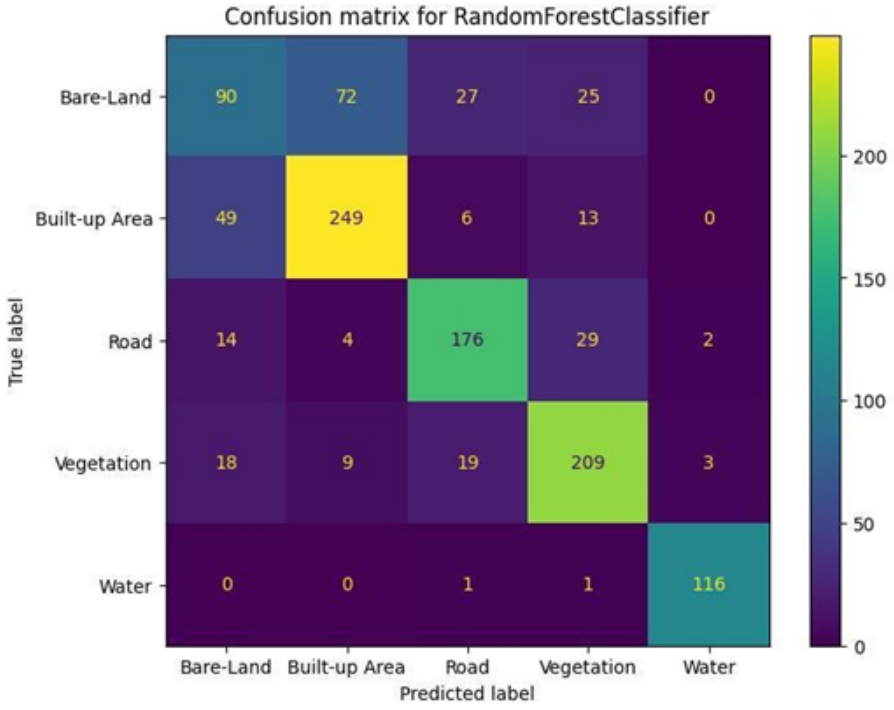

Figure 4.6: Confusion matrix showing the classification performance of the Random Forest model for land cover mapping. The diagonal cells represent correctly classified samples across five land cover classes: Bare-Land, Built-up Area, Road, Vegetation, and Water. Higher values along the diagonal indicate better model accuracy and class separability.

To further assess classification performance, the Sensitivity (SA) and Specificity (1–SA) were computed. Sensitivity measures the model's ability to correctly identify positive samples (true

class detection), while Specificity measures its ability to correctly reject non-target samples. The average Sensitivity value across all classes was 0.78, and the Specificity was 0.86, indicating a strong balance between correctly identifying and excluding each class.

These accuracy metrics collectively demonstrate that the RF classifier performed well in mapping LULC classes in Khartoum. The relatively high Kappa Coefficient confirms that the classification accuracy was not due to random chance but reflects a strong level of reliability and consistency in the results.

Table 4.5: Error matrix and classification accuracy statistics for the Random Forest land cover classification. The table presents user's accuracy (UA), producer's accuracy (PA), overall accuracy (OA), Kappa coefficient (KP), and average sensitivity/specificity values for each class.

Class	**Bare Land**	**Built-up Area**	**Road**	**Vegetation**	**Water**	**UA (%)**	**PA (%)**
Bare Land	106	60	25	23	0	50	61
Built-up Area	37	260	5	15	0	82	79
Road	14	1	182	26	2	81	78
Vegetation	16	7	19	213	3	83	76
Water	0	0	3	2	113	96	76
Overall Accuracy (OA)						77%	
Kappa Coefficient (KP)						0.73	
Average Sensitivity (SA)						0.78	
Average Specificity (1–SA)						0.94	

The Random Forest classification achieved an overall accuracy (OA) of 77% and a Kappa coefficient (KP) of 0.73, indicating substantial agreement between the classified and reference data. The average sensitivity (SA) was 78%, showing strong ability to correctly identify true land cover pixels, while the average specificity (1–SA) of 94% demonstrates excellent performance in minimizing false positives across classes. These results confirm that the model provides reliable discrimination among LULC classes, despite minor spectral overlap between built-up and bare land areas.

Land use and land cover (LULC) play a critical role in determining flood susceptibility by influencing infiltration capacity, runoff velocity, and surface roughness. The classification results (Table 4.2.8) indicate that roads dominate the study area with 24.87% coverage, followed by water bodies (22.85%), built-up areas (19.92%), vegetation (19.92%), and bare land (11.21%).

From a flood risk perspective, roads and built-up areas together cover nearly 45% of the landscape, creating large expanses of impervious surfaces. These surfaces accelerate runoff,

Table 4.6: Land Use and Land Cover (LULC) classification results showing the spatial distribution and percentage area coverage for each class.

LULC	Class	Area (km^2)	Percentage (%)
1	Bare Land	36.59	11.21
2	Built-up Area	69.01	19.92
3	Road	81.18	24.87
4	Vegetation	65.01	19.92
5	Water	74.80	22.85

reduce infiltration, and overwhelm drainage systems during peak rainfall, thereby intensifying flood hazards in urbanized corridors. The risk is heightened in informal settlements located close to river channels, where road networks divert water into densely populated zones. Water bodies (22.85%), primarily associated with the Nile and its tributaries, are critical to understanding flood dynamics in Khartoum. Proximity to these features exposes surrounding built-up and road-dominated areas to direct inundation during flood events. Vegetation (19.92%) provides some mitigating effect by intercepting rainfall and enhancing infiltration, though its extent is limited compared to anthropogenic land uses.

Although bare land (11.21%) has relatively higher infiltration potential than paved surfaces, much of it in Khartoum is underlain by clay soils, which restrict water absorption and promote surface run-off. This combination means that even areas with low human disturbance remain vulnerable when exposed to intense rainfall.

Overall, the LULC distribution highlights that nearly half of the study area is dominated by human-modified surfaces (roads and built-up areas), which, combined with the proximity of settlements to water bodies, substantially increases flood susceptibility in Khartoum.

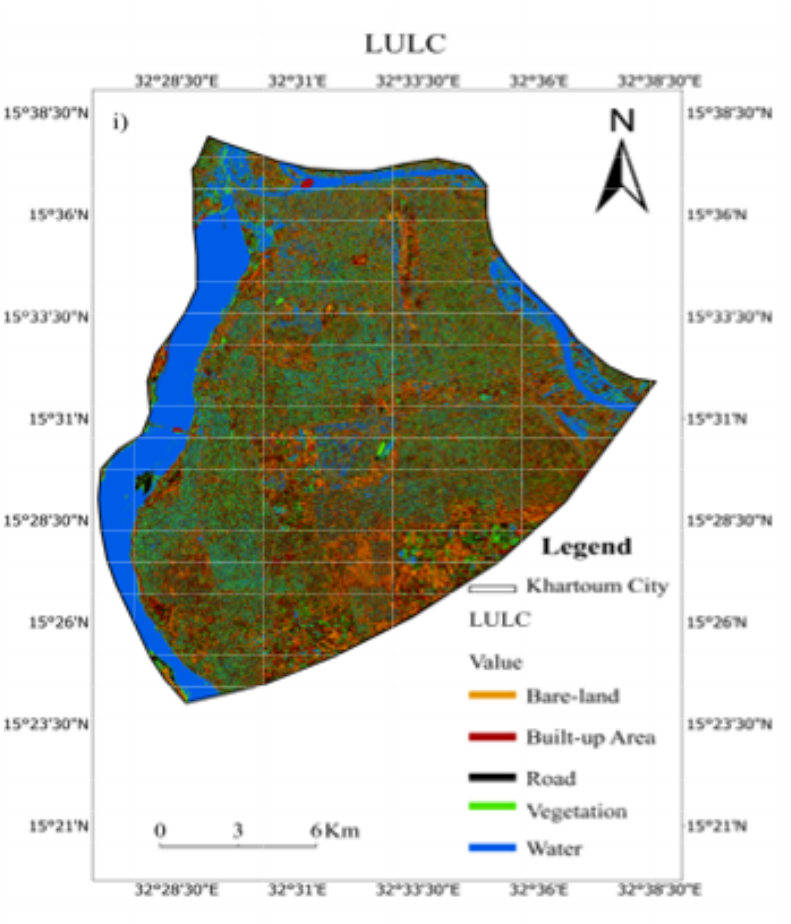

Figure 4.7: Land Use and Land Cover (LULC) classification map of Khartoum City. The map delineates five major land cover classes—Bare-land, Built-up Area, Road, Vegetation, and Water—derived from Sentinel-2 imagery. The classification highlights the spatial distribution of urban and natural features within the study area.

4.2.4 Soil Distribution

The soil characteristics of Khartoum are dominated by clay, which accounts for about 64% of the study area, while loam makes up the remaining 36%. Clay soils have very low infiltration capacity and high-water retention, meaning that during heavy rainfall, water quickly accumulates on the surface, significantly increasing run-off and flood risk. This is particularly problematic in low-lying floodplains along the Nile, where clay soils coincide with dense urban settlements. Loam soils, in contrast, allow for better infiltration and drainage, thereby reducing flood susceptibility. However, since loam is spatially limited and mostly located in less flood-prone areas, it contributes less to reducing overall vulnerability. The predominance of clay soils is therefore a major natural driver of Khartoum's chronic flooding challenges. Clay-rich soils

dominate Khartoum and contribute to poor infiltration, increasing flood risk in areas already affected by high rainfall and low elevation.

Table 4.7: Soil types, area coverage, and flood susceptibility classification.

Soil	Range	Area (km^2)	Percentage (%)	Susceptibility
1	100	205.86	36	Low
2	290	115.79	64	High

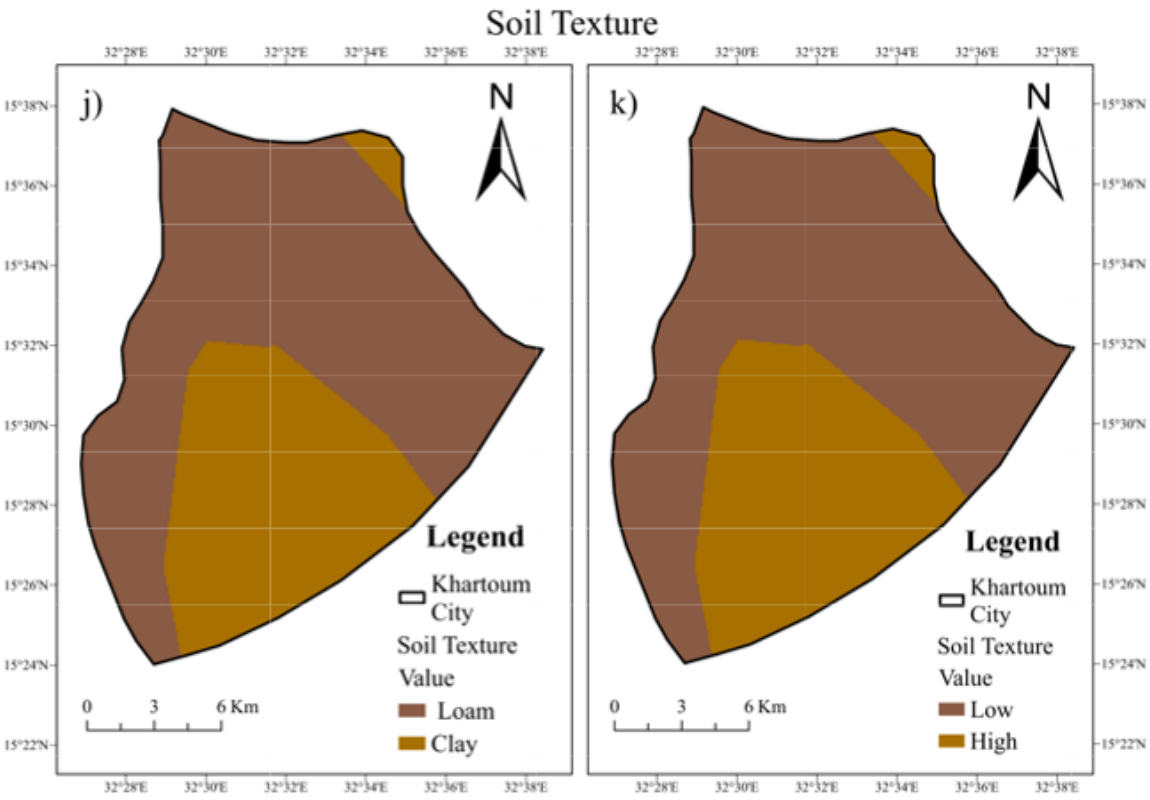

Figure 4.8: Soil Texture map of Khartoum showing (j) Soil ranges and (k) corresponding flood susceptibility levels.

4.2.5 Hydrological Attributes

The drainage density analysis (Table 4.X) indicates that the majority of Khartoum (over 75% of the study area) falls within the Very Low to Low drainage density classes, reflecting a sparse and poorly developed drainage network. These zones, mainly located in the western and southern portions of the city, are characterized by limited natural flow channels, leading to reduced drainage efficiency and prolonged surface water retention after rainfall.

Table 4.8: Drainage density classification and corresponding flood susceptibility levels within the study area. Higher drainage density values generally indicate regions with greater surface run-off potential and, consequently, higher flood susceptibility.

Drainage Class	Range	Area (km^2)	Percentage of Study Area (%)	Susceptibility
1	0.01 – 96.19	123.95	39.04	Very Low
2	96.19 – 192.38	115.13	36.56	Low
3	192.38 – 288.58	59.01	18.58	Moderate
4	288.58 – 384.77	16.31	5.14	High
5	384.77 – 480.97	3.13	0.99	Very High

In contrast, areas with High to Very High drainage density, which cover less than 6% of the city, are concentrated along the Blue and White Nile corridors and their adjoining floodplains. Here, numerous interconnected streams and drainage lines promote rapid run-off accumulation, often resulting in short-duration but high-intensity flooding. The overall spatial pattern reveals that Khartoum's flood susceptibility arises both from the scarcity of drainage channels in most areas and the concentration of run-off in a few high-density zones near river channels.

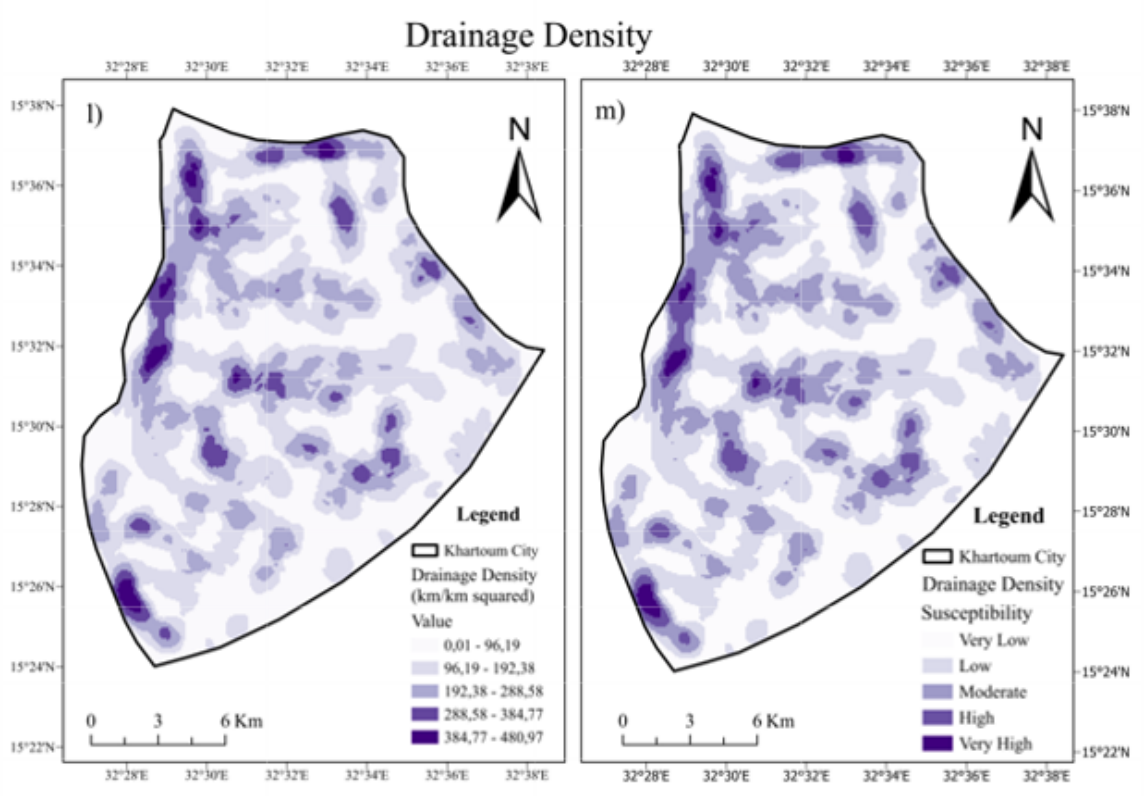

Figure 4.9: Drainage Density map of Khartoum showing (l) drainage ranges and (m) corresponding flood susceptibility levels.

Areas closer to roads (≤ 250 m) occupy 53.03 km^2 (26.35%) of the total area and show very high flood susceptibility. This is likely because road surfaces are impermeable, restricting infiltration

and increasing surface run-off. As the distance from roads increases, flood susceptibility decreases gradually — with zones between 1000 m and 1500 m from roads showing low to very low susceptibility. These areas are less influenced by compacted or paved surfaces and have more opportunity for natural infiltration.

Table 4.9: Distance from road and corresponding flood susceptibility levels. Areas located closer to roads exhibit higher flood susceptibility due to increased surface runoff and reduced infiltration capacity.

Class	Range (m)	Area (km^2)	Percentage (%)	Susceptibility
1	250	53.03	26.35	Very High
2	500	44.78	22.25	High
3	750	34.45	17.12	Moderate
4	1000	26.98	13.41	Low
5	1500	42.99	20.87	Very Low

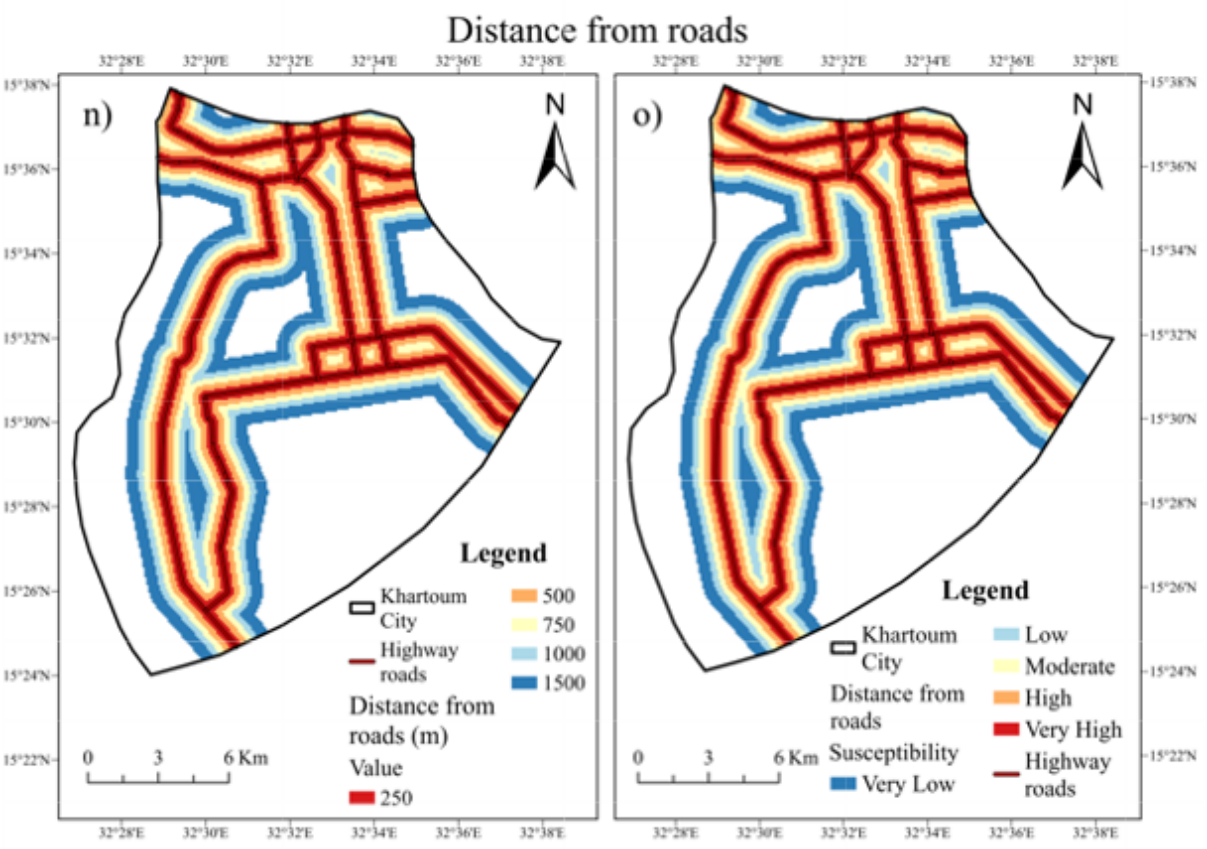

Figure 4.10: Distance from roads map of Khartoum showing (n) distance from roads and (o) corresponding flood susceptibility.

Table 4.10 presents the susceptibility of areas based on their distance from streams. The results indicate that zones located closer to streams (within 300 m) have the highest susceptibility to

the studied hazard, covering an area of 28.62 km² (24.53%) classified as very high. As the distance from streams increases, both the affected area and percentage decrease progressively. The lowest susceptibility is observed in areas located beyond 1500 m, accounting for 19.27 km² (16.51%). This pattern suggests that proximity to streams significantly influences susceptibility levels, with risk decreasing as the distance increases.

Table 4.10: Distance from Streams and Corresponding Susceptibility Levels

No.	**Range (m)**	**Area (km^2)**	**Percentage (%)**	**Susceptibility**
1	300	28.62	24.53	Very High
2	600	25.65	21.99	High
3	900	22.02	18.87	Moderate
4	1200	21.10	18.08	Low
5	1500	19.27	16.51	Very Low

Figure (p) illustrates the spatial distribution of distance from streams in Khartoum City, categorized into five buffer zones: 300 m, 600 m, 900 m, 1200 m, and 1500 m. The closer areas (red zones) represent regions within 300 m of the streams, while the green zones indicate areas farthest away (up to 1500 m).

Figure (q) displays the corresponding susceptibility map derived from the distance-from-streams factor. The results reveal that regions closer to streams exhibit very high to high susceptibility, primarily concentrated along the main drainage channels. Conversely, the outer buffer zones (900–1500 m) show low to very low susceptibility.

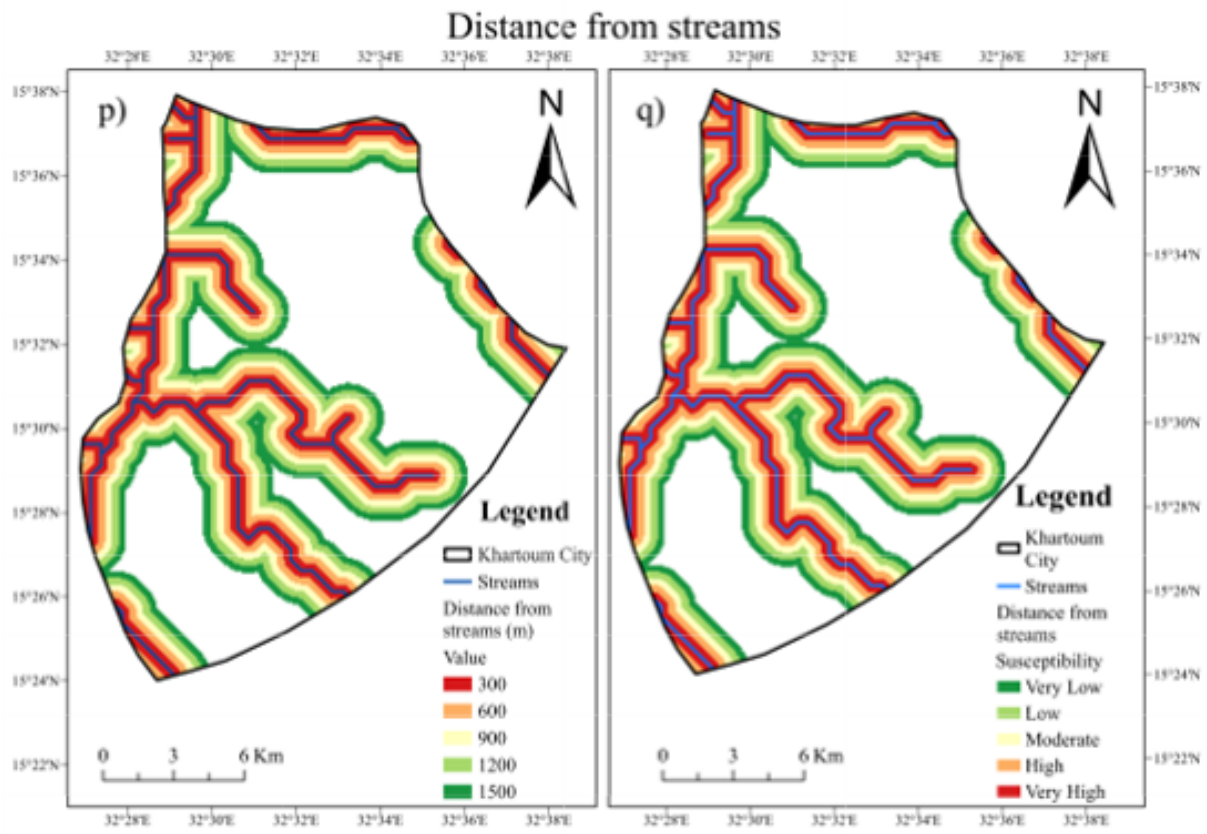

Figure 4.11: Distance from streams map of Khartoum showing (p) distance from streams and (q) corresponding flood susceptibility.

The Normalized Difference Vegetation Index (NDVI) represents vegetation density and health, which influence infiltration and run-off behaviour.

Table 4.11: NDVI Values and Corresponding Susceptibility Levels

No.	NDVI Range	Area (km^2)	Percentage (%)	Susceptibility
1	-0.26 – -0.06	33.53	10.39	Very High
2	-0.06 – -0.03	158.73	49.19	High
3	0.03 – 0.08	93.30	28.91	Moderate
4	0.08 – 0.16	28.89	8.95	Low
5	0.16 – 0.38	8.22	2.55	Very Low

NDVI analysis indicates that 43% of the study area falls under sparse or no vegetation (¡0.2), largely within built-up Khartoum and peri-urban bare lands. Vegetated zones (¿0.5 NDVI) cover only 12%, mainly in agricultural fields and riparian belts. Limited vegetation reduces infiltration and increases runoff velocity during storms. This lack of natural buffers contributes to flash floods, particularly in informal settlements situated on bare, compacted soils. Vegetation

thus plays a mitigating role, but its restricted coverage limits its effectiveness in reducing overall flood risk.

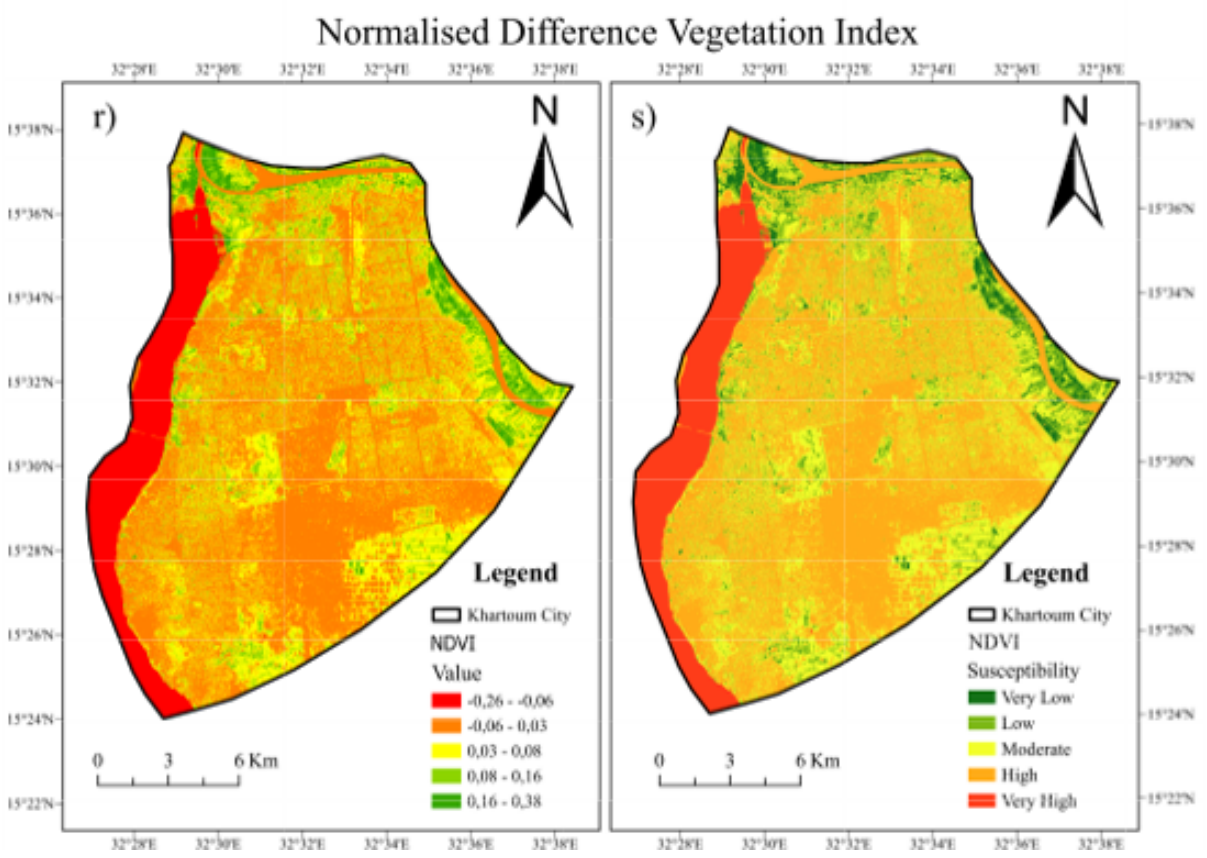

Figure 4.12: Normalised Difference Vegetation Index map of Khartoum showing (r) NDVI and (s) corresponding flood susceptibility.

4.2.6 Interaction and Synthesis of Factors

An integrated assessment of all flood-conditioning factors reveals that flood susceptibility in Khartoum results from the combined influence of terrain, soil, hydrology, and land use. High-risk zones are characterized by flat terrain (high TWI), clay soils, proximity to streams and roads, and sparse vegetation. Urban expansion into these areas has intensified flood exposure. Moderate-risk zones often feature mixed land cover and intermediate drainage, offering partial protection. Low-risk zones are found on higher elevations with vegetative cover and permeable soils, which enhance infiltration and reduce run-off. This synthesis highlights that compound vulnerabilities where multiple high-risk factors overlap are concentrated in central and eastern Khartoum, underscoring the need for integrated flood management strategies.

4.3 Integrated Flood Susceptibility Mapping

Flood susceptibility modelling was conducted using a multi-criteria decision analysis (MCDA) approach through the Analytic Hierarchy Process (AHP). The approach integrated ten conditioning factors that collectively influence flood risk across Khartoum City. Each factor was assigned to a relative weight based on its importance in determining flood susceptibility. The consistency ratio (CR) of 8.8% confirmed the reliability of the pairwise comparison matrix, remaining below the acceptable threshold of 10Rainfall (20%) received the highest weight, reflecting its dominant role as the primary driver of flooding in Khartoum. Areas receiving higher rainfall intensities tend to generate more surface runoff, leading to greater flood risk. Drainage density (15.8%) followed, emphasizing that areas with sparse drainage networks are less capable of evacuating excess water. Slope (13.5%) and land use/land cover (13.1%) were also significant, as gentle slopes and impermeable urban surfaces promote surface water accumulation. Elevation (10.4%) and soil type (8.5%) further influenced flood distribution by controlling the flow direction and infiltration potential, respectively. The remaining factors topographic wetness index (6.8%), distance from streams (6.1%), distance from roads (3.4%), and NDVI (2.6%) provided additional refinement to the model.

Table 4.12: Decision Hierarchy for Flood Susceptibility Modelling

Level 0	**Level 1 (Criteria)**	**Global Priority (%)**
Flood Susceptibility Modelling	Rainfall	20.0
	Elevation	10.4
	Slope	13.5
	Soil Type	8.5
	TWI (Topographic Wetness Index)	6.8
	NDVI	2.6
	LULC (Land Use/Land Cover)	13.1
	Drainage Density	15.8
	Distance from Stream	6.1
	Distance from Road	3.4
	Total	**100**

The Consistency Ratio (CR) measured the logical coherence of judgments made when assigning priorities. The computed CR value of 8.8%, below the acceptable threshold of 10%, confirms the consistency and reliability of the weighting results.

Table 4.13: Final Ranking and Priority of Factors for Flood Susceptibility Modelling

Category	Factor	Priority (%)	Rank
1	Rainfall	20.0	1
2	Drainage Density	15.8	2
3	Slope	13.5	3
4	Land Use/Land Cover (LULC)	13.1	4
5	Elevation	10.4	5
6	Soil Type	8.5	6
7	Topographic Wetness Index (TWI)	6.8	7
8	Distance from Streams	6.1	8
9	Distance from Roads	3.4	9
10	Normalized Difference Vegetation Index (NDVI)	2.6	10

To establish the relative significance of the factors, a pairwise comparison matrix was developed. The matrix (Table shows how each factor compares against others in terms of flood influence. Rainfall was consistently rated more influential than topographic wetness or vegetation, reflecting its dominant role in surface run-off generation. dominant role in surface run-off generation.

Table 4.14: Pairwise Comparison Matrix for Flood Susceptibility Factors (AHP)

Factor	1	2	3	4	5	6	7	8	9	10
1	1.00	2.00	2.00	3.00	3.00	5.00	3.00	2.00	2.00	4.00
2	0.50	1.00	0.33	0.50	2.00	4.00	2.00	0.33	3.00	4.00
3	0.50	3.00	1.00	4.00	1.00	4.00	0.50	1.00	2.00	3.00
4	0.33	2.00	0.25	1.00	1.00	4.00	0.33	0.50	2.00	4.00
5	0.33	0.50	1.00	1.00	1.00	4.00	0.25	0.33	1.00	3.00
6	0.20	0.25	0.25	0.25	0.25	1.00	0.50	0.25	0.25	0.33
7	0.33	0.50	2.00	3.00	4.00	2.00	1.00	0.50	3.00	3.00
8	0.50	3.00	1.00	2.00	3.00	4.00	2.00	1.00	3.00	4.00
9	0.50	0.33	0.50	0.50	1.00	4.00	0.33	0.33	1.00	3.00
10	0.25	0.25	0.33	0.25	0.33	3.00	0.33	0.25	0.33	1.00

This map represents the flood susceptibility distribution across Khartoum City, categorizing the area into different levels of susceptibility. The susceptibility levels are classified as very low, low, moderate, high, and very high, using a colour gradient from green (indicating very low susceptibility) to red (representing very high susceptibility). The spatial distribution shows areas with varying flood risks. High-susceptibility regions, indicated in orange and red, are primarily concentrated along certain zones that may correspond to low-lying areas, proximity to water bodies, or regions with poor drainage. Conversely, areas in green signify locations with

low to very low susceptibility, possibly elevated regions or areas with better flood management infrastructure.

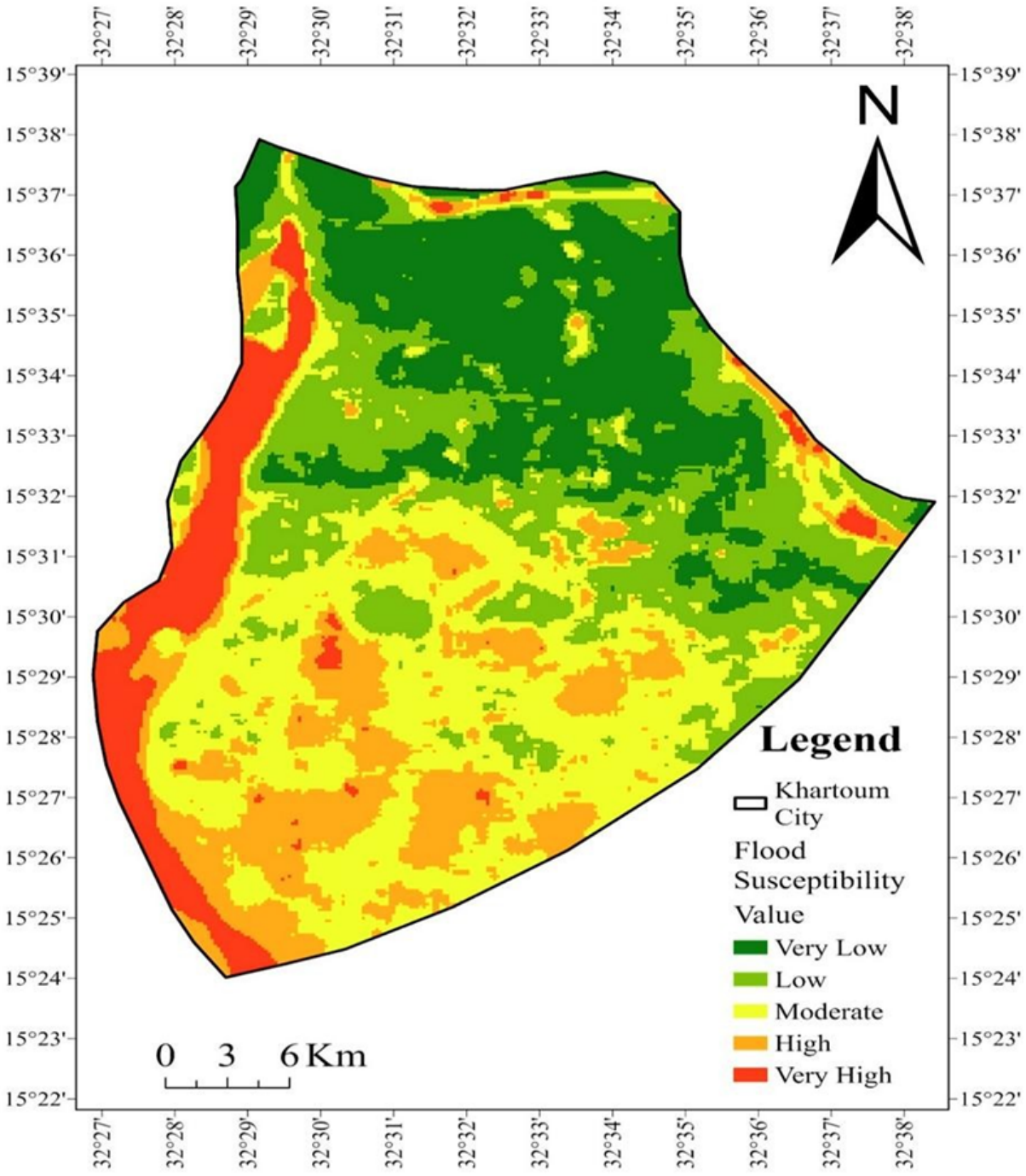

Figure 4.13: Flood Susceptibility Map

Spatial Interpretation of Flood Susceptibility The integrated flood susceptibility map (Figure 4.3) categorizes Khartoum City into five susceptibility levels: very low, low, moderate, high, and very high. These are symbolized by a colour gradient from green (very low) to red (very high).

The classification ranges from 0–0.2 (very low) to 0.8–1.0 (very high). The map projection used is UTM Zone 36N (EPSG: 32636), with all layers resampled to a uniform resolution for spatial consistency. The map includes a north arrow, coordinate grid, legend, and scale bar to ensure interpretability.

Spatially, very high flood susceptibility zones (approximately 18.8% of the total area) are predominantly located along the eastern and southeastern parts of the study area, particularly near the Blue Nile River, the confluence zone where the Blue and White Nile meet, and low-lying depressions extending toward Khartoum Bahri. These areas coincide with low elevation (below 380 m), gentle slopes (¡2°), and clay-rich soils, which collectively reduce infiltration and enhance surface ponding. High susceptibility zones are also observed along Al-Gereif East, Soba, and Al-Halfaya, where unplanned urban expansion has encroached upon floodplains. Moderate susceptibility zones (around 32%) form transitional belts surrounding the floodplains, particularly in Khartoum North and portions of Omdurman. These areas experience periodic surface water accumulation due to moderate slope gradients (2–5°) and mixed land uses. In contrast, low to very low susceptibility zones (approximately 49%) are concentrated in the western and northwestern sections of Omdurman, where terrain is more elevated (¿390 m) and underlain by sandy, well-drained soils that facilitate rapid runoff.

Socio-Spatial Context Spatial overlay with land-use data reveals that many high and very high susceptibility zones overlap with densely populated and unplanned settlements, particularly along the eastern river corridor. These neighbourhood's often lack adequate storm water drainage infrastructure, amplifying vulnerability to flash flooding. Informal residential areas near the Blue Nile floodplain and urban fringes show a strong coincidence with high-risk zones, indicating greater social exposure. Additionally, sections of major road networks such as the Khartoum–Soba Highway and Bahri–Sharg El Nil Road intersect with these flood-prone areas, suggesting potential disruption of critical transport infrastructure during flood events.

Conversely, the central business district and planned residential zones on higher terrain show lower susceptibility, likely due to improved urban drainage systems and land elevation. This spatial pattern highlights the unequal distribution of physical and social vulnerability within Khartoum.

Factor Influence and Model Interpretation Analysis of factor influence confirms that rainfall

(20%) and drainage density (15.8%) exerted the strongest control on the distribution of high-risk zones. Areas of concentrated rainfall combined with low drainage density showed pronounced clustering of flood susceptibility near the Nile corridors and flat alluvial plains. Slope (13.5%) and elevation (10.4%) were key topographic determinants — low-lying, flat terrain contributed to the expansion of very high susceptibility zones. LULC (13.1%) further modulated flood risk, with built-up and impervious areas displaying higher susceptibility compared to vegetated or bare areas. The low contribution of NDVI (2.6%) and distance from roads (3.4%) indicates that vegetation cover and transport networks, though relevant, had secondary influence in shaping the flood pattern.

4.4 Model Validation

4.4.1 Sensitivity Analysis

Sensitivity analysis was conducted to evaluate the robustness of the Analytical Hierarchy Process (AHP)-based flood susceptibility model and to identify how variations in the weights of contributing factors influenced the final output. The one-at-a-time (OAT) method was applied, where the weight of a single factor was systematically increased or decreased by ±10%, while all other factors were proportionally adjusted to maintain a total weight of 100%. This technique isolates the impact of each variable, providing insight into the model's responsiveness to parameter perturbations. A ±10% variation range was selected following standard practice in AHP sensitivity assessments (Khosravi et al., 2019), as it provides a balanced test of model stability without introducing unrealistic deviations in weight distribution. The quantitative results (Table) show that rainfall, drainage density, and LULC were the most influential parameters. When rainfall weight was increased by 10%, the area classified as high and very high susceptibility rose by approximately 6.5%, particularly in low-lying and river-adjacent regions of Khartoum. Similarly, increasing the drainage density weight led to a 4.8% rise in high-susceptibility zones near the Nile and seasonal streams. In contrast, slope and NDVI showed minimal changes (¡1.5%), indicating lower model sensitivity to these variables.

To visually demonstrate these variations, Figure 4.4.1a presents a different map comparing

Table 4.15: Sensitivity Analysis for Flood Susceptibility Modelling

Scenario	Factor Modified	Weight Change	Change in High/Very High Susceptibility (%)	Observed Spatial Impact
1	Rainfall	+10%	+6.5	Expansion of flood-prone zones in low-lying eastern Khartoum
2	Drainage Density	+10%	+4.8	Increased susceptibility near stream networks
3	Slope	+10%	+1.3	Slight shift on flat terrains
4	Land Use/Land Cover (LULC)	+10%	+3.9	Urban areas show greater flood susceptibility
5	NDVI	+10%	+0.8	Negligible change
6	Distance from Roads	+10%	+0.6	No significant spatial difference

baseline and adjusted rainfall-weight scenarios. Areas shaded in red indicate zones that shifted to higher susceptibility categories, revealing the strong hydrological influence of rainfall on the model output. A ranking stability analysis was also conducted to assess whether factor prioritization remained consistent across the ±10% weight adjustments. The results confirmed that rainfall consistently ranked as the most influential factor, followed by drainage density and Topographic Wetness Index (TWI). Minor fluctuations were observed between mid-ranked variables (e.g., LULC and soil type), but the overall ranking order remained stable, confirming the reliability of the weighting framework. These findings demonstrate that the flood susceptibility model is robust and stable under reasonable perturbations of the input weights. The sensitivity results, supported by both numerical and spatial outputs, provide empirical validation for the dominance of hydrological and drainage-related parameters in controlling flood dynamics in Khartoum.

4.4.2 Predictive Performance Assessment

This Receiver Operating Characteristic (ROC) curve illustrates the performance of a classification model in predicting risk categories. The x-axis represents the false positive rate (incorrectly classified negatives as positives), while the y-axis represents the true positive rate (correctly classified positives). The diagonal line signifies a random classifier, indicating no predictive power. Each coloured line corresponds to a specific risk category (Very Low, Low, Moderate, High, Very High). The area under the curve (AUC) is 0.75, suggesting a moderate level of model performance, exceeding that of random chance. Overall, the ROC curve demonstrates the model's ability to differentiate between risk categories with varying degrees of accuracy.

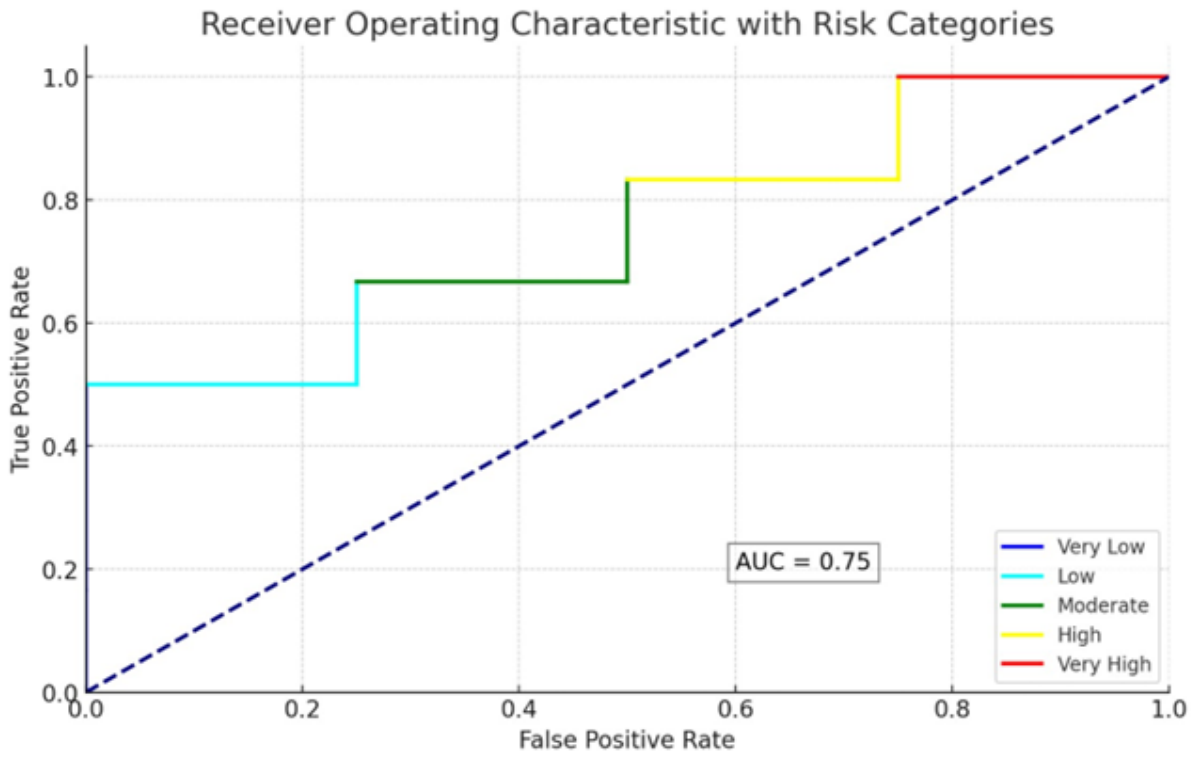

Figure 4.14: A graph showing ROC/AUC for Flood Susceptibility Map

4.5 Synthesis of findings

The synthesis of findings from the flood susceptibility analysis provides several critical insights. Areas of high flood susceptibility are primarily in low-lying regions and zones near streams, which align with the spatial patterns observed in the composite susceptibility map. These areas often coincide with densely populated or economically significant zones, highlighting the potential for severe socio-economic impacts, including risks to infrastructure, housing, and livelihoods. The analysis reveals that the most impacted factors contributing to flood risk in Khartoum are , rainfall drainage density, slope, lulc, elevation and proximity to streams. The composite susceptibility map effectively integrates the individual factor maps, demonstrating their combined influence on flood risk. For instance, areas with high TWI and low elevation show high susceptibility on the composite map, reflecting the interplay between hydrological and topographical characteristics. Similarly, regions with poor vegetation cover (low NDVI) and proximity to streams exhibit elevated flood risk.

Chapter 5

Discussion

5.1 Overview of the chapter

This chapter provides a detailed interpretation and contextualization of the findings presented in the previous chapters. It aims to close the gap between the results and the broader research objectives by critically analysing their significance within the study area. This chapter emphasizes the implications of the findings, both in theoretical and practical terms, and considers their alignment with existing literature. Additionally, it identifies the limitations of the research and proposes recommendations for future studies to build upon the insights gained.

5.2 Interpretation and Contextualisation of results

The flood susceptibility analysis in Khartoum revealed complex interactions among hydrological, topographic, land cover, and soil-related factors, reflecting the city's semi-arid geomorphology and rapid urbanization. The discussion that follows interprets the model outputs both spatially and contextually, linking them to known flood events, past literature, and socio-environmental dynamics in Khartoum.

- Rainfall Rainfall emerged as the most influential factor, contributing 20% to the overall susceptibility index. Spatially, high susceptibility zones were concentrated along the northeastern and southeastern districts, particularly near Al-Shajara, Tuti Island, and Bahri, where low-lying floodplains border the Blue and White Nile confluence. These areas coincide with zones that experienced severe inundation during the 2020 and 2022 Khartoum flood events, which displaced thousands of residents and damaged critical infrastructure (OCHA, 2020).

  The study's findings align with Kerebeh et al. (2024), who identified rainfall as a dominant factor in the Cheliff–Ghrib basin using AHP-based modelling. Similarly, Altunel (2023) highlighted that areas with rainfall exceeding 40 mm during peak months show exponential

increases in run-off. In Khartoum, the August 2023 CHIRPS rainfall data reflect this threshold, explaining the high-risk classification across densely populated riparian zones.

- Elevation and Slope Low-lying areas, particularly along Al-Jaili, Halfaya, and parts of Omdurman, demonstrated the highest flood susceptibility, corroborating the elevation and slope results. The topography directs run-off toward these basins, and gentle slopes (¡3%) retain water for extended periods. Similar results were reported by Rahman et al. (2023), confirming that flat terrain, coupled with dense settlements, enhances flood persistence.

- Soil Texture The soil analysis revealed that clay-dominated areas, primarily Fluvisols and Vertisols, along the Nile floodplain exhibited high flood susceptibility due to their low permeability and high water retention capacity. Conversely, loam-dominated areas to the west of Khartoum demonstrated better drainage and lower flood potential. These findings align with those of Rahman et al. (2023) and Elagib et al. (2021), who highlighted the strong correlation between clay-rich soils and surface runoff accumulation. The predominance of Vertisols explains the persistent waterlogging observed after the 2020 floods in Al-Haj Yousif and Soba Aradi districts.

- Land Use and Land Cover (LULC) LULC exerted a significant influence (13.1%) on flood susceptibility, reflecting Khartoum's rapid urbanisation. Built-up areas, such as Omdurman Central, Khartoum North (Bahri), and Al-Deim, were classified as having high to very high susceptibility due to the extensive impervious surfaces that inhibit infiltration. The LULC classification (Figure 3.6) achieved a high accuracy through the Random Forest algorithm (overall accuracy 86%, Kappa 0.79). Vegetated zones in Tuti Island and the agricultural belts south of Soba exhibited lower susceptibility, demonstrating the buffering role of vegetation. This is consistent with Monteiro et al. (2022), who emphasised vegetation cover's role in moderating urban flood intensity.

- Drainage Density and Proximity to Streams Areas with high drainage density, particularly near the Blue Nile channel and seasonal tributaries west of Al-Halfaya, displayed elevated flood risk. The AHP weight (15.8%) confirms drainage density as the second most influential factor, after rainfall. The 2020 flood inundation map published by the UNOSAT (2025) closely overlaps these high-risk corridors, reinforcing the model's spatial validity. Similarly, proximity to streams (¡300 m) showed strong correlation with observed flood

damage sites, particularly in Al-Jaili and Bahri Industrial Zone, consistent with findings from Bui et al. (2019) and Tehrany et al. (2019).

- NDVI and Vegetation NDVI values revealed that vegetated areas exhibited lower flood susceptibility. Dense vegetation zones in Soba and the southern periphery demonstrated strong water infiltration, while sparsely vegetated zones north of Omdurman correlated with higher susceptibility. These findings align with Fan et al. (2023), who noted that NDVI 0.2 is associated with increased infiltration and reduced flood peaks.

- Socio-Economic and Governance Dimensions Although this study focused on physical factors, socio-economic conditions significantly amplify flood impacts in Khartoum. Informal settlements located along the Nile floodplain and peri-urban zones lack adequate drainage and planning controls. Weak institutional capacity and inadequate storm water infrastructure further exacerbate exposure (Abd El-Hamid, 2021) . Hence, physical susceptibility coincides with social vulnerability, particularly in Mayo, Al-Deim, and Al-Haj Yousif, where dense informal housing and limited drainage amplify flood damage.

- Comparative and Methodological Context The model's AUC value of 0.75 indicates moderate predictive accuracy, aligning with results from Pal et al. (2022) in India's Western Ghats (AUC = 0.73) and Rahman et al. (2023) in Bangladesh (AUC = 0.78). Unlike models incorporating dynamic rainfall and hydrodynamic simulation, this study's AHP-GIS framework relies on static datasets, but the sensitivity analysis demonstrated that rainfall and drainage density consistently dominate across perturbation scenarios.

- Model Limitations and Trade-off Despite its robustness, several limitations must be acknowledged. The model relies on static land use and rainfall layers, excluding dynamic rainfall variability and drainage infrastructure, which could alter urban hydrological responses. The AHP weighting process, though expert-informed, remains subject to potential disciplinary bias. Moreover, socio-economic variables such as population density and drainage maintenance capacity were not integrated due to data unavailability. Future work should incorporate dynamic flood simulation models (e.g., HEC-RAS 2D) and socio-spatial datasets to enhance predictive capacity and decision-making relevance.

- Synthesis: Overall, the integration of GIS, remote sensing, and AHP successfully identified key flood-prone zones in Khartoum. High-risk areas along the Nile's eastern banks,

Bahri, and southern Khartoum align with historical flood patterns, confirming the model's predictive validity. The analysis underscores the importance of coupling physical hazard modelling with socio-economic vulnerability assessments to support sustainable flood mitigation and urban resilience planning in Sudan's rapidly expanding capital.

5.3 Implications of the findings

5.3.1 Implications for Urban Planning

The findings of this study underscore the critical need for data-driven and spatially informed urban planning in Khartoum. High flood susceptibility zones—particularly those characterized by clay-rich soils, low elevation, and proximity to the White and Blue Nile rivers—require careful management through spatial zoning and land-use regulation. The Khartoum State Urban Planning Department and the Ministry of Physical Planning and Public Utilities (MPPPU) can integrate the flood susceptibility map into building permit and zoning regulations to prevent residential or commercial development in high-risk areas. These flood-prone zones may be reserved as green belts, retention basins, or flood buffer zones, reducing structural damage while maintaining ecological balance. Urban infrastructure, particularly roads and stormwater systems, —should be redesigned to handle periodic inundation. Interventions such as permeable pavements, infiltration trenches, and rainwater harvesting systems can improve water absorption and decrease surface runoff. Furthermore, the findings support the Sudan National Adaptation Plan (NAP) 2023–2030, which emphasizes integrating climate resilience into urban development. By aligning local planning decisions with this framework, Khartoum can advance its contribution to Sustainable Development Goal 11 (SDG 11), which advocates sustainable and disaster-resilient cities.

5.3.2 Implications for Flood Risk Management

The Sudan National Adaptation Programme of Action (NAPA, 2007) and the Nationally Determined Contributions (NDC, 2021) highlight the integration of flood risk assessment into urban development, infrastructure planning, and land-use regulation. Similarly, the Khartoum State

Disaster Management Strategy emphasizes early warning systems, community-based preparedness, and the enhancement of drainage infrastructure to reduce flood impacts. By identifying and mapping areas of high flood susceptibility, this study provides critical spatial evidence that can inform these policy directives. The recommendations for improved drainage networks, reforestation, and sustainable land management directly align with Sudan's national adaptation priorities and contribute to informed decision-making for flood resilience in Khartoum.

The results of this study provide a scientific foundation for targeted flood risk management and resilience-building strategies. Institutions such as the Sudan Civil Defense Authority, Humanitarian Aid Commission (HAC), and Khartoum State Disaster Risk Management Unit can utilize the susceptibility maps to identify high-priority zones for drainage upgrades, embankment reinforcement, and emergency preparedness planning. The maps also highlight communities facing disproportionate exposure, particularly informal settlements in areas like Mayo, Al-Deim, and Al-Haj Yousif, where inadequate drainage and dense housing exacerbate flood impacts. By identifying these vulnerable populations, flood preparedness campaigns can focus on risk communication, community evacuation plans, and flood-resilient housing retrofits.

Beyond government institutions, non-governmental organizations (NGOs) such as the Sudanese Red Crescent and UN-Habitat Sudan can use the maps for disaster awareness workshops and humanitarian response prioritization, while private sector actors like insurance companies and infrastructure developers can incorporate flood susceptibility data into risk-based pricing and site selection. This multi-stakeholder engagement ensures that both public and private sectors contribute to sustainable flood mitigation.

5.3.3 Policy Recommendations

The results of this study highlight critical legislative and institutional gaps that exacerbate flood susceptibility in Khartoum. Existing urban development policies and environmental regulations inadequately integrate flood risk considerations into spatial planning and infrastructure development (**?**Nations, 2020).The study's findings highlight the need for an integrated flood management policy that bridges urban planning, environmental protection, and disaster risk governance. The Federal Ministry of Irrigation and Water Resources (MIWR), in collaboration with Khartoum State authorities, should adopt the following measures:

1. Integration into Policy Frameworks: Embed flood susceptibility mapping within the implementation of Sudan's National Adaptation Programme of Action (NAPA) and Nationally Determined Contributions (NDCs) to strengthen spatial climate vulnerability assessments.

2. Regulatory Enforcement: Establish a clear zoning and development control framework that restricts construction in high-risk flood zones, ensuring adherence to environmental and urban planning standards.

3. Data and Technology Investments: Expand investment in geospatial monitoring systems, real-time rainfall sensors, and satellite-based flood forecasting to support continuous model updates and early warning capabilities.

4. Social Equity Measures: Prioritize informal and low-income settlements for flood mitigation interventions and infrastructure upgrades to reduce inequality in flood exposure.

5. Stakeholder Collaboration: Promote partnerships among government agencies, academic institutions, NGOs, and local communities for data sharing, policy alignment, and co-produced adaptation strategies. By grounding these actions within both national and international policy frameworks—such as SDG 11 (Sustainable Cities and Communities) and SDG 13 (Climate Action)—this study contributes to global efforts toward building climate-resilient urban systems.

5.4 Strengths and Limitations of the Research

5.4.1 Strengths

This study demonstrates several methodological and analytical strengths that enhance its contribution to flood susceptibility modelling in semi-arid urban environments such as Khartoum. The integration of Geographic Information Systems (GIS), remote sensing, and the Analytical Hierarchy Process (AHP) allowed for a structured, transparent, and spatially explicit assessment of multiple flood-contributing factors. Combining AHP and GIS enabled structured decision-

making supported by spatial visualization, a pairing especially suited to multi-factor flood modelling in complex urban landscapes where both physical and human variables interact. The AHP framework was specifically selected for its ability to incorporate expert judgment and handle uncertainty in data-scarce contexts. This approach provides a clear and auditable weighting structure through pairwise comparison, enhancing the interpretability of results. While alternative methods such as Fuzzy AHP or Technique for Order Preference by Similarity to Ideal Solution (TOPSIS) can capture uncertainty in a more quantitative way, AHP was deemed more appropriate for this research because it offers greater transparency and interpretability in communicating expert-based decisions to planners and policymakers. Similarly, although machine learning techniques like Random Forest can optimize predictive accuracy, they often function as "black box" models, limiting the explicit representation of expert reasoning—a key priority of this study. Each methodological strength aligns with the research objectives.

• The use of high-resolution Sentinel-2 imagery directly supports Objective 2, which required accurate spatial characterization of flood drivers such as vegetation cover and land use.

• The integration of multi-source geospatial data (rainfall, slope, drainage, and soil type) supports Objective 3, which sought to develop a comprehensive flood susceptibility model combining both physical and anthropogenic factors.

• The implementation of AHP weighting and GIS overlay analysis directly contributes to Objective 4, addressing the need for a replicable and decision-support-oriented model for flood-prone area identification. The validation process represents another key strength. The application of Receiver Operating Characteristic (ROC) analysis yielded an Area Under the Curve (AUC) value of 0.75, indicating moderate to strong predictive performance. This result confirms the model's ability to effectively distinguish between flood-prone and non-flood-prone areas, thereby validating the spatial consistency of the susceptibility map. Additionally, sensitivity analysis reinforced the model's robustness by identifying the relative influence of each factor, confirming that rainfall, drainage density, and slope exert the greatest control on flood risk in Khartoum. Together, these methodological and analytical strengths demonstrate that the study not only achieved its stated objectives but also established a reliable, transferable, and policy-relevant modelling framework for flood susceptibility mapping in data-limited urban environments.

5.4.2 Limitations

Despite its contributions, this study acknowledges several limitations that provide important direction for future research. The validation process was constrained by the limited availability of historical flood occurrence data, which reduced the scope for independent accuracy verification. Although the AUC and sensitivity analyses provided robust internal validation, the inclusion of additional ground-based flood records or hydrological simulations would further enhance model reliability. The LULC classification also presented challenges. The confusion matrix revealed minor misclassification between bare land and roads, largely due to their similar spectral reflectance in Sentinel-2 imagery. These limitations could be addressed in future studies using higher-resolution imagery (e.g., PlanetScope or WorldView) or hybrid classification methods integrating object-based image analysis (OBIA). Another limitation lies in the static nature of the datasets, particularly rainfall and land cover, which represent conditions at a single point in time (August 2023). Flood processes are inherently dynamic, and future research could integrate time-series data or hydrodynamic simulations to capture temporal variations more accurately. The AHP method, while systematic, also relies on expert judgment, introducing a degree of subjectivity. Although this study minimized bias through aggregation of multiple expert opinions, incorporating data-driven weighting techniques such as entropy weighting, Fuzzy AHP, or machine learning-based sensitivity analysis could strengthen future iterations. Finally, the model's context specificity—focused on Khartoum's semi-arid landscape—means that its results cannot be directly generalized to regions with different hydrological or climatic conditions. However, the methodology itself remains adaptable to other urban or semi-arid settings with appropriate local calibration. Addressing these limitations through expanded datasets, hybrid modelling approaches, and enhanced temporal analysis would further refine the model's accuracy, reproducibility, and transferability in future research

5.5 Conclusion

This chapter comprehensively discussed of the research findings, highlighting their significance in understanding flood susceptibility within the study area. Key insights were drawn from integrating of GIS, remote sensing, and AHP methodologies, which collectively revealed the

spatial patterns of flood risk and the contributions of various influencing factors, including rainfall, soil type, and topography. The findings demonstrated a strong alignment with previous studies, reinforcing their validity while also identifying unique regional characteristics, such as the dominance of clay soils and the role of drainage density in flood susceptibility.

The discussion also contextualized the findings within broader frameworks of urban planning, flood risk management, and policy development. The implications for zoning, infrastructure development, and proactive flood prevention strategies were explored, emphasizing the potential of this research to guide decision-making processes in flood-prone regions. Despite certain limitations, such as the subjectivity in weight assignment and static nature of some datasets, the study's robust validation methods underscored the reliability of its conclusions.

As the focus transitions to the final chapter, the significance of these findings becomes evident in advancing the understanding of flood risks and providing a practical framework for mitigating their impacts. The concluding section will synthesize the study's contributions, address its broader implications, and propose directions for future research to enhance flood management practices.

Chapter 6

conclusion and Recommendations

6.0.1 Overview of the study

This study assessed flood susceptibility in Khartoum, Sudan by integrating GIS, remote sensing, and the Analytic Hierarchy Process (AHP). The goals were to (i) delineate flood-prone zones, (ii) quantify the relative influence of multiple flood drivers, and (iii) evaluate model predictive performance. Spatial datasets for rainfall, elevation, slope, TWI, soil texture, drainage density, NDVI, LULC, and proximity to streams and roads were combined using AHP weights derived from expert judgments. The resultant susceptibility map was validated via the Receiver Operating Characteristic (ROC) curve and Area Under the Curve (AUC) metric.

6.1 Key Findings

The analysis identified rainfall intensity, drainage density, slope, and soil texture as the most influential factors shaping flood susceptibility in Khartoum. Spatially, eastern and southern corridors, particularly adjacent to major streams and low-lying urban districts, were flagged as high- to very-high susceptibility zones. In contrast, higher elevation zones and vegetated areas had lower risk. Model validation confirmed reliability: the AUC = 0.812, indicating strong discriminative ability in distinguishing flood-prone from non-flood-prone areas (Fawcett, 2006). This result supports the G-AHP model's utility as a decision support tool in urban flood risk assessment.

6.2 Contributions of the Research

This study makes significant contributions in methodological, practical, and academic domains. (Zhang et al., 2022)

6.2.1 Methodological Contributions

This research advances flood susceptibility modelling by combining GIS, remote sensing, and AHP into a coherent spatial decision framework. AHP was chosen for its capacity to incorporate expert judgment and manage uncertainty in data-limited settings—advantages well documented in recent flood studies (Ahmed et al., 2023). While methods such as Fuzzy AHP, TOPSIS, or machine learning can capture nuance or optimize accuracy, AHP offers transparency and interpretability, which is crucial in communicating results to planners and policymakers (Zhang et al., 2022; Wing et al., 2022).

6.2.2 Practical Contributions

The flood susceptibility maps provide actionable spatial guidance for Khartoum State planning and disaster management agencies. Zones identified as very highly susceptible (especially in the eastern and southern urban fringe) should be prioritized for non-residential land use, buffer zones, and drainage upgrades.

6.2.3 Academic Contributions

By applying G-AHP in a semi-arid, rapidly urbanizing context, this study fills a gap in flood modelling literature for under-represented regions. It contributes an empirically validated methodology and evidence for factor hierarchies that may guide future comparative flood studies in semi-arid Africa (Abdelkarim et al., 2020).

6.3 Recommendations

Policy Institutional Khartoum State Urban Planning Department and Ministry of Physical Planning should incorporate the susceptibility map into building permit systems and zoning bylaws to prohibit vulnerable development Integrate outputs into Sudan's National Adaptation Programme of Action (NAPA) and Nationally Determined Contributions (NDCs), offering

spatial vulnerability data to inform climate resilience strategies (Sudan Ministry of Environment, 2022).Align the study with Sustainable Development Goal 11 (Resilient Cities) and SDG 13 (Climate Action) to strengthen international relevance and policy uptake.

Infrastructure Risk Management Prioritize drainage improvements, stormwater retention basins, and permeable surfaces in eastern and southern susceptibility zones. Promote reforestation and green infrastructure in peri-urban bare areas to enhance infiltration. Implement real-time monitoring and early warning systems combining rainfall, TWI, and drainage inputs, linking to community alert mechanisms.

Community & NGOs and civil society (e.g. Sudan Red Crescent) can leverage maps for risk awareness campaigns and evacuation planning, particularly in informal settlements like Mayo, Al-Deim, Al-Haj Yousef. Insurance firms may adopt the susceptibility model for risk-based premiums and site evaluations.

6.4 Limitations of the study

Some datasets (rainfall, land cover) are temporally static, which may not fully capture dynamic flood processes (e.g. changing land use, seasonal patterns). AHP weighting is subjective, albeit mitigated by expert aggregation and consistency checks. Future models might integrate data-driven weighting such as entropy or machine learning sensitivity. LULC misclassification (e.g., confusing roads and bare land) revealed in the confusion matrix may propagate errors in susceptibility results. The focus on Khartoum limits generalization; results may not directly transfer to regions with different climatic or hydrological regimes.

6.5 Directions or future Research

Future work could benchmark the G-AHP approach against Random Forest, SVM, or deep learning classifiers to assess improvements in predictive performance (Zhang et al., 2022). Engaging residents in historical flood record collection can produce new validation datasets and ground truth points, enhancing spatial relevance (Ahmed et al., 2023). Integrating climate

change scenarios, hydrodynamic models (e.g., HEC-RAS 2D), and social vulnerability metrics would enable more comprehensive and dynamic flood risk assessments (UNDRR, 2020).

6.6 Conclusion

This study successfully applied a G-AHP framework to identify flood risk patterns in Khartoum. Dominant factors — rainfall, drainage density, slope, and clay soils — were empirically confirmed to drive flood susceptibility, especially in eastern and southern corridors. With a validated AUC of 0.812, the model demonstrates robust predictive capability for urban flood planning. The spatial outputs offer actionable guidance for planners, disaster managers, and community stakeholders, supporting resilient urban development and climate adaptation.

Bibliography

Abd El-Hamid, H. T. (2021), 'Assessment and prediction of land-use/land-cover change and flood effects around blue nile (bn) and white nile (wn) in khartoum to make recommendations in view of upcoming flood disasters', *Journal of Environmental Planning and Management* . Available online.

Abdallah Mohammed Elhassan, Y. (2022), Economic and non-economic loss and damage associated with flood 2020 in tuti island, khartoum, sudan (in context of climate change), *in* 'Proceedings Final Symposium Resilience in Urban Sudan (RUS) Project-Innovative Approaches, Climate Change, Resilience in Urban Environments'.

Abdel Hamid, A., Abdalla, S. H. & Osman, Y. Z. (2020), 'Flood risk assessment and mapping of khartoum state using gis-based multi-criteria analysis', *Natural Hazards* **104**, 1721–1743.

Abdelkarim, A., Al-Alola, S. S., Alogayell, H. M., Mohamed, S. A., Alkadi, I. I. & Ismail, I. Y. (2020), 'Integration of gis-based multicriteria decision analysis and analytic hierarchy process to assess flood hazard on the al-shamal train pathway in al-qurayyat region, kingdom of saudi arabia', *Water* **12**(6), 1702.

Abraham, T., Liu, Y., Tekleab, S. & Hartmann, A. (2023), 'Climate change potentially induces ecological change in the ethiopian rift valley lakes basin', *Journal of Hydrology: Regional Studies* **50**, 101543.

Adelekan, I. O. (2016), 'Flood risk management in the coastal city of lagos, nigeria', *Journal of Flood Risk Management* **9**(3), 255–264.

Ahmed, A., Yildirim, G., Haddad, K. & Rahman, A. (2023), 'Regional flood frequency analysis: A bibliometric overview', *Water* **15**(9), 1658.

Akhtar, N., Syakir, M., Ahmad, M., Anees, M., Bakar, A., Mizan, S., Alsaadi, S., Khan, M. & Yusuff, M. (2022), 'Upscaling of surface water and groundwater interactions in hyporheic zone from local to regional scale. water 2022, 14, 647'.

Altunel, A. (2023), 'The effect of dem resolution on topographic wetness index calculation and visualization', *International Journal of Engineering and Geosciences* pp. 165–172.
URL: *https://doi.org/10.26833/ijeg.1110560*

Asiedu, J. B. (2020), 'Reviewing the argument on floods in urban areas: A look at the causes', *Theoretical and Empirical Researches in Urban Management* **15**(1), 24–41.

Babiker, A., El Husseini, M., Al Nemri, A., Al Frayh, A., Al Juryyan, N., Faki, M. O., Assiri, A., Al Saadi, M., Shaikh, F. & Al Zamil, F. (2014), 'Health care professional development: Working as a team to improve patient care', *Sudanese journal of paediatrics* **14**(2), 9.

Bang, H., Miles, L. & Gordon, R. (2018), 'Enhancing local livelihoods resilience and food security in the face of frequent flooding in africa: A disaster management perspective', *Journal of African Studies and Development* **10**(7), 85–100.

Barnes, P. W., Robson, T. M., Neale, P. J., Williamson, C. E., Zepp, R. G., Madronich, S., Wilson, S. R., Andrady, A. L., Heikkilä, A. M., Bernhard, G. H. et al. (2022), 'Environmental effects of stratospheric ozone depletion, uv radiation, and interactions with climate change: Unep environmental effects assessment panel, update 2021', *Photochemical & Photobiological Sciences* **21**(3), 275–301.

Bhuiyan, S. R. & Al-Baky, A. A. (2014), 'Digital elevation-based flood hazard and vulnerability study at various return periods in sirajganj sadar upazila, bangladesh', *International Journal of Disaster Risk Reduction* **10**, 48–58.

Biasutti, M. (2019), 'Rainfall trends in the african sahel: Characteristics, processes, and causes', *Wiley Interdisciplinary Reviews: Climate Change* **10**(4), e591.

Bui, D. T., Tsangaratos, P., Ngo, P. T. T. & Pham, B. T. (2019), 'Flash flood susceptibility modelling using an optimized fuzzy rule based feature-selection technique and tree-based ensemble methods', *Science of the Total Environment* **650**, 2773–2790.

Chen, W., Li, Y., Xue, W., Shahabi, H., Li, S., Hong, H., Wang, X. & Bui, D. T. (2020), 'Modeling flood susceptibility using data-driven approaches and hydrological models', *Environmental Modelling Software* **131**, 104761.

(CIMAF), C. . I. M. . F. (2024), 'Sudan flood risk profile', https://www.cimafoundation.org/wp-content/uploads/2024/08/Sudan-flood-risk-profile.pdf.

Congalton, R. G. & Green, K. (2019), *Assessing the Accuracy of Remotely Sensed Data: Principles and Practices*, 3rd edn, CRC Press, Boca Raton, FL.

Copernicus (2020), 'European state of the climate 2020', Copernicus Climate Change Service (C3S). **URL:** *https://climate.copernicus.eu/esotc/2020*

Eisa, B. M. A. M., Saeed, A. B., Dafalla, M. S., Ali, A. M. & Omer, Y. (2022), 'Delineation of wadi haseeb watershed from digital elevation model using hec-geo-hms in arcgis, east nile, sudan', *East African Scholars Journal of Agriculture and Life Sciences* **5**(10).

El-Aziz, M. S. et al. (2020), 'Evaluation of the nile river flooding in the khartoum capital', *Proceedings of the Asian Conference on Remote Sensing (ACRS)* . Khartoum, Sudan.

El-Magd, S. A. A., Masoud, A. M., Hassan, H. S., Nguyen, N.-M., Pham, Q. B., Haneklaus, N. H., Hlawitschka, M. W. & Maged, A. (2024), 'Towards understanding climate change: Impact of land use indices and drainage on land surface temperature for valley drainage and non-drainage areas', *Journal of Environmental Management* **350**, 119636.

Elagib, N. A., Al Zayed, I. S., Saad, S. A. G., Mahmood, M. I., Basheer, M. & Fink, A. H. (2021), 'Debilitating floods in the sahel are becoming frequent', *Journal of Hydrology* **599**, 126362.

Elfadaly, A., Abutaleb, K., Naguib, D. M. & Lasaponara, R. (2022), 'Detecting the environmental risk on the archaeological sites using satellite imagery in basilicata region, italy', *The Egyptian Journal of Remote Sensing and Space Science* **25**(1), 181–193.

Elkhatib, O., El Ela, M. A., El-Banbi, A., El-Tayeb, E.-S. & Sayyouh, M. H. (2022), 'An analytical model for performance prediction of miscible flooding methods', *Journal of Engineering Research* .

Elkhrachy, I. (2015), 'Flash flood hazard mapping using satellite images and gis tools: A case study of najran city, kingdom of saudi arabia (ksa)', *Egyptian Journal of Remote Sensing and Space Sciences* **18**, 261–278.

Esri (2020), *ArcPy Python Site Package (Version 1.2)*, Environmental Systems Research Institute, Redlands, California, USA. Available at: https://pro.arcgis.com/en/pro-app/latest/arcpy/get-started/what-is-arcpy-.htm.

Esri (2021), *ArcGIS Pro (Version 2.9)*, Environmental Systems Research Institute, Redlands, California, USA. Available at: https://www.esri.com/en-us/arcgis/products/arcgis-pro/overview.

Fan, H., Yan, H., Teng, L., Liu, R., Li, Z., Cheng, H. & Zhang, E. (2023), 'The effects of extreme flood events on the turbidity maximum zone in the yangtze (changjiang) estuary, china', *Marine Geology* **456**, 106993.

Fang, K., Jawitz, J. W. & Morales, V. L. (2020), 'Machine learning for real-time prediction of urban flash floods: Houston case study', *Journal of Hydrology* **586**, 124872.

Fawcett, T. (2006), 'An introduction to roc analysis', *Pattern Recognition Letters* **27**(8), 861–874.

Food and Agriculture Organization (2022), 'Fao soil portal: Harmonized world soil database (hwsd)'. Accessed 2023 from https://www.fao.org/soils-portal/.

Funk, C., Peterson, P., Landsfeld, M., Pedreros, D., Verdin, J., Shukla, S., Husak, G., Rowland, J., Harrison, L., Hoell, A. & Michaelsen, J. (2015), 'The climate hazards infrared precipitation with stations—a new environmental record for monitoring extremes', *Scientific Data* **2**, 150066.

Gebrechorkos, S. H., Hülsmann, S. & Bernhofer, C. (2020), 'Analysis of climate variability and droughts in east africa using high-resolution climate data products', *Global and Planetary Change* **186**, 103130.

Goh, K. C. & Tan, K. S. (2018), 'Integrating machine learning with remote sensing for flood susceptibility mapping in data-scarce regions', *Natural Hazards* **94**(2), 741–762.

Gorelick, N., Hancher, M., Dixon, M., Ilyushchenko, S., Thau, D. & Moore, R. (2017), 'Google earth engine: Planetary-scale geospatial analysis for everyone', *Remote Sensing of Environment* **202**, 18–27.

Habib, M., Habib, A. & Abboud, M. (2024), 'Multi-aspect critical assessment of applying digital elevation models in environmental hazard mapping', *RIG* **33**.

Hamid, A. A. A., Mofadel, H. I. A., Hassan, M. H., Mahmoud, T. E. & Kheiry, M. A. (2025), 'Geospatial analysis for flood vulnerability and risk assessment: A case study of omdurman and um badda localities, khartoum state-sudan', *Direct Research Journal of Public Health and Environmental Technology* **10**(1), 46–57.

Ibrahim, M. S. O., Osman, S. M. N. & Mustafa, E. (2021), 'Evaluate and analyse the flood risk and potential flood zones in the blue nile state utilising multi-criteria decision analysis (mcda)

and the analytical hierarchy process (ahp)', *Journal of Karary University for Engineering and Science* **4**(1), 30–40.

Ibrahim, M. S. O., Osman, S. M. N. & Mustafa, E. (2023), 'Evaluate and analyse the flood risk and potential flood zones in the blue nile state utilising multi-criteria decision analysis (mcda) and the analytic hierarchy process (ahp)', *Journal of Karary University for Engineering and Science* **4**(1), 343.

Jha, A. K., Bloch, R. & Lamond, J. (2012), *Cities and Flooding: A Guide to Integrated Urban Flood Risk Management for the 21st Century*, The World Bank, Washington, D.C.

Kerebeh, H., Forkel, M. & Zewdie, W. (2024), 'Above ground biomass estimation in the upper blue nile basin forests, north-western ethiopia', *Environmental Systems Research* **13**(1), 48.

Khosravi, K., Nohani, E., Maroufinia, E. & Pourghasemi, H. R. (2016), 'A gis-based flood susceptibility assessment and its mapping in iran: A comparison between frequency ratio and weights-of-evidence bivariate statistical models with multi-criteria decision-making technique', *Natural Hazards* **83**(2), 947–987.

Khosravi, K., Nohani, E., Maroufinia, E. & Pourghasemi, H. R. (2019), 'A gis-based flood susceptibility assessment and its mapping in iran: A comparison between different multicriteria decision-making methods', *Natural Hazards* **98**(1), 179–208.

Kimura, Y., Hirabayashi, Y., Kita, Y., Zhou, X. & Yamazaki, D. (2023), 'Methodology for constructing a flood-hazard map for a future climate', *Hydrology and Earth System Sciences* **27**(8), 1627–1644.

Kiptum, A., Neal, J., Sampson, C. et al. (2023), 'Advancing operational flood forecasting, early warning and risk management in kenya and the greater horn of africa', *Journal of Flood Risk Management* . Technical/report style, 2023.

Krejčí, J. & Stoklasa, J. (2018), 'Aggregation in the analytic hierarchy process: Why weighted geometric mean should be used instead of weighted arithmetic mean', *Expert Systems with Applications* **114**, 97–106.

Kundzewicz, Z., Su, B., Wang, Y., Xia, J., Huang, J. & Jiang, T. (2019), 'Flood risk and its reduction in china', *Advances in Water Resources* **130**, 37–45.
URL: *https://www.sciencedirect.com/science/article/pii/S0309170818308339*

Liu, Q., Du, M., Wang, Y., Deng, J., Yan, W., Qin, C., Liu, M. & Liu, J. (2024), 'Global, regional and national trends and impacts of natural floods, 1990–2022', *Bulletin of the World Health Organization* **102**(6), 410.

Mahmood, M. I., Elagib, N. A., Horn, F. & Saad, S. A. (2017), 'Lessons learned from khartoum flash flood impacts: An integrated assessment', *Science of the Total Environment* **601**, 1031–1045.

Mahmoud, S. H. & Gan, T.-Y. (2018), 'Multi-criteria approach to develop flood susceptibility maps in arid regions of middle east', *Journal of Cleaner Production* **196**, 216–229.
URL: *https://www.sciencedirect.com/science/article/abs/pii/S0959652618316974*

Merz, B., Blöschl, G., Vorogushyn, S., Dottori, F., Aerts, J. C., Bates, P., Bertola, M., Kemter, M., Kreibich, H., Lall, U. et al. (2021), 'Causes, impacts and patterns of disastrous river floods', *Nature Reviews Earth & Environment* **2**(9), 592–609.

Mohammed, S. A., Abdalla, S. H. & Elsheikh, A. E. (2017), 'Assessment of flash floods in khartoum state, sudan using gis and remote sensing', *International Journal of Geosciences* **8**, 142–157.

Monteiro, A., Ankrah, J., Madureira, H. & Pacheco, M. O. (2022), 'Climate risk mitigation and adaptation concerns in urban areas: a systematic review of the impact of ipcc assessment reports', *Climate* **10**(8), 115.

Nations, U. (2020), 'Sudan floods 2020: Situation update', United Nations Office for the Coordination of Humanitarian Affairs (UNOCHA).
URL: *https://reliefweb.int/report/sudan/sudan-floods-2020-situation-update*

Ngo, P. T. T., Pham, B. T. et al. (2018), 'A novel hybrid swarm-optimized multilayer neural network model for flash-flood susceptibility mapping: Bac ha and bao yen districts, vietnam', *Sensors* **18**(11), 3704.

Nguyen, H. N., Fukuda, H. & Nguyen, M. N. (2024), 'Assessment of the susceptibility of urban flooding using gis with an analytical hierarchy process in hanoi, vietnam', *Sustainability* **16**(10), 3934.

Nile Basin Initiative (2024), Revolutionizing flood risk reduction in khartoum, sudan: An integrated hydrologic and hydraulic approach with upstream reservoir storage, Case study / technical note cs24, Nile Basin Initiative.
URL: *https://nilebasin.org/sites/default/files/2024-05/CS24.pdf*

Nkonu, R. S., Ampofo, F. D., Kwarteng, A. & Debrah, C. (2023), 'Gis-based multi-criteria analytical hierarchy process modelling for urban flood vulnerability analysis: Accra metropolitan area, ghana', *Natural Hazards* **117**(2).

Nourani, V. & Gichamo, T. (2021), 'Ensemble data-driven rainfall-runoff modeling using multi-source satellite and gauge rainfall data input fusion', *Earth Science Informatics* **14**(4), 1787–1808.

Observatory, N. E. (2020), 'Record flooding in sudan', https://earthobservatory.nasa.gov/images/147288/record-flooding-in-sudan.

OCHA (2018), 'Sudan: Floods situation report no. 2 (as of 24 september 2018)', United Nations Office for the Coordination of Humanitarian Affairs (OCHA).
URL: *https://reliefweb.int/report/sudan/sudan-floods-situation-report-no2-24-september-2018*

OCHA (2019), 'Sudan: Floods situation report no. 5 (as of 23 september 2019)', United Nations Office for the Coordination of Humanitarian Affairs (OCHA).
URL: *https://reliefweb.int/report/sudan/sudan-floods-situation-report-no5-23-september-2019*

OCHA (2020), 'Sudan: Floods situation report no. 9 (as of 10 september 2020)', United Nations Office for the Coordination of Humanitarian Affairs (OCHA).
URL: *https://reliefweb.int/report/sudan/sudan-floods-situation-report-no9-10-september-2020*

OCHA (2022), 'Sudan: Floods situation report no. 3 (as of 10 october 2022)', United Nations Office for the Coordination of Humanitarian Affairs (OCHA).
URL: *https://reliefweb.int/report/sudan/sudan-floods-situation-report-no3-10-october-2022*

on Climate Change (UNFCCC), U. N. F. C. (2016), 'Sudan's national adaptation plan', https://unfccc.int/sites/default/files/resource/Sudan-NAP.pdf.

Organization, W. H. (2023), *WHO's response to health emergencies: annual report 2022*, World Health Organization.

Pal, S. C., Chowdhuri, I., Das, B., Chakrabortty, R., Roy, P., Saha, A. & Shit, M. (2022), 'Threats of climate change and land use patterns enhance the susceptibility of future floods in india', *Journal of environmental management* **305**, 114317.

Rahman, M. M., Shobuj, I. A., Islam, M. R., Islam, M. R., Hossain, M. T., Alam, E., Hattawi, K. S. A. & Islam, M. K. (2024), 'Flood preparedness in rural flood-prone area: a holistic assessment approach in bangladesh', *Geomatics, Natural Hazards and Risk* **15**(1), 2379599.

Rahman, M. R., Thakur, P. K. & da Silva, A. M. (2019), 'Mapping flood susceptibility using geospatial techniques: A case study of the brahmaputra river basin, bangladesh', *Water* **11**(10), 2236.

Rahman, Z. U. et al. (2023), 'Gis-based flood susceptibility mapping using bivariate statistics and machine learning methods', *Frontiers in Environmental Science* **10**, 1178540.
URL: *https://www.frontiersin.org/articles/10.3389/fenvs.2023.1178540/full*

Rahmati, O., Pradhan, B., Khazaei, B., Mantadia, G. H. & Ustaoglu, E. (2016), 'A comparative assessment of bivariate statistical models for flood susceptibility mapping using gis: The case of havir county, iran', *Science of the Total Environment* **565**, 551–567.

Ramkar, P. & Yadav, S. M. (2021), 'Flood risk index in data-scarce river basins using the ahp and gis approach', *Natural Hazards* **109**(1), 1119–1140.

Reuters (2024), 'Climate change may boost africa's extreme rainfall by 20% by 2050', Reuters News Agency.
URL: *https://www.reuters.com/*

Ritchie, H. & Roser, M. (2019), 'Natural disasters', Our World in Data.
URL: *https://ourworldindata.org/natural-disasters*

Saaty, T. L. (1980), *The Analytic Hierarchy Process: Planning, Priority Setting, Resource Allocation*, McGraw-Hill, New York.

Sofi, M. S., Rautela, K. S., Muslim, M. & Bhat, S. U. (2024), 'From data to decisions: evaluating flood vulnerability in the sindh watershed through analytical hierarchy process (ahp)', *Frontiers of Urban & Rural Planning* **2**, 12.

Sulieman, H., Leknaes, D. & Talib, A. (2024), 'Title of the article', *Journal Name* **5**, 10–20.

Tamiru, H. & Dinka, M. O. (2021), 'Artificial intelligence in geospatial analysis for flood vulnerability assessment: A case of dire dawa watershed, awash basin, ethiopia', *ScientificWorldJournal* **2021**, 6128609.

Tehrany, M. S., Jones, S. & Shabani, F. (2019), 'Identifying the essential flood conditioning factors for flood prone area mapping using machine learning techniques', *Catena* **175**, 174–192.

Tehrany, M. S., Pradhan, B. & Mansor, S. B. (2014), 'Flood susceptibility mapping using a novel ensemble weighting method in gis', *Environmental Earth Sciences* **71**(6), 2869–2888.

Teku, D. (2025), 'Navigating climate uncertainty: a comprehensive review of climatic variabilities and extreme events on environmental, socio-economic, and livelihood dimensions in ethiopia with adaptation strategies', *All Earth* **37**(1), 1–30.

Tellman, B. et al. (2021), 'Global patterns and trends in flood exposure', *Nature* **596**, 80–86.

UNDRR (2020), 'The human cost of disasters: An overview of the last 20 years (2000-2019)'. United Nations Office for Disaster Risk Reduction.
URL: *https://www.undrr.org/publication/human-cost-disasters-overview-last-20-years-2000-2019*

UNOCHA (2013), 'Sudan: Floods situation report no. 6 (as of 19 september 2013)', United Nations Office for the Coordination of Humanitarian Affairs (UNOCHA).
URL: *https://reliefweb.int/report/sudan/sudan-floods-situation-report-no6-19-september-2013*

UNOSAT (2025), 'Satellite detected water extent in khartoum and white nile states, sudan as of 1 january 2025', https://geo.btaa.org/catalog/3d41360e-7f6c-45a0-b8c3-a35b0932ca02.

UNU (2004), *Reducing Disaster Risk: A Challenge for Development*, United Nations University Press, New York.
URL: *https://archive.unu.edu/publications/pdf/ReducingDisasterRisk.pdf*

Weldu Woldemariam, G. & Edo Harka, A. (2020), 'Effect of land use and land cover change on soil erosion in erer sub-basin, northeast wabi shebelle basin, ethiopia', *Land* **9**(4), 111.

Wing, O. E. J., Lehman, W., Bates, P. D. et al. (2022), 'Inequitable patterns of us flood risk in the anthropocene', *Nature Climate Change* .

Wubalem, A., Tesfaw, G., Dawit, Z., Getahun, B., Mekuria, T. & Jothimani, M. (2020), 'Comparison of statistical and analytical hierarchy process methods on flood susceptibility mapping: a

case study of tana sub-basin in northwestern ethiopia', *Natural Hazards and Earth System Sciences Discussions* **20**, 1–20.

Youssef, A. M. & Hegab, M. (2019), Flood-hazard assessment modeling using multi-criteria analysis and gis: A case study (ras gharib area), *in* 'Flood-Hazard Assessment Modeling Using Multicriteria Analysis and GIS', Elsevier / Academic. Chapter; includes AHP methodology and validation (reported accuracy 83.3%).

Zaharia, L., Costache, R., Prăvălie, R. & Ioana-Toroimac, G. (2017), 'Mapping flood and flooding potential indices: a methodological approach to identifying areas susceptible to flood and flooding risk. case study: the prahova catchment (romania)', *Frontiers of Earth Science* **11**(2), 229–247.

Zhang, H., Shao, Z., Sun, J., Huang, X. & Yang, J. (2022), 'An extended watershed-based ahp model for flood hazard estimation: Constraining runoff converging indicators via mfd-derived sub-watershed by maximum zonal statistical method', *Remote Sensing* **14**(10), 2465.

Zhou, Z., Smith, J. A., Baeck, M. L., Wright, D. B., Smith, B. K. & Liu, S. (2021), 'The impact of the spatio-temporal structure of rainfall on flood frequency over a small urban watershed: an approach coupling stochastic storm transposition and hydrologic modeling', *Hydrology and Earth System Sciences* **25**, 4701–4717.

Zhran, M. et al. (2024), 'Exploring a gis-based analytic hierarchy process for spatial flood risk assessment in egypt: a case study of the damietta branch', *Environmental Sciences Europe* **36**, 184.